

Techno-economic and environmental comparative assessment of two renewable methanol production routes

Sebastian Quevedo



Techno-economic and environmental comparative assessment of two renewable methanol production routes

by

Sebastian Quevedo

to obtain the degree of Master of Science
at the Delft University of Technology,
to be defended publicly on Friday July 9, 2021 at 01:00 PM.

Student number:	5021294	
Project duration:	November 1, 2020 – July 9, 2021	
Thesis committee:	Prof. dr. ir. Andrea Ramirez Ramirez,	TU Delft, supervisor
	Prof. dr. ir. Wiebren de Jong,	TU Delft, co-supervisor
	Dr. Paola Ibarra,	TU Delft, co-supervisor

An electronic version of this thesis is available at <http://repository.tudelft.nl/>.

Summary

The threats posed by global warming require the rapid transition of high emitting sectors to sustainable alternatives. In this framework, methanol has the potential to influence the decarbonization of two hard-to-abate sectors of the economy: the chemical industry and the large transport sector. In order to achieve this, methanol production needs to shift from its current fossil fuel based methods. There are already two promising technologies that could be used for this purpose. One is the hydrogenation of captured CO_2 , and the other is through the gasification of plastic wastes. However, more research is needed to identify trade-offs and, particularly, to assess the influence of contaminants and their purification requirements in the overall performance of the technologies.

This report aims to evaluate the competitiveness of the CO_2 hydrogenation route and the plastic-to-methanol process by means of a techno-economic and environmental evaluation. The design of both processes considers the treatment of contaminants to reach the target levels required by the catalyst used in methanol production. CO_2 from a Carbon Capture and Sequestration network is considered for the CO_2 hydrogenation case study, while the plastic share of the Municipal Solid Wastes in the Netherlands is chosen as main feedstock for the plastic-to-methanol route. The design processes are simulated using Aspen Plus software to calculate technical, economic, and environmental key performance indicators. These are then used to find process bottlenecks and trade-offs between the technologies.

The study finds neither of the technologies outperforms the other in every dimension. From an economic perspective, the plastic-to-methanol process showed better results. Particularly, this production route benefits from cheaper raw materials in comparison to the hydrogen costs. On the other hand, the generation of combustion gases during gasification and the liquid waste streams produced during the cleaning of the syngas hinder the environmental footprint of the plastic-to-methanol route. Moreover, TARs production is found to consume around 25% of the carbon content in the plastics, which considerably reduces the efficiency of the technology. Therefore, a lower overall carbon conversion is obtained, despite the fact that methanol production from syngas experiences better reaction rates compared to the interaction between CO_2 and H_2 .

The outcomes of the research are subject to the boundaries and limitations of the process model, however, the findings highlight the relevance of the purification units. This is more noticeable in the plastic-to-methanol route, where carbon losses and waste generation end up reducing the potentials for the technology. On the contrary, the CO_2 purification system has little impact on the efficiency of the CO_2 hydrogenation process. In fact, less than 5% of the inlet CO_2 is lost during the purification steps. Nonetheless, the system plays a major role in achieving the right conditions for the methanol reaction. Added to the fact that it contributes to about a third of the overall cost of the process, it is concluded that the system is highly relevant for the correct assessment of the technology.

Preface

This report marks the culmination of an 8-month investigative work, of which I am very proud. Two years ago I made the decision to get off the path I was walking and follow my guts. Although it was difficult at times, I know that I made the right decision. In the same way that I know that I could not be where I am right now without the help of many others. To all those who have accompanied and supported me during this stage of my life, I will be eternally grateful.

First of all, I want to thank my thesis supervisor, Prof. dr. Andrea Ramirez, for giving me the chance of doing this research and trusting that I was up to the task. But more importantly, for always keeping an eye on her team and making us feel welcomed.

To my co-supervisor, Prof. dr. Wiebren de Jong, for taking the time and interest to help me accomplish this project. Your inputs to the research were highly valuable.

My warmest gratitude to my weekly supervisor Dr. Paola Ibarra. Thank you so much for your patience, your kind spirit, and for mentoring me during the whole process. I will miss our weekly chats.

I also want to thank everybody from Andrea's group. You were kind enough to help me improve the models of my thesis, and even though I didn't get to meet you in person, I enjoyed every group meeting.

Of course, I want to thank my friends from TU Delft and Boom Xior (you know who you are). You made my master's experience an awesome period of my life and we will meet again sometime.

Finally and most importantly, I want to thank my family. To my brothers, sister, and especially my parents. Everything I am I owe it to you. To my girlfriend's family, for always cheering me up and constantly worrying about us. And to gigi, thank you for everything you do for us and for taking care of everything while I lived in the computer chair.

Sebastian Quevedo
Delft, June 2021

Contents

Summary	i
List of Figures	v
List of Tables	vii
1 Introduction	1
1.1 Background on Methanol Production	3
1.2 State of the Art	7
1.3 Knowledge Gaps	8
1.4 Thesis Aim	8
1.4.1 Specific Objectives of the Thesis	9
1.5 Thesis Outline	9
2 Project Scope and Methodology	10
2.1 Project Scope	10
2.2 Methodology	10
2.3 Key Performance Indicators	13
2.3.1 Technical KPIs	13
2.3.2 Economic KPIs	14
2.3.3 Environmental KPIs:	16
3 Case Studies	18
3.1 Raw Materials	18
3.1.1 Carbon Dioxide	19
3.1.2 Hydrogen	19
3.1.3 Plastics	20
3.2 Case Study 1: CO_2 hydrogenation route	21
3.3 Case Study 2: Plastic-to-Methanol route	22
4 Process Design and Modeling	24
4.1 CO_2 Purification System	25
4.1.1 Process Design	25
4.1.2 Process Modeling	27
4.2 CO_2 Hydrogenation	28
4.2.1 Process Design	28
4.2.2 Process Modeling	30
4.3 Plastic-to-methanol	31
4.3.1 Process Design	31
4.3.2 Process Modeling	34
5 Pedigree Analysis	36
5.1 Background on Process Model Uncertainty	36
5.2 Pedigree Analysis	37
5.2.1 Pedigree Workshops	37
5.2.2 Results from Pedigree workshops	40
6 Results	45
6.1 Mass and Energy Balances	45
6.2 Results from Technical KPIs	47
6.3 Results from Economic KPIs	50
6.4 Results from Environmental KPIs	52

7 Sensitivity Analysis	54
7.1 Sensitivity analysis on key input parameters	54
7.2 Alternative Hydrogen Supply for the CO_2 Hydrogenation Route	56
7.2.1 Background on Water Electrolysis	56
7.2.2 Comparison between different hydrogen sources	58
8 Discussion	60
9 Conclusions and Future Works	64
Bibliography	65
A Pedigree Analysis	72
A.1 Components evaluated.	72
A.2 Pedigree Criteria	73
B Regeneration Units	74
B.1 Dual-alkali process	74
B.2 LO-CAT process	75
C Aspen Flowsheets	77
D Economic Evaluation	83

List of Figures

1.1	Global temperature change relative to 1850-1900 (°C). Measured data since 2015 to 2018 is shown in blue. The orange line represents the projection at current warming rate, and in green is a hypothetical pathway where emissions peak in 2020 and reach net-zero by 2055. Sourced from IPCC, 2018	2
1.2	Overview of the Netherlands energy system by fuel and sector, 2018. Sourced from (IEA, 2020b). * <i>Total supply includes bunker fuels for international aviation and shipping (not part of TPES)</i> . ** <i>Other renewables includes wind, solar, hydro, and geothermal</i>	2
1.3	Derivatives of methanol and main markets. Adapted from (IRENA, 2021)	3
1.4	Share of sources for methanol production. Adapted from (Chatterton, 2019)	4
1.5	Possible routes for methanol production classified by carbon intensity. TRL of alternative routes included (Albo et al., 2015; IRENA, 2021; Pérez-Fortes & Tzimas, 2016; Solis & Silveira, 2020). ¹ The TRL depends on the specific electrolyser technology. Alkaline and Polymer Electrolyte Membrane (PEM) electrolysis have a higher TRL of 8 - 9, while Solid Oxide Electrolysers (SOEC) are in the range 6 - 7.	5
1.6	CO_2 hydrogenation pathways	6
2.1	Methodology approach for the techno-economic and environmental evaluation of two renewable methanol production routes.	11
3.1	Simplified block diagram with the system boundaries of case study 1: CO_2 hydrogenation	21
3.2	Simplified block diagram with the system boundaries of case study 2: plastic-to-methanol	22
4.1	Process Flow Diagram of the CO_2 purification system	26
4.2	Process Flow Diagram of the CO_2 hydrogenation plant	29
4.3	Process Flow Diagram of the plastic-to-methanol plant	32
5.1	Examples of inputs in a process model with underlying uncertainty	37
5.2	Stages in the modeling procedure in which Pedigree Analysis was conducted and the components evaluated.	38
6.1	Mass demand of individual inputs in kg/kg_{MeOH}	47
6.2	Utility demand distribution between the purification steps and the methanol synthesis	48
6.3	Hot and cooling utility demand by unit operations in the methanol synthesis step	49
6.4	Comparison between overall and reactor conversion efficiencies.	50
6.5	Breakdown of CAPEX costs	51
6.6	Contribution of CAPEX and OPEX to the LCOMeOH of the different technologies.	51
6.7	Breakdown of OPEX costs. VCP are shown with a pattern fill in the upper half. FCP are shown with a solid fill in the lower half.	52
6.8	Carbon footprint of the technologies compared to two reference cases.	52
6.9	Energy yield ratio of the different case studies and two reference cases.	53
7.1	Sensitivity analysis on economic and environmental parameters for the CO_2 hydrogenation route	55
7.2	Sensitivity analysis on economic and environmental parameters for the plastic-to-methanol route	55
7.3	Types of water electrolysis technologies. Sourced from (IRENA, 2020)	57
7.4	Energy losses from mechanical compression of hydrogen, based on percentage of hydrogen LHV. Sourced from (IRENA, 2020)	58
7.5	Financial indicators of the CO_2 hydrogenation route under different scenarios of hydrogen supply	59

8.1	Contribution of the CO_2 Purification System to the levelized cost of MeOH	62
9.1	Comparative assessment of two renewable methanol production routes	64
B.1	Schematic of an absorption and regeneration process for a dual-alkali process. Sourced from (Bezuidenhout et al., 2012)	74
B.2	Schematic representation of the LO-CAT technology. Sourced from (MERICHEM, n.d.)	75
C.1	Simulation flowsheet of the CO_2 purification system	78
C.2	Simulation flowsheet of the CO_2 hydrogenation	79
C.3	Simulation flowsheet of the gasification and syngas conditioning units	80
C.4	Simulation flowsheet of the methanol synthesis from syngas	81
C.5	Matlab code for the alkaline water electrolyser	82

List of Tables

2.1	Breakdown of CAPEX and OPEX calculation (Pérez-Fortes et al., 2016)	15
2.2	Carbon content in utilities	16
3.1	Contaminant target levels for methanol synthesis in mg/Nm^3 (Abdoulmoumine et al., 2015; Block et al., 2019; Woolcock & Brown, 2013)	18
3.2	Composition of the CO_2 feedstock for the CO_2 hydrogenation case study. Based on (Harkin, Sick, et al., 2017)	20
3.3	Specification for the plastic feedstock	20
4.1	Property methods used in the simulations	25
4.2	Design parameters of the Plug-flow reactor and catalyst (Nyári et al., 2020)	30
5.1	Pedigree matrix for the assessment of data uncertainty in the State of the Art. Based on Spek et al., 2016.	39
5.2	Pedigree matrix for the assessment of data uncertainty in the Simulations. Based on Spek et al., 2016.	39
5.3	Pedigree scores for the data uncertainty in the State of the Art of the CO_2 purification system. Median values range from 0 (high uncertainty) to 4 (low uncertainty). Colours are used to highlight the uncertainty level	40
5.4	Pedigree scores for the data uncertainty in the Simulation components of the CO_2 purification system. Median values range from 0 (high uncertainty) to 4 (low uncertainty). Colours are used to highlight the uncertainty level	40
5.5	Pedigree scores for the data uncertainty in the State of the Art of the CO_2 hydrogenation process. Median values range from 0 (high uncertainty) to 4 (low uncertainty). Colours are used to highlight the uncertainty level	41
5.6	Pedigree scores for the data uncertainty in the Simulation components of the CO_2 hydrogenation process. Median values range from 0 (high uncertainty) to 4 (low uncertainty). Colours are used to highlight the uncertainty level	41
5.7	Pedigree scores for the data uncertainty in the State of the Art of the plastic to methanol process. Median values range from 0 (high uncertainty) to 4 (low uncertainty). Colours are used to highlight the uncertainty level	42
5.8	Pedigree scores for the data uncertainty in the Simulation components of the plastic to methanol process. Median values range from 0 (high uncertainty) to 4 (low uncertainty). Colours are used to highlight the uncertainty level	42
5.9	Improvements made to the process models	44
6.1	Mass balance of the different case studies.	45
6.2	Energy balance of the different case studies.	46
6.3	Mass demand of individual inputs	48
6.4	Utility demand of the technologies	48
6.5	Economic KPIs	50
7.1	Input parameters used in the sensitivity analysis.	54
7.2	Break-even values	55
7.3	Specifications for the alkaline electrolyser. Based on Armijo, 2019; IRENA, 2020; Nel Hydrogen, 2019; Sánchez et al., 2020	58
8.1	Comparative table with key performance indicators	60
D.1	Prices of raw materials, utilities, and product	84

D.2	Total installation cost of equipment for the Plastic Gasification and Syngas Conditioning process	84
D.3	Total installation cost of equipment for the Methanol Synthesis process	85
D.4	Total installation cost of equipment for the CO_2 Purification System	85
D.5	Total installation cost of equipment for the CO_2 Hydrogenation process	86
D.6	Yearly cash flows	87

Introduction

Anthropogenic greenhouse gas emissions (GHG) are rising the world's temperature to dangerously high levels. A 2018 study from the Intergovernmental Panel on Climate Change showed the dangers to natural and human ecosystems if temperatures were to reach 2 °C, or even 1.5 °C above pre-industrial levels (IPCC, 2018). Although subject to particular characteristics such as geographic location, rate of warming, or level of vulnerability, amongst others, these climate-related risks include increasing frequency and intensity of droughts, heavy precipitations with tropical cyclones, flooding related to sea level rise, and many more. The same report warned policy-makers that the current rate of warming could exceed the temperature targets in the next decades if no action is taken, as depicted in Figure 1.1. The evidence is so overwhelming that developed economies have acknowledged this as a globalized threat. However, international commitments from developed countries have proven to be insufficient. So far, optimistic projections considering governments decarbonization targets and Nationally Determined Contributions (NDCs) are only on track of keeping the global temperature below 2.9 °C by the end of the century (Climate Tracker, 2020). Additional and timely efforts are thus needed to maintain the negative effects of climate change at bay.

The Netherlands has joined the global agenda and committed to reduce CO_{2eq} emissions with respect to 1990 levels by 49% in 2030 and 95% by 2050 (The Minister of Justice and Security, 2019), with a strong focus in renewable energy generation and the development of low carbon hydrogen and carbon capture sequestration and use technologies (CCS and CCU) (Government of The Netherlands, 2020; IEA, 2020b; Netherlands Enterprise Agency, 2020). Despite clear policies supporting the transition to a more sustainable energy system, The Netherlands is lagging behind and needs to at least double the pace of emission reductions to meet its 2030 target (PBL Netherlands Environmental Assessment Agency, 2020).

Decarbonizing the industry sector is paramount for The Netherlands to reach its emission reduction goals. As Figure 1.2 shows, the country's total energy consumption is dominated by oil and gas, particularly for the emission-intensive chemical and refining industries. On the other hand, natural gas alone amounts to 42% of Total Primary Energy Supply (TPES), the highest share among the International Energy Agency (IEA) member countries (IEA, 2020b). Nonetheless, natural gas production has fallen in the last couple of years transforming the Netherlands from a historically gas exporter country into a net importer. Incidentally, adding a point of threat to national energy security. Moreover, the goals from the Dutch Climate Agreement and the phase out plan of natural gas production from the Groningen gas field, due to safety concerns, are pressing for a quick and major reduction of gas consumption in the national energy system (IEA, 2020b).

The political landscape and technological advancements represent an attractive opportunity to decarbonize industry processes. The chemical industry is the subsector with the highest energy demand and one of the largest CO₂ emitters, behind cement and iron & steel production (IEA, 2020a). Within the chemical industry, finding production alternatives is key. Particularly in the Netherlands, where 2/5 of the largest multinational chemical companies have operations (VNCI, 2018). In this context, methanol

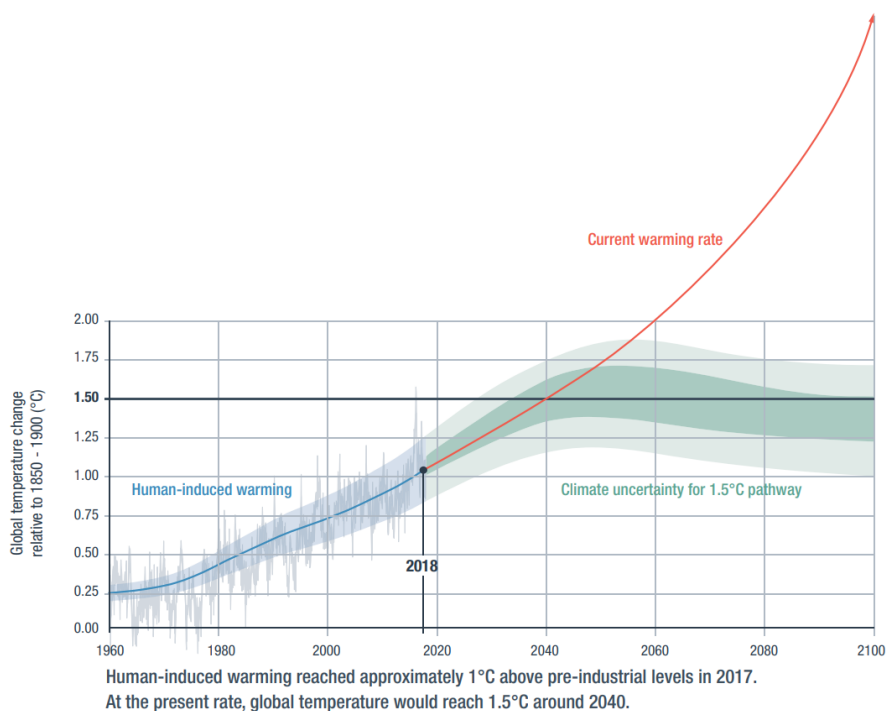


Figure 1.1: Global temperature change relative to 1850-1900 (°C). Measured data since 1955 to 2018 is shown in blue. The orange line represents the projection at current warming rate, and in green is a hypothetical pathway where emissions peak in 2020 and reach net-zero by 2055. Sourced from IPCC, 2018

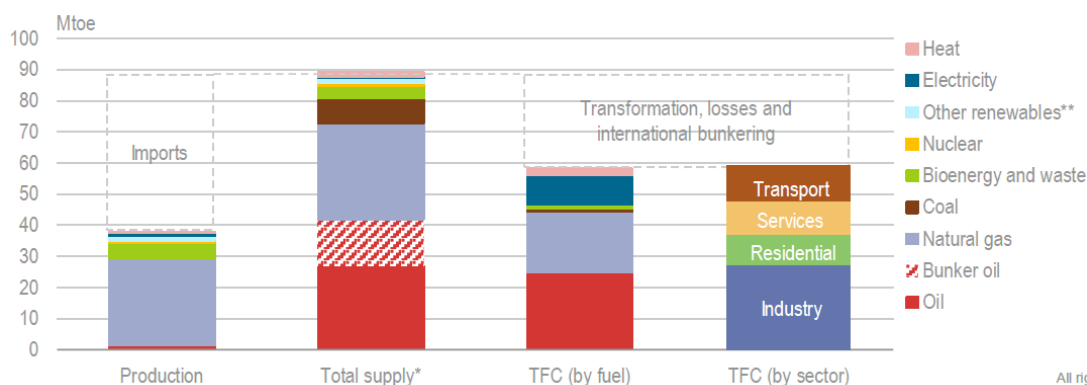


Figure 1.2: Overview of the Netherlands energy system by fuel and sector, 2018. Sourced from (IEA, 2020b). * *Total supply includes bunker fuels for international aviation and shipping (not part of TPES).* ***Other renewables includes wind, solar, hydro, and geothermal.*

stands out as a an interesting opportunity. Not only is it extremely relevant to the industry as a building block for other materials, but its manufacturing process consumes large amounts of natural gas. Therefore, changing to more sustainable feedstock and production technologies helps reducing GHG emissions and is also in line with the national goal of phasing out natural gas demand (IEA, 2020b). Furthermore, the government's strategy for the industry transition promotes measures such as the use of blue/green hydrogen¹, CCU & CCS, and accelerating circularity (e.g. waste-to-chemicals), which can be directly implemented when considering renewable pathways for methanol synthesis (Government of The Netherlands, 2019).

¹Green hydrogen refers to hydrogen produced through water electrolysis powered by renewable sources. Blue hydrogen is produced from steam methane reforming with CO₂ sequestration.

1.1. Background on Methanol Production

Methanol is a platform material which can be derived into a number of applications. It is mainly used as a building block for the chemical industry, acting as a starting point for a variety of products, such as plastics and fuel additives (IRENA, 2021). Figure 1.3 shows the derivatives of methanol and the main markets in which it participates. Formaldehyde remains the largest chemical derived from methanol, used mainly as a precursor for the manufacturing of resins. Methanol-to-Olefins process is the second largest source of demand. It is a relatively new technology that has seen tremendous growth over the last decade, particularly in China, as an alternative route from naphtha-based synthesis of ethylene and propylene. From virtually no production in 2010 it now accounts for approximately 25% of global methanol consumption (MMSA, 2021). Another application of methanol that has also grown rapidly is fuels. Whether methanol is used as a fuel by itself, blended with gasoline, derived into biofuel, or used in the form of methyl tert-butyl ether (MTBE) and dimethyl ether (DME), it accounts for around 31% of global demand.

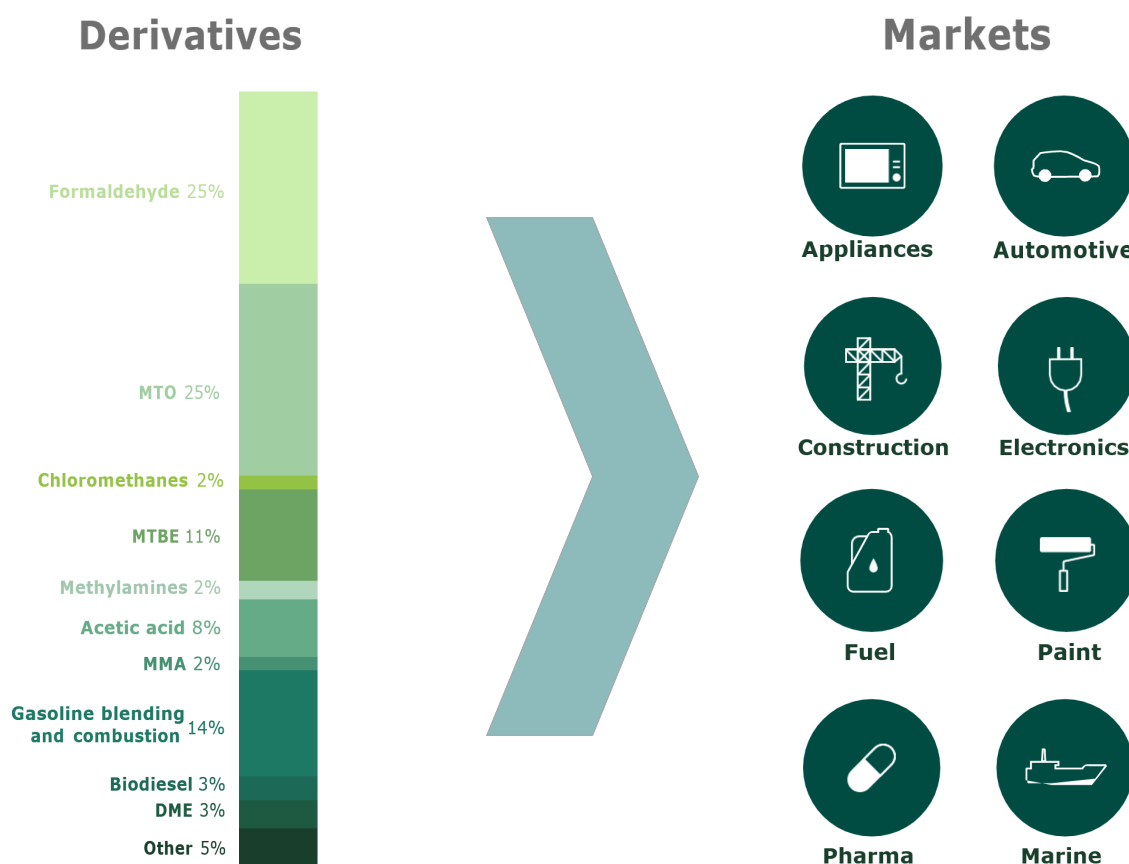


Figure 1.3: Derivatives of methanol and main markets. Adapted from (IRENA, 2021)

The established technology for large scale methanol production is based on the catalytic conversion of synthesis gas (syngas) over a copper-based catalyst (Sheldon, 2017). Syngas is a mixture of hydrogen, carbon monoxide, and some minor shares of carbon dioxide. The formation of methanol from this mixture is determined by the following reactions (Lee et al., 2020):



After years of improvement, the optimal reaction conditions have been developed to drive methanol formation. Conversions of CO and CO_2 to methanol (equations 1.1 and 1.3) are exothermic, hence they are favored by lower temperatures. However, the reaction rates in both cases increase with higher temperature (Lee et al., 2020). Additionally, the conversion rate of CO is superior than the one from CO_2 . Thus, shifting the equilibrium of equation 1.2 to the right benefits the methanol yield, which in turn is favored by an increase in temperature. A balance is reached by operating in the range of 200 - 300 °C. Furthermore, and according to the Le Chatelier's principle, the reduction in the number of molecules indicates that the methanol yield is maximized with higher pressures. Nowadays, conventional synthesis reactors operates in the 50 - 100 bar range (De Jong & Van Ommen, 2014).

To maximize productivity, an optimum ratio of H_2 to carbon in the syngas is required. This optimum composition is determined by the stoichiometric number S (Ott et al., 2012):

$$S = \frac{\text{Moles of } H_2 - \text{Moles of } CO_2}{\text{Moles of } CO + \text{Moles of } CO_2} \quad (1.4)$$

The value of S in the syngas should be close to 2. On the one hand, values below the stoichiometric optimum indicate that there is a hydrogen deficiency. Which results in a considerable reduction in the selectivity of methanol (Ott et al., 2012). On the other hand, S values greater than 2 mean that there is an excess of hydrogen. In this case, larger amounts of unreacted gases are trapped in the synthesis loop and, consequently, the size of the equipment increases. Therefore, conditioning processes to adjust the synthesis gas composition to its optimum level are most often necessary.

Today, methanol is predominantly produced from fossil fuels, as Figure 1.4 depicts. Natural gas accounts for about 65% of methanol production, while the rest is almost entirely sourced from coal. Only around 0.2% comes from alternative sources (IRENA, 2021). The vast majority of methanol production from coal is located in China, where large coal reserves are available. In the rest of the world, natural gas is the preferred choice of feedstock because of better economic conditions and its lower impurity content.

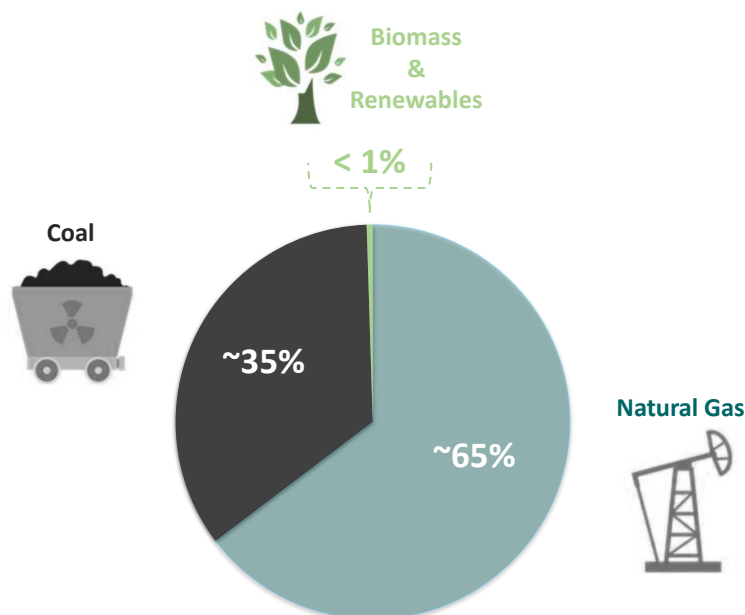


Figure 1.4: Share of sources for methanol production. Adapted from (Chatterton, 2019)

Reducing the large consumption of fossil fuels and the subsequent GHG emissions is the major driver for finding alternative production routes. Common technologies to produce syngas for methanol synthesis include steam reforming (from natural gas or light naphthas) and partial oxidation (used with heavy oils or carbon) (Pérez-Fortes et al., 2016). Both processes have a similar energy consumption: $33.4 - 36.5 \text{ GJ}/t_{\text{MeOH}}$ for steam reforming and $37.15 \text{ GJ}/t_{\text{MeOH}}$ used in partial oxidation. However, the emissions are significantly different depending on the feedstock. Typical GHG emissions associated with methanol production from natural gas are close to $0.5 \text{ CO}_2\text{-eq}/\text{kg}_{\text{MeOH}}$ (Pérez-Fortes et al., 2016), while emissions from coal are in the range of $2.97 - 3.8 \text{ CO}_2\text{-eq}/\text{kg}_{\text{MeOH}}$ (IRENA, 2021; Kajaste et al., 2018).

Furthermore, addressing the emissions generated in the production of methanol is key for the decarbonization of the chemical industry and the transport sector. The International Energy Agency (IEA) estimates that emissions from primary chemicals (such as methanol) need to drop below 10% from today's level by 2030 if the world is to meet the Sustainable Development Scenario (SDS)² (IEA, 2020a). Methanol production accounts for nearly 10% of the total CO_2 emissions in the chemical and petrochemical sector (IRENA, 2021). Thus, shifting to sustainable methods of methanol synthesis can have a major impact. Moreover, the characteristics of methanol makes it a natural alternative to fossil-based fuels, particularly for the harder to electrify transport sectors such as aviation and maritime (Methanex, 2020; P. Schmidt & Weindorf, 2016).

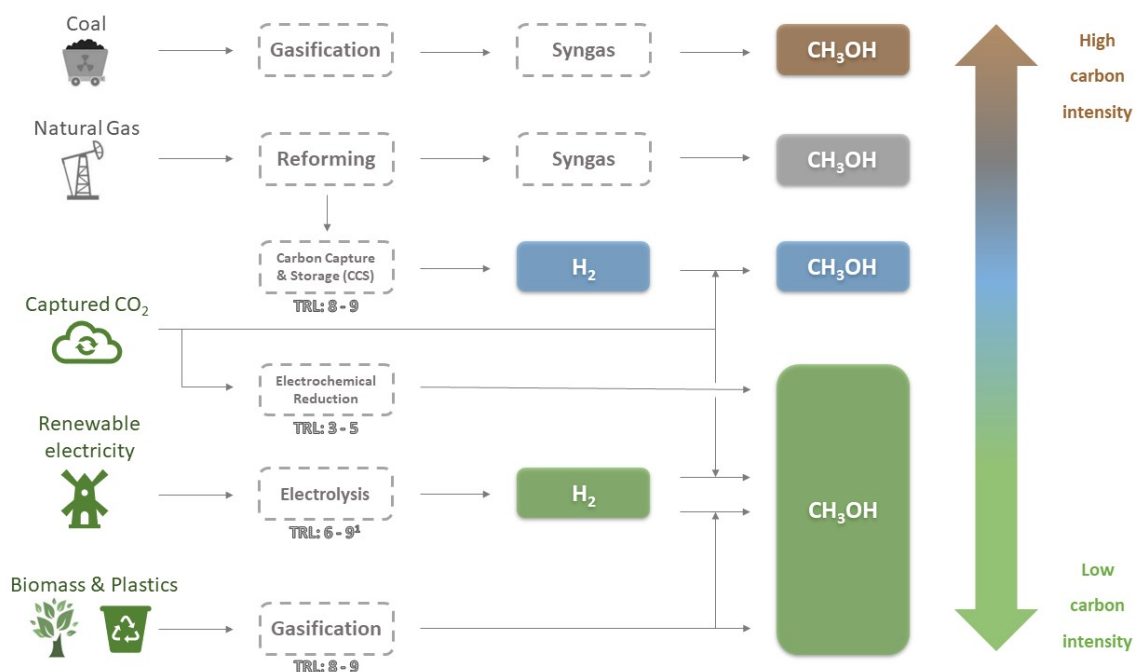


Figure 1.5: Possible routes for methanol production classified by carbon intensity. TRL of alternative routes included (Albo et al., 2015; IRENA, 2021; Pérez-Fortes & Tzimas, 2016; Solis & Silveira, 2020).

¹The TRL depends on the specific electrolyser technology. Alkaline and Polymer Electrolyte Membrane (PEM) electrolysis have a higher TRL of 8 - 9, while Solid Oxide Electrolysers (SOEC) are in the range 6 - 7.

Because of its versatility and relevance for the decarbonization of hard to abate sectors, there is great interest in the research and development of renewable processes for methanol synthesis. Figure 1.5 shows a diagram with possible routes for methanol production, including the Technology Readiness Level (TRL) of the alternatives. Methanol can be produced from several carbonaceous sources and may or may not require additional hydrogen. Depending on the source of the carbon, the technology used to produce the hydrogen, and the associated GHG emissions of the whole process, methanol can be characterized as low or high carbon intensity (IRENA, 2021).

²The SDS outlines a shift in the global energy system to meet the targets of the Paris Agreement, without relying on technologies for net negative emissions. <https://www.iea.org/reports/world-energy-model/sustainable-development-scenario>

In particular, two alternative productions have shown the most potential. Both technologies already with cases of commercial applications (CRI, 2011; Solis & Silveira, 2020). The first one is CO_2 hydrogenation using blue or green hydrogen and captured CO_2 . The second one is through the gasification of biomass or plastic waste (plastic-to-chemical process). This gasification process results in a synthesis gas which can then be converted to methanol. There is a third renewable alternative, through the electrochemical reduction of CO_2 . However it has not yet reached the same maturity level. Therefore, this study will focus on the first two technologies.

CO_2 hydrogenation can be performed in two different ways. In one step, through the direct interaction of CO_2 and hydrogen (Adnan & Kibria, 2020; Kotowicz et al., 2021) or in two steps, using Reverse Water Gas Shift (RWGS) reaction to produce synthesis gas (syngas) and then use the better conversion rates between CO and H_2 for the production of methanol (Elsernagawy et al., 2020; Gao et al., 2020). Figure 1.6 gives a simplified overview of the two alternatives. There is no consensus among researchers over which approach represents the best alternative for the industry. Nonetheless, this work will concentrate on the one-step CO_2 hydrogenation process. The decision is made after a literature review on the subject showed both alternatives achieve similar results, but the complexity of the system is reduced using the direct approach (Lee et al., 2020; Rafiee, 2020).

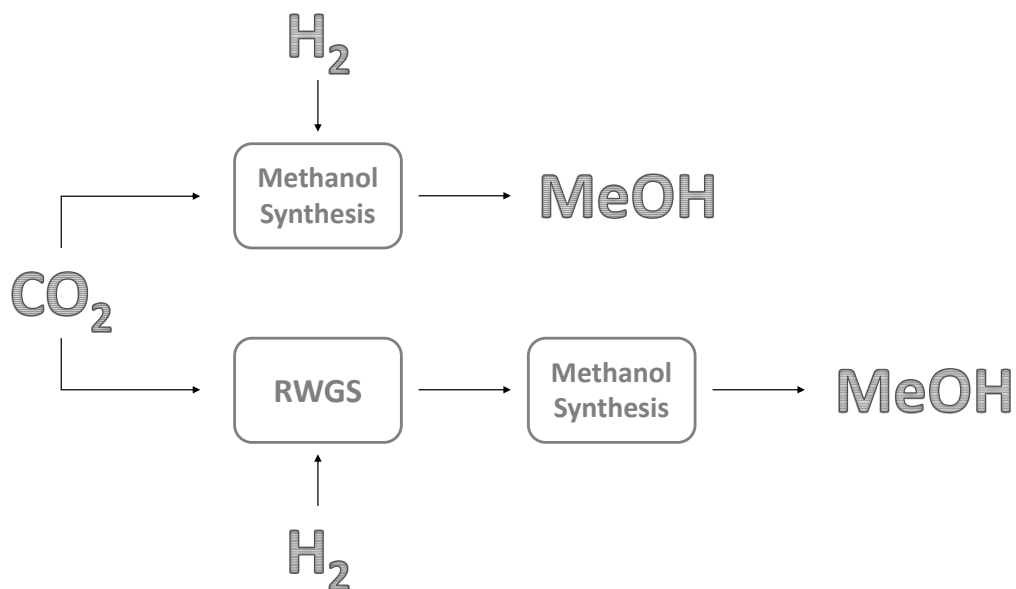


Figure 1.6: CO_2 hydrogenation pathways

On the other hand, the gasification of waste to produce value-added chemicals has drawn attention for its potential to promote circularity in the industry as an alternative to current practices for waste disposal and methanol production. In particular, the chemical recycling of plastics via gasification is considered a very attractive technology (Solis & Silveira, 2020). Most plastic waste is still disposed in landfills or incinerated (European Commission, 2018). However, incineration and landfilling do not align with the circular economy perspective, as the feedstock cannot be recovered (Davidson et al., 2021). Consequently, the replacement of new plastic material is required, which today means production based on fossil fuels. Alternatively, plastics can be recycled by mechanical or chemicals methods. Mechanical recycling is the most common alternative. Although, it suffers from strict requirements of homogeneity in the raw material. Thus, it makes it difficult to implement on a larger scale (Davidson et al., 2021). Chemical recycling through plastic gasification has the advantage of having more flexibility in the variability of the feedstock (Lopez et al., 2018). Therefore, the plastic-to-chemical process has the opportunity to create added value products (such as methanol) from residual raw material outside the scope of mechanical recycling methods.

1.2. State of the Art

Both CO₂ hydrogenation and waste-to-chemicals technologies have been extensively studied. Pérez-Fortes et al. (Pérez-Fortes et al., 2016) evaluated the economic viability and environmental benefits of a methanol (MeOH) plant using H₂ from water electrolysis and CO₂ captured from a CCU unit. The results showed the process is not financially viable mainly because of the high cost of H₂ production. However, the CO₂ emissions are reduced. Szima and Cormos (Szima & Cormos, 2018) also studied the production of MeOH from captured CO₂ and renewable H₂. Their work included the use of a gas turbine and organic Rankine cycles to reduce the energy consumption, without considering the electrolyzer unit. They found that the MeOH plant is energetically fully self-sufficient but still not economically viable. Adnan and Golam (Adnan & Kibria, 2020) compared the techno-economic and environmental performance of 3 renewable MeOH production routes against the conventional one. The proposed technologies included the reaction of captured CO₂ and renewable H₂, electrolysis of CO₂ to CO and subsequent syngas conversion to MeOH, and direct CO₂ electrolysis. The study found production costs 2 - 4 times higher than current market price for the renewable pathways. However, future projections looked favorable for all the technologies under electricity prices below 3 US\$ cents/kWh. A cradle-to-gate life-cycle-analysis on the three alternative routes showed that the electricity needs to be sourced with a CO₂ content below 130 g/kWh to reduce emissions over the conventional route.

Most of the research in waste gasification to produce methanol has focused in the use of refused derived fuel (RDF) and landfill gas (LFG). Salladini et al. (Salladini et al., 2020) evaluated a MeOH production plant using syngas from waste gasification and enriched with green H₂. The hybrid scheme was compared against the waste-to-methanol and direct power-to-methanol processes, based on CO₂ emissions and economic performance. They also included the bio-fraction content of each alternative for the economic evaluation. Their results suggest current waste-to-methanol process is the most economically attractive solution, although future share of renewable energy and decreasing electricity prices will make the hybrid scheme consistently more attractive. The influence of feedstock composition in the production of MeOH from RDF was assessed by Borgogna et al (Borgogna et al., 2019). They modeled the gasification of RDF with different compositions to identify the main parameters affecting syngas production, and subsequently, the effect on yield, energy consumption, and emissions from the overall process. Their model proved satisfactory and they found that the conversion of waste into methanol has higher environmental benefits as opposed to the waste to energy process. The study found the potential for CO₂ reduction can be up to 68% depending on the percentage of renewable energy use. Moreover, their analysis identified RDF's LHV as the most influential parameter to consider in the preliminary design steps. Gao et al. (Gao et al., 2020) compared techno-economic performance indicators between two options of renewable MeOH production from LFG, excluding the syngas pre-treatment process. Both options achieve optimum syngas ratio by either additional H₂ supply or by using a membrane to separate the excess CO₂ from the LFG. The study showed the first option is more energy efficient and environmentally favorable, while the second process has better economic performance.

The literature available on plastic-to-chemical processes is limited and mainly focused in the gasification section. Li et al. (Li et al., 2021) investigated the gas composition of PET gasification in a lab-scale bubbling fluidized bed reactor. Specifically, the authors studied the effect of temperature, steam/fuel ratio, and residence time. The results showed temperature was the most influential parameter in the gas distribution, with higher temperatures achieving better yields of H₂ and CO₂, in the range of 700 - 800 °C. Additionally, they found more than half of the carbon in PET was converted to TARs, an undesired byproduct comprised of a mixture of condensable hydrocarbons. Wilk and Hofbauer (Wilk & Hofbauer, 2013) studied the gasification of several mixtures of plastics in a dual fluidised bed (DFB) pilot reactor. Steam was used as gasifying agent and the combustion chamber was fluidized with air. The heat was transported by using olivine as bed material, and to reach the required gasification temperatures, additional fuel was added to the combustion reactor. The composition of product gas was measured for PE, PP, and mixtures of PE+PET, PE+PS, and PE+PP. The volatile nature of the plastics and the low ash content resulted in virtually no dust and minimum amount of char in the produce gas. The TAR content, on the other hand, was considerably high compared to biomass or coal gasification. Although, in line with concentrations found by other authors. Remarkably, PE and PP showed the highest TAR

concentrations, while the mixture of the two polymers resulted in the lowest of all the samples. The decrease was around 80 - 85%. They concluded that the interactions between the different decomposition products enhanced the TAR reforming reactions. Additionally, they found significant differences in the H_2 and CO yields between pure substances and mixtures. Particularly, higher concentrations were achieved for PE+PS and PE+PP, even though there is no oxygen molecule in either polymer. This suggests that the decomposition products of the mixture of polymers favors the reaction of carbon with steam.

Furthermore, a review of Life Cycle Assessment (LCA) studies in the context of chemical recycling of plastic wastes was conducted by Davidson et al. (Davidson et al., 2021). Their findings showed pyrolysis is the most researched method, even though there is evidence to support the comparative advantages of other technologies such as hydrocracking and gasification. This disproportion in the quantity and quality of data can cause an unintended bias towards pyrolysis technologies. The review also concludes plastic gasification has the advantage of high TRL level. However, the lack of data and limited number of projects in operation makes it difficult to make a proper economic feasibility study. The findings highlight the need for more research into plastics gasification to increase the availability of quality data and enable better technology comparisons.

1.3. Knowledge Gaps

Notwithstanding the extensive literature on methanol production, significant gaps can be found in the design and techno-economic evaluation of alternative renewable routes. First, the literature on waste-to-chemical conversion processes is limited to the use of organic materials. Moreover, studies including the use of plastic feedstock are mostly focused on the gasification step. It is necessary to investigate the effects of the use of plastics as the main source of raw material for the production of methanol (plastic-to-methanol). Second, there is a lack of Key Performance Indicators (KPI) benchmarking between CO_2 hydrogenation and plastic-to-methanol processes. Techno-economic and environmental comparative assessments amongst potential technologies are needed to better understand the trade-offs and help steer future research. Third, there is a lack of research in the effect of purification steps in the overall performance of the different alternatives. For instance, catalysts used for methanol production are very sensitive and require strict levels of contaminants. Therefore, the conditioning of raw materials needs to be included in techno-economic assessments to understand the limitations for scaling the technologies. Lastly, with the growing penetration of renewable energy generation, green H_2 will play an increasingly more important role in the chemical industry. It is of particular interest then to analyze the effect that different sources of H_2 production will have particularly on the economic feasibility of renewable methods for methanol production. This will also provide insight into the main bottlenecks that hinder the large-scale introduction of the technology.

Consequently, given the absence of comparative literature on the aforementioned topics, this study will focus on the evaluation of techno-economic and environmental KPI for the direct CO_2 hydrogenation and plastic-to-methanol processes, using consistent and rigorous simulations. Emphasis will be made in the conditioning steps needed to achieve the high purity levels of raw materials required for the catalytic reactions. Furthermore, different scenarios of H_2 production and their influence on the economic performance of the technologies will be assessed.

1.4. Thesis Aim

The aim of this study is to *assess the competitiveness of the CO_2 hydrogenation and the plastic-to-methanol processes as alternative methods for methanol production, to promote the transition towards a more sustainable chemical industry.* To achieve this, the performance of both technologies is evaluated using techno-economic and environmental key performance indicators. Furthermore, the source of carbon and the impurity content vary depending on the technology. Therefore, purification steps are adapted for the characteristics of each process and included in the assessment.

1.4.1. Specific Objectives of the Thesis

To reach the main goal, the following specific objectives are considered:

- Synthesize and design of the CO₂ hydrogenation and plastic-to-methanol processes.
- Design the purification system required for each synthesis route, depending on the conditions and composition of the carbon source.
- Assess the bottlenecks for both production methods and determine the techno-economic and environmental trade-offs for the use of the different technologies as an alternative to conventional methanol synthesis.

1.5. Thesis Outline

The first step of the research project is to design a methodology to achieve the aim of the thesis. This includes steps considered to address the objectives and the main goal of this study. These are presented in Chapter 2. Afterward, the case studies included in the assessment need to be defined. This is done in Chapter 3, which includes the characterization of the raw materials and an overview of the unit operations selected for each methanol production route. Once the case studies are introduced, the information has to be translated into a process flow diagram and then into a simulation environment. Therefore, the design of the processes and the modeling parameters used in the simulation are provided in Chapter 4. Then, in order to evaluate the qualitative uncertainties of the process models, a pedigree analysis was conducted. The results from this uncertainty assessment are given in Chapter 5. Subsequently, the outcomes of the modeling procedure, including material and energy balances and KPIs calculations are specified in Chapter 6. Next, Chapter 7 illustrates the outcomes of the sensitivity analysis and in the next Chapter, the results from the KPI evaluation and the uncertainty assessments are discussed. This is done in Chapter 8, with the goal to identify bottlenecks and trade-offs between the technologies. Finally, the conclusions of the thesis project are given in Chapter 9.

2

Project Scope and Methodology

In this Chapter, the scope of the research is introduced and described in section 2.1. Subsequently, an overview of the methodology is given in section 2.2, explaining the steps taken to achieve the specific objectives of the thesis. Finally, the selection of the key performance indicators and their formulas are provided in section 2.3.

2.1. Project Scope

The focus of this study lies on the synthesis, design and evaluation of sustainable routes for methanol production. To achieve this goal two process routes were selected as main case studies and a methodology was developed to assess the bottlenecks for both production methods and determine the techno-economic and environmental trade-offs of using each technology as an alternative to conventional methanol synthesis. The comparison is based on a functional unit of 1 kg of methanol for a production plant of 220 kton per year, located in the Port of Rotterdam. A detailed description on the methodology is presented in Section 2.2.

2.2. Methodology

To achieve the main goal of this thesis project, three specific research objectives are formulated. Figure 2.1 depicts the approach and steps taken to reach those objectives. Details on each step are given after the diagram.

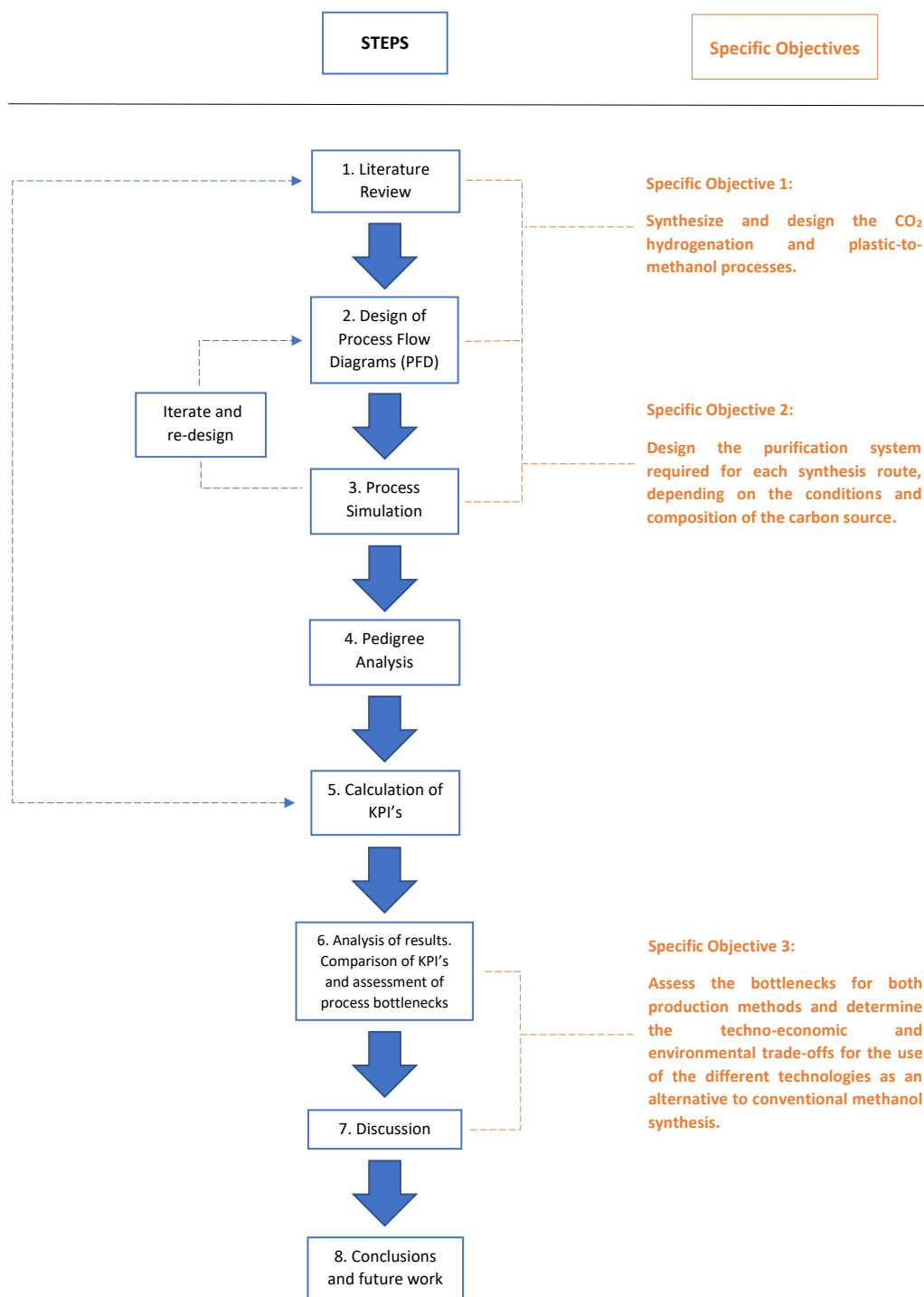


Figure 2.1: Methodology approach for the techno-economic and environmental evaluation of two renewable methanol production routes.

1. **Literature Review:** The first step involves a literature review on the alternative methods for methanol production. The goal is to collect information on feedstock composition and operating conditions of unit operations. Likewise, the amount and type of impurity content of each manufacturing route is identified, depending on the characteristics of the carbon source. This is then contrasted with the target levels required by the catalysts used in methanol synthesis. Subsequently, this information is used as input for the design of the purification units. In addition, to assess the strength of the data gathered from the state of the art, a Pedigree analysis is conducted in step number 4. .
2. **Design of Process Flow Diagram (PFD):** The second step considers the selection of unit operations, operating conditions, and feed stream compositions to design the process flow diagrams of both production routes. Similarly, depending on the impurity levels from the raw materials of each technology, purification units are included. This step sets up the basis for the process modelling.
3. **Process Simulation:** Rigorous simulations of both alternative production routes are performed using Aspen Plus. The software is used to calculate mass and energy balances, and estimate equipment costs using Aspen Process Economic Analyzer (APEA). The inputs for the calculations (unit operations, feed-stream composition, thermodynamic property package, etc) are based on the information gathered in steps 1 and 2. Moreover, for materials or unit operations not available in Aspen, the information is entered via user-defined components. Additionally, iteration between the process design and the simulations is carried out to achieve an optimum set-up.
4. **Pedigree Analysis:** The quality of the data from the state of the art and the simulations is assessed through a Pedigree analysis. To achieve this, two Pedigree workshops are conducted with the help from researchers from TU Delft's Energy Systems and Services Department. Furthermore, the outcomes of the qualitative assessment are used to improve the simulations.
5. **Calculation of KPI's:** In this step, the calculation of the KPIs is performed based on the outcomes from steps 3 and 4. Depending on the metric, these are divided in technical, economic, or environmental indicators. The list of the estimated KPIs for each production pathway is given below:
 - Technical:
 - Mass demand of individual inputs per kg of MeOH produced
 - Overall electricity, heat, and cooling requirements per kg of MeOH produced
 - Raw materials conversion efficiency (η_{CO_2} , η_{CO} , η_{H_2} , η_{carbon})
 - Economic:
 - Capital Expenditure (CAPEX) and Operational Expenditure (OPEX)
 - Net Present Value (NPV)
 - Levelized Cost of MeOH ($LCOMeOH$)
 - Environmental:
 - Carbon footprint (CF)
 - Energy yield ratio (E_y)

Furthermore, the details for the selection of the KPIs and their formulas are given in section 2.3

6. **Analysis of Results. Comparison of KPI's and assessment of process bottlenecks :** In the sixth step, the technical, economic, and environmental KPI's of both production routes are compared against each other and the benchmark. Furthermore, process bottlenecks are identified and the influence of main inputs on the performance of the technologies are assessed through a sensitivity analysis. These results are used to encourage the discussion in step number 7.
7. **Discussion:** The results from steps 4, 5, and 6 are used to find trade-offs between the technologies, as well as to analyze the impacts from the purification requirements.
8. **Conclusions and Future Work:** Finally, conclusions from the study are made based on the methodology, results, and discussion. In addition, recommendations for further research in the field are outlined.

2.3. Key Performance Indicators

To achieve the aim of this thesis, technical, economic, and environmental key performance indicators are selected to assess different dimensions of the technologies. The selection of these KPIs is meant to facilitate the benchmarking between both routes and the conventional process. In addition, the KPIs are used to identify the main bottlenecks from each technology. Furthermore, in order to ensure a common basis of comparison, the list of KPIs is validated with the results from previous techno-economic studies (Nyári et al., 2020; Pérez-Fortes et al., 2016; Szima & Cormos, 2018).

2.3.1. Technical KPIs

Technical KPIs are defined based on the efficiency of the technologies, which is estimated through the consumption of raw materials and the energy requirements. Additionally, the energy demand is divided between electricity, hot utility, and cooling utility. It is important to make this distinction to understand the different sources of energy consumption and identify opportunities for improvement. Particularly, when the utility consumption is compared against the results from other techno-economic studies with heat integration networks.

The raw materials and energy consumption metrics are complemented with the conversion efficiency of key components. This KPI is widely used in research to compare technology performance. It allows to identify limitations in process design, such as the optimum inlet composition to reactors. Moreover, to assess the production routes from different perspectives, two conversion efficiencies are calculated: the overall process efficiencies of hydrogen and carbon, and the conversion efficiencies in the reactor.

Previous literature on the subject has used overall CO_2 conversion as performance metric, instead of measuring the variation in the carbon content (Nyári et al., 2020; Pérez-Fortes et al., 2016; Szima & Cormos, 2018). The decision to change the parameter is founded on two reasons. First, to allow a comparison basis between the CO_2 hydrogenation and the plastic-to-methanol route. Second, the methodology used to calculate the overall CO_2 conversion fails to include every interaction in the process. It is based on estimating the mass flow variation of CO_2 between the inlet and outlet streams (i.e., CO_2 present in the product stream and waste streams) to the plant. However, it does not consider the CO_2 responsible for the production of by-products, such as CO or CH_3OCH_3 . This can lead to an overestimation of the process efficiency. Therefore, the overall carbon conversion is chosen for this study, as a more comprehensive performance indicator.

The equations that determine the technical KPIs are:

$$MD_i = \left(\frac{m_{i-inplant}}{m_{MeOH}} \right) \quad (2.1)$$

$$E_i = \left(\frac{Ut_i}{m_{MeOH}} \right) \quad (2.2)$$

$$\eta_{ireactor} = \left(\frac{m_{i-inreact} - m_{i-outreact}}{m_{i-inreact}} \right) \quad (2.3)$$

$$\eta_{ioverall} = \left(\frac{m_{MeOH} \times M_i \times n_i}{M_{MeOH} \times m_{i-inplant}} \right) \quad (2.4)$$

In which:

- MD_i : Mass demand of individual inputs [kg/kg_{MeOH}]
- $m_{i-inplant}$: Mass flow inlet of component i to the plant [kg/h]
- m_{MeOH} : Mass flow of MeOH in product stream [kg/h]

- E_i : Specific demand of utility i (i : electricity, hot utility, and cooling utility) [kWh/kg_{MeOH}]
- Ut_i : Consumption of utility i [kWh/h]
- $\eta_{ireactor}$: Conversion efficiency of component i in the reactor
- $m_{i-inreact}$: Mass flow inlet of component i to the reactor [kg/h]
- $m_{i-outreact}$: Mass flow outlet of component i to the reactor [kg/h]
- $\eta_{ioverall}$: Overall conversion efficiency of component i in the plant
- M_i : Molar weight of component i [$kg/kmol$]
- n_i : Moles of component i in methanol in the product stream [$kmol/kmol_{MeOH}$]

2.3.2. Economic KPIs

The economic dimension of the technologies is assessed, first, through the calculation of Capital and Operational Expenditures (CAPEX and OPEX). For each technology, the breakdown of CAPEX and OPEX is determined to identify the items with greater influence on the overall cost. Likewise, the results can be used to compare the studied technologies against the benchmark.

The methodology used for calculating the CAPEX was based on the factorial method from (Towler & Sinnott, 2013), reported in the work of (Pérez-Fortes et al., 2016). CAPEX is deconstructed in the sum of the Total Fixed Capital Cost (TFCC) and the Working Capital. TFCC includes Inside Battery Limits capital costs (ISBL), Offsite Battery Limits capital costs (OSBL), engineering costs, and contingency. A description of the items that make up CAPEX and OPEX is provided in table 2.1.

In addition, the case studies are also evaluated from an investor point of view, to assess the economic feasibility of implementing either technology. To achieve this, Net Present Value (NPV) and Levelized Cost of MeOH ($LCOMeOH$) are used as metric. NPV is a strong indicator that incorporates the yearly cash-flows, the project's discount rate, and its lifetime into the economic evaluation. While the $LCOMeOH$ allows for an easy comparison into the feasibility of the manufacturing technologies against the benchmark. The formulas for the calculations of these KPIs are provided in equations 2.7 and 2.8.

To estimate these economic indicators, the following assumptions are used (based on (Nyári et al., 2020; Pérez-Fortes et al., 2016; Towler & Sinnott, 2013)):

- The project is assessed for a lifetime of 25 years.
- Capital expenses are divided in three years prior to the start of operations: 30% in year 1, 60% in year 2, and 10% in year 3.
- No taxes or depreciation are considered. This decision is made to allow the comparison with previous techno-economic assessments on the same basis.
- Revenues start in year 3. Additionally, only 30% and 70% of revenues are considered for years 3 and 4. From year 5 onward, 100% of revenues are expected.
- Prices of raw materials, utilities, and products are constant during the 25 years. The details of the prices used for the calculations can be found in Table D.1 in Appendix D.
- A real discount rate of 8% is used.

Table 2.1: Breakdown of CAPEX and OPEX calculation (Pérez-Fortes et al., 2016)

Economic Parameter	Item	Description	Source
CAPEX	Total Fixed Capital Cost (TFCC)		
	ISBL capital costs	Purchased equipment costs, erection of equipment, piping, insulation, instrumentation and control, electrical system, civil works and site preparation	APEA
	OSBL capital costs	Investment needed for the modification of site infrastructure	35% of ISBL
	Engineering costs	Costs associated with detailed engineering, costs and civil engineering, administrative charges, project management, contractors, etc	20% of ISBL and OSBL
	Contingency	To account for errors in the estimated budget	30% of ISBL and OSBL
		Working Capital	
OPEX	Variable Costs of Production (VCP)		
	Raw materials costs	Depending on the consumption from each case study	Mass balance and market prices
	Catalyst consumption	Consumption of catalyst in the MeOH reactor	(Nyári et al., 2020)
	Utility consumption	Electricity, hot utility, and cooling utility requirements	Energy balance and market prices
	Fixed Costs of Production (FCP)		
	Salaries	40000 €/year per operator. 5 operators working in 3 shift rotations	
	Supervision	Cost of supervision staff	25% of salaries
	Overheads	Charges for corporate overhead functions	45% of salaries and supervision
	Maintenance		3% of ISBL
	Interests		6% of Working Capital

Economic KPIs:

$$CAPEX = TFCC + WorkingCapital \quad (2.5)$$

$$OPEX = VCP + FCP \quad (2.6)$$

$$NPV = \left(\sum_{n=1}^{n=t} \frac{CF_n}{(1+i)^n} \right) \quad (2.7)$$

$$LCOMeOH = \left(\frac{NPV_{costs}}{\sum_{n=1}^{n=t} \frac{M_{MeOH}}{(1+i)^n}} \right) \quad (2.8)$$

In which:

- CF_n : Cash flow in year n [m€/year]
- t : Lifetime of the project in years
- i : Discount rate
- NPV_{costs} : Net Present Value of total costs over lifetime [€]
- M_{MeOH} : Yearly production of methanol [kg]

2.3.3. Environmental KPIs:

Finally, the environmental performance of each route is evaluated by means of two parameters. First, the technologies are assessed by their carbon footprint (CF), which includes direct emissions from the manufacturing process and indirect emissions from the energy consumption. To calculate the indirect emissions, the carbon content of utilities is used (Table 2.2). The motivation for doing research in renewable alternatives for methanol production is to reduce the CO_2 emissions. Which underscores the importance of understanding whether or not the alternative processes have a positive impact versus the conventional route, in terms of GHG emissions. However, it is worth mentioning that the assessment is made from a gate-to-gate perspective. Thus, the emissions from the production and supply of the raw materials, as well as the end of life treatment of the product, are not accounted for. A more detailed description of the boundaries of the systems can be found in Chapter 3.

Table 2.2: Carbon content in utilities

Utility	Carbon content ($kgCO_2/kWh$)	Reference
Electricity	0.390	Average value for the Netherlands in 2019 (European Environment Agency, 2019)
Low pressure steam	0.237	Aspen Plus
High pressure steam	0.237	Aspen Plus
High temperature needs	0.237	Aspen Plus
Cooling water	0	Aspen Plus
Chilling water	0	Aspen Plus
Refrigerant	0.201	Aspen Plus

Second, energy analysis can be used to determine the sustainability of the system and compare efficiency losses between technologies. This category is assessed by calculating the Energy Yield Ratio (E_y), which is a measure of the ratio between the energy provided to the system and the energy content in the product stream. The equations used to estimate the environmental KPIs are described below:

$$CF = \left(\frac{m_{CO_2-in} - m_{CO_2-out} - m_{CO_2-indirect}}{m_{MeOH}} \right) \quad (2.9)$$

$$E_y = \left(\frac{LHV_{MeOH} \times m_{MeOH}}{m_x \times LHV_x + E_{hu} + E_{el}} \right) \quad (2.10)$$

$$(2.11)$$

In which:

- m_{CO_2-in} : CO_2 mass flow inlet to the plant [kg/h]

- m_{CO_2-out} : CO_2 mass flow outlet from the process, in product streams and waste streams [kg/h]
- $m_{CO_2-indirect}$: CO_2 emissions from utility consumption [kg/h]
- m_{MeOH} : $MeOH$ mass flow outlet from the process [kg/h]
- LHV_{MeOH} : Low heating value of $MeOH$ [kWh/kg]
- m_x : Mass flow inlet of H_2 or plastics, depending on the case study [kg/h]
- LHV_x : Low heating value of H_2 or plastics, depending on the case study [kWh/kg]
- E_{nu} : Hot utility consumption [kWh/h]
- E_{el} : Electricity consumption in [kWh/h]

3

Case Studies

Chapter 3 provides an overview of the case studies used for the techno-economic and environmental assessment. First, section 3.1 introduces the main raw materials and their specifications. Then, the case studies based on the CO_2 hydrogenation and the plastic-to-methanol routes are presented in sections 3.2 and 3.3, respectively.

3.1. Raw Materials

The inlet gas to the methanol reactor has to meet strict levels of impurities to ensure the optimum operation of the catalyst. Otherwise, catalyst deactivation can affect the performance of the process by reducing the available area for activity. More importantly, the introduction of contaminants can have a negative effect on methanol selectivity (Twigg & Spencer, 2003). For example, chloride poisoning can block catalyst sites, accelerate the damage from other species such as H_2S , or react with the Zn present in the catalyst and cause sintering problems. Similarly, sulfur compounds can reduce the lifetime of the catalyst by reacting with copper to produce Cu_2S . This was improved with the large scale implementation of desulfurisation technologies and the introduction of Zn to the Cu-based catalyst (Twigg & Spencer, 2003). Nonetheless, the high sensitivity to sulfur content requires low levels of the contaminant at the feed (Kung, 1992).

Several studies, particularly in the applications of syngas from biomass, agree on the maximum limit permissible of impurities to avoid damage to the catalysts used for methanol synthesis (Abdoulmoumine et al., 2015; Block et al., 2019; Woolcock & Brown, 2013). These include the presence of sulfur and nitrogen compounds, halides, and TARs. All of which must be present in concentrations at least below $1\text{ mg}/Nm^2$. Table 3.1 shows the contaminant target levels sourced from the literature review and used as basis for the design of the purification units.

Table 3.1: Contaminant target levels for methanol synthesis in mg/Nm^3 (Abdoulmoumine et al., 2015; Block et al., 2019; Woolcock & Brown, 2013)

Impurity	Target level
TARS	< 0.1 - 1
Sulfur compounds	< 1
Nitrogen compounds	< 0.1
Halides	< 0.1

Taking into account the requirements for contaminant levels, the source of the raw materials becomes an important aspect for the assessment. Depending on the composition, different purification units have to be included and the effect on the overall performance of the technology can vary. Therefore, the first step in the design of the case studies is determining the source and conditions of the feedstock.

3.1.1. Carbon Dioxide

The assessment of the methanol plant is based in the Port of Rotterdam, thus, it can benefit from process integration with other industries. In the Port, there is a project for building a CCS network called Porthos, scheduled to start operations in 2024 (European Commission, 2020). The goal of the project is to capture 5 $MtCO_2/yr$ during the first phase, with the option to increase the capacity to 10 $MtCO_2/yr$, and store it in a geological site under the sea. To achieve this, Porthos will be sourced primarily by the refineries and chemical industries in the area (IOGP & European Commission, 2019). This concentration of high emitting sources improves the business cases of capture technologies, which under current conditions exceed the incentives to decrease emissions from the Emissions Trading System (ETS). This is accomplished by creating an industrial network that benefits from economies of scale and the shared use of transport infrastructure. Therefore, the CO_2 used for the CO_2 hydrogenation case study is assumed to be sourced from industries, specifically from the Porthos infrastructure.

A CO_2 transport network from industrial sources must meet a series of technical conditions, such as the operating temperature and pressure range or the maximum levels of pollutants. However, these targets for impurity content can be orders of magnitude higher than the limits required for methanol synthesis. Consequently, the importance of contaminants and their role in the process must be taken into account.

The waste gases generated from industrial process can contain a number of impurities, such as H_2S , SO_2 , NO_x , CS_2 , and others. Nonetheless, most of them are regulated and have to meet the maximum permissible levels imposed by the EU emissions standards (Harkin, Filby, et al., 2017). Likewise, the implementation of a shared pipeline infrastructure comes by the hand of setting minimum conditions to join in the network. In this context, the specification for the CO_2 was based on the results from the CarbonNet project (Harkin, Sick, et al., 2017). This study was chosen for two main reasons: i) it has similar characteristics to the Porthos project. For instance, it also considers a CCS hub-based network with a capacity of 5 $MtCO_2/yr$ to be stored at a geological site beneath the sea; ii) the methodology used to calculate the optimum CO_2 pipeline conditions can be replicated to address the goal of Porthos. In this sense, the study aims to minimize the whole project's CCS costs and to encourage potential sources to invest in carbon capture technologies and connect to the network.

Table 3.2 shows the composition and conditions for the CO_2 . The specification considers constraints from CO_2 capture technologies, as well as limitations imposed by pipeline materials and hydraulics, health and safety regulations, geological storage conditions, and commercial implications (Harkin, Sick, et al., 2017). All of these aspects are taken into consideration to define the contaminant levels in the feedstock stream. Based on these levels of impurities, the CO_2 purification system is designed to achieve the optimum conditions for the catalyst in the methanol reactor. Furthermore, a temperature of 15 °C and a pressure of 100 bar is considered to allow the CO_2 to stay in a dense phase through the whole length of the network.

3.1.2. Hydrogen

To produce methanol from CO_2 , additional hydrogen needs to be supplied to the process. Nowadays, there are several technologies for the manufacturing of hydrogen, including coal or biomass gasification, anaerobic digestion & dark fermentation, steam methane reforming (SMR), or water electrolysis. However, only coal gasification, SMR and water electrolysis are at TRL of commercial application and can be expected to source an industrial-scale methanol plant (Rijk & Van Dinther, 2019). Moreover, SMR is the dominating technology in the market with the lowest production costs. Therefore, considering the best economic alternative and to ensure a continuous supply of raw material, hydrogen is assumed to be sourced from a SMR plant for the CO_2 hydrogenation case study.

The condition and composition of the feedstock are based on a hydrogen production model for a central natural gas plant without CCS (NREL, 2018). According to the results from this model, the purity of the H_2 outlet is above 99.5%, with minor traces of CO_2 and N_2 . However, to simplify the assessment and considering these low levels of CO_2 and N_2 won't influence the operation of the methanol catalyst,

Table 3.2: Composition of the CO_2 feedstock for the CO_2 hydrogenation case study. Based on (Harkin, Sick, et al., 2017)

Component	Units	Value
Temperature	°C	15
Pressure	bar	100
CO_2	vol.%	95
CO	ppmv	2000
H_2O	ppmv	100
Ar	vol.%	4.08
NO	ppmv	900
NO_2	ppmv	100
SO_2	ppmv	1000
H_2S	ppmv	100

*The share of NO/NO_2 was defined as 9:1 (De Jong & Van Ommen, 2014)

the purity of the grey H_2 is assumed to be 100%. Furthermore, a temperature of 80 °C and 30 bars was considered at the inlet of the CO_2 hydrogenation process. These are determined based on the temperature and pressure of H_2 produced in a SMR plant and pipeline transport conditions (NREL, 2018; Takahashi, 2009).

The environmental benefits of alternative supply of green H_2 can become economically feasible in the short to medium term. Therefore, two sensitivity analysis are included for the CO_2 hydrogenation route, considering renewable source of hydrogen. These are discussed in more detail in section 7.2: Alternative Hydrogen Supply for the CO_2 Hydrogenation Route.

3.1.3. Plastics

Table 3.3: Specification for the plastic feedstock

Component	Units ¹	Value
Proximate analysis		
Moisture content	wt% (ar)	10
Ash content	wt% (dry)	4.40
Volatile content	wt% (dry)	95.6
Ultimate analysis		
Carbon	wt% (daf)	84.84
Hydrogen	wt% (daf)	13.95
Nitrogen	wt% (daf)	0.12
Halides ²	wt% (daf)	0.22
Sulphur	wt% (daf)	0.01
Oxygen	wt% (daf)	0.87

¹ar: as received, including ash and moisture; dry: weight percentage from dry material, including ash; daf: dry and ash free.

²The content of halides was assumed to be 100% Chlorine (TNO, n.d.)

For the plastic-to-methanol route, the plastic share of the Municipal Solid Wastes from the Netherlands is considered. There are several kinds of materials present in plastic waste streams, such as polyethylene, polypropylene, polystyrene, or polyethylene terephthalate. The gasification of each one produces a synthesis gas with different characteristics. Moreover, the combination of these plastic materials can alter the results and generate a syngas with completely different composition, including the H_2/CO ratio and the level of contaminants (Wilk & Hofbauer, 2013). Both important parameters for the catalytic conversion of syngas to methanol. Therefore, it is important to define the composition and physico-chemical properties of the feedstock before conducting a techno-economic assessment. Furthermore,

because the project is based in the Netherlands, TNO's Phyllis database is used as source to define the properties of the raw material. In particular, the plastic fraction from the MSW of the Netherlands is chosen (TNO, n.d.). Additionally, it is assumed that the raw material is already sorted and ready to enter the gasifier with the composition defined. Table 3.3 presents the proximate and ultimate analysis of the plastics considered in the process model.

Although the physico-chemical composition of the feedstock is known, information on the share of bio-wastes or the types of plastics is unavailable. This limits the depth of the assessment, particularly when analysing the environmental impact. Nonetheless, the proximate and ultimate composition are sufficient to model the produced syngas from the gasification process.

3.2. Case Study 1: CO_2 hydrogenation route

The methanol production from the CO_2 hydrogenation route is divided in two plants: the CO_2 purification system and the CO_2 hydrogenation. Moreover, the boundaries of the assessment are consistent with an R&D perspective for studies of substitute products, i.e., from gate-to-gate (Zimmermann et al., 2020). Figure 3.1 shows a simplified block diagram of the process with its main elements, inputs, outputs, and system boundaries.

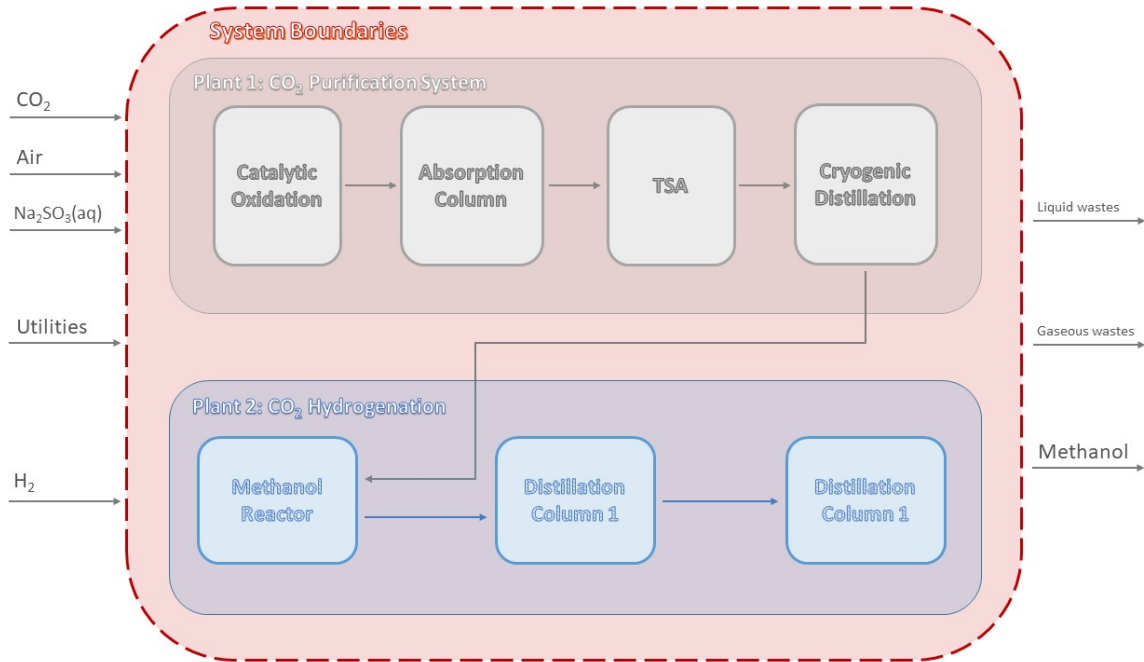


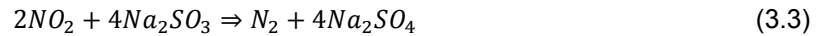
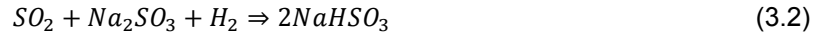
Figure 3.1: Simplified block diagram with the system boundaries of case study 1: CO_2 hydrogenation

The process starts with CO_2 sourced from a CCS network with a 95 vol.% purity. Thus, before entering the methanol reactor, the impurities must be reduced to safe levels for the operation of the catalyst. To achieve this, a CO_2 purification system is designed based on the process from (Heim & Gupta, 1999). First, the H_2S is converted to SO_2 in a catalytic oxidation unit, according to equation 3.1:



In the second step, both SO_2 and NO_2 are removed in an absorption column using an aqueous solution of Na_2SO_3 . The reactions between the impurities and scrubbing solution are given in equations 3.2 and

3.3. Next, the CO_2 stream is sent to a Temperature Swing Adsorption system to remove the moisture content. Finally, the rest of non-condensable gases, such as Ar , CH_4 , NO , and N_2 are separated in a cryogenic distillation column. The waste gases leave from the top, while CO_2 is produced at the bottom with a 99.99 wt% purity. The product stream is then compressed to pipeline transport conditions and sent to the CO_2 hydrogenation plant.



In the second plant, the carbon dioxide is mixed with hydrogen to produce the methanol product. The raw materials are first conditioned to the right pressure and then heated to achieve the optimum conditions for methanol synthesis. The inlet flow of hydrogen is also defined to match the stoichiometric requirements (defined in equation 1.4). After the reactor, the products are cooled down to separate the unreacted gases from the liquid methanol stream. A small fraction of the gases are purged and the rest is re-compressed and recycled back to the reactor. The liquid stream is expanded to remove the rest of unreacted gases, before entering the first distillation column. This step is designed to remove the majority of the water. Finally, a second distillation tower is used to achieve a chemical-grade methanol of 99.9 wt% purity.

A more detailed explanation of the two plants is given in Chapter 4: Process Design and Modeling.

3.3. Case Study 2: Plastic-to-Methanol route

The plastic-to-methanol route consists of one plant that can be divided in two main sections. The first comprises the stages of gasification and conditioning of the synthesis gas, and the second consists of the methanol synthesis. A block diagram with the main operations, inputs, outputs, and system boundaries is depicted in Figure 3.2

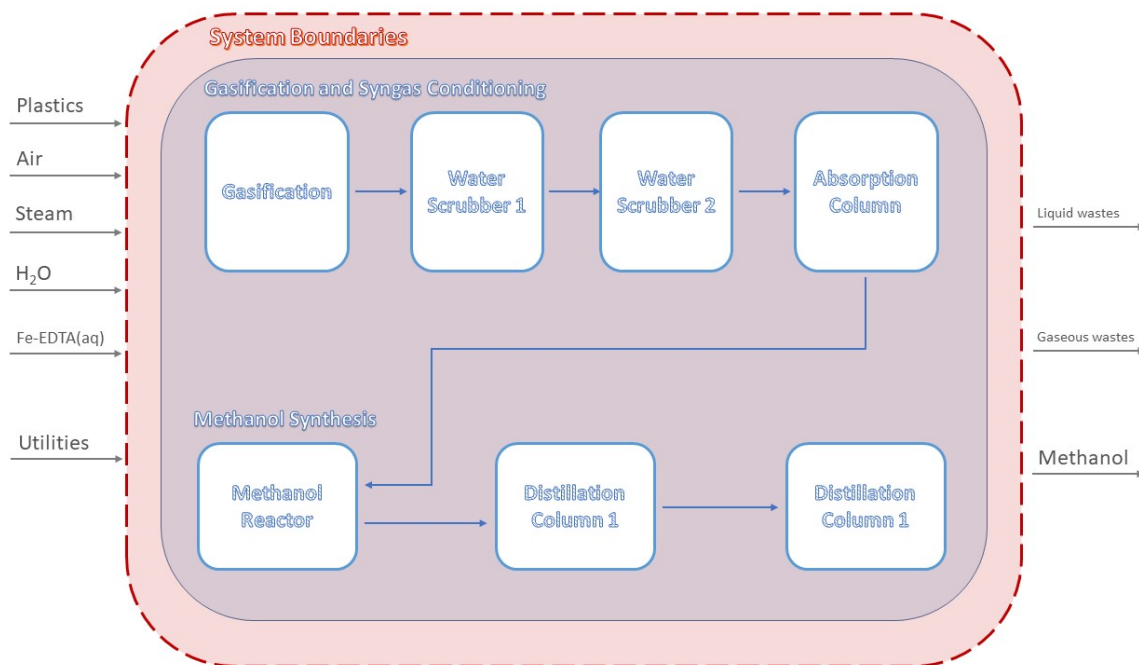
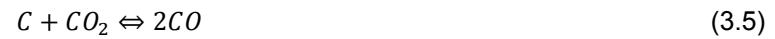


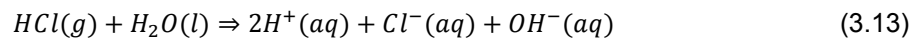
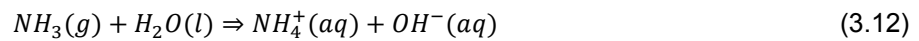
Figure 3.2: Simplified block diagram with the system boundaries of case study 2: plastic-to-methanol

The plant starts with the gasification unit, using plastic wastes as feedstock. These plastic materials react with a gasifying agent at high temperature to produce synthesis gas and some impurities. These

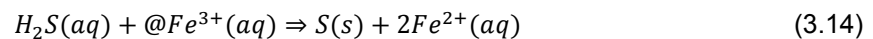
last ones depend on the elemental composition of the raw material, and in this case consist of TARs, NH_3 , HCl , and H_2S . Moreover, in order to generate the right share of H_2 , CO , and CO_2 , a mixture of air and steam is used as gasifying agent. A summary of the main gasification reactions is provided below:



The heat to drive the gasification is generated in the combustion chamber of the gasifier by burning the unreacted char and additional natural gas. To transport the heat from the combustion to the gasifier, sand is used as bed material. Afterward, the produce gas is sent to three cleaning stages to remove the contaminants. The first unit is a water quench designed to reduce the temperature and remove condensed TARs, NH_3 , and HCl . Equations 3.14 and 3.13 describe the interactions in the scrubber between water and the polar impurities:



The second unit is a subsequent water scrubber used to eliminate the remaining NH_3 from the gas stream. Then, a third absorption column removes the H_2S using an aqueous iron-chelate solution. In this third purification unit, the Fe^{3+} irons in the solvent interact with H_2S to form elemental sulfur according to the following reaction:



Next, the clean syngas is sent to a 4-stage compression train to achieve the 50 bars required for the methanol synthesis. Additionally, the temperature is increase to 230 °C before entering the reactor. The process then has the same set-up as the CO_2 hydrogenation route, without the addition of hydrogen. The products from the reactor are cooled down and expanded. The majority of unreacted gases are recycled back, re-compressed, and mixed with the inlet stream. While the liquid raw methanol is sent to two distillation columns to separate the remaining water and gases to achieve chemical-grade methanol.

More details on the design of the plastic-to-methanol process is provided in Chapter 4: Process Design and Modeling.

4

Process Design and Modeling

The process design and the assumptions for the simulation of the case studies previously defined in sections 3.2 and 3.3 are given in this Chapter. Section 4.1 introduces the process flow diagram, the design details, and the simulation characteristics of the CO_2 purification system. Next, section 4.2 does the same for the CO_2 hydrogenation plant. Finally, the detailed description of the plastic-to-methanol route and the simulation assumptions are provided in section 4.3.

Process design is a key step to the assessment of the technologies. It includes the selection and sequence of unit operations to achieve the desired outcomes, as well as the choice of operating conditions, such as temperature and pressure. Depending on these decisions, the results from the process model can be greatly affected. Moreover, the uncertainty of the model is increased with lower levels of confidence in the data used for the decision making. Therefore, the design of the alternative methanol production routes is based on previous research studies and patented systems. Likewise, the selection of unit operations is focused on high TRL processes.

After the layout and conditions of the unit operations are defined, the process is translated into a simulation environment. Process modeling allows to replicate chemical operations without the need of conducting expensive industrial or laboratory scale experiments. In this research study, Aspen Plus V8.8 is used as process simulation tool to calculate the mass and energy balances. The software is widely-used in research and industry because of its modeling potentials and flexibility. Particularly, Aspen has the advantage of having a vast number of libraries of predetermined unit operation models and chemical properties, which simplify the modeling procedure. Furthermore, the total installation costs of the unit operations is estimated using Aspen Process Economic Analyzer (APEA). APEA is a build-in cost estimating software that generates Capital and Operating costs based on the process design. However, APEA is only used in the Capital Cost calculations. The operating expenditures associated to the raw materials and utility consumption are estimated separately based on the mass and energy balances and defined market prices.

Property Methods

The most important decision when designing the simulation is the selection of the property method. This determines the parameters used to calculate the interaction of materials in the unit operations. Therefore, it has a major impact in the outcomes of the process models. Moreover, there are different types of thermodynamic property methods available in commonly used simulators, such as Aspen Plus. These can be divided in Equation-of-State Models, Activity Coefficient Models, and Specially Customized Models. Each one with its own assumptions, advantages, and practical limitations, depending on the application.

The thermodynamic property models chosen for the simulations are based on the characteristics of the processes (temperatures, pressures, chemical compounds) and previous research. Table 4.1 gives a summary of the property methods selected for each process:

Table 4.1: Property methods used in the simulations

Process	Property Method	Reference
CO_2 Purification System	RKS-BM	(Aspen Plus, 2001)
Absorption Column in CO_2 Purification System (CDP-T01)	ELECNRTL	(Aspen Plus, 2001)
CO_2 hydrogenation	RK-Soave	(Kiss et al., 2016)
Distillation columns in CO_2 hydrogenation (MEOH-T01, MEOH-T02)	NRTL-RK	(Aspen Plus, 2001)
Gasification and syngas conditioning	PR-BM	(Mutlu & Zeng, 2020; Puig-Gamero et al., 2018)
Methanol Synthesis	RK-Soave	(Kiss et al., 2016)
Distillation columns in plastic-to-methanol (PTC-T04, PTC-T05)	NRTL-RK	(Aspen Plus, 2001)

4.1. CO_2 Purification System

4.1.1. Process Design

The process flow diagram of the CO_2 purification system is depicted in Figure 4.1. In addition, the design characteristics of the process and the assumptions for the simulation are discussed in the following paragraphs.

As mentioned in Section 3.2, the purification system starts with a catalytic oxidation unit (CDP-R1). This step is designed to convert the H_2S from the CO_2 feed stream into SO_2 , a compound that is more easily removed by absorption methods. Another alternative is to treat both sulfur compounds separately. In fact, H_2S can be removed using solvent-based techniques with amines, selexol, or methanol (Adams et al., 2014), as well as through the use of metal oxides (Marcantonio et al., 2020). Likewise, SO_2 is commonly removed using wet flue gas desulfurization technologies, such as limestone or dual-alkali FGD systems (Córdoba, 2015). However, the methods to treat H_2S are generally expensive and, more importantly, the SO_2 can be removed simultaneously with NO_2 to reduce the number of unit operations. Therefore, a combined treatment of H_2S oxidation to SO_2 with a subsequent scrubbing unit is chosen.

First, the CO_2 stream is mixed with oxygen in the presence of a sulfur tolerant catalyst at 22 bar and 400 °C (Dalrymple, 2014; Heim & Gupta, 1999; Karpuk, 2003). This catalyst is platinum based and can withstand the concentration of sulfur species and other impurities from the gas stream (Karpuk, 2003). To reach the conditions of the unit operation, liquid CO_2 is expanded from 100 to 22 bar using two turbines (CDP-C01, CDP-C02) and two heaters (CDP-E01, CDP-E02). Air on the other hand, is compressed from atmospheric pressure to 22 bar using a 2-stage compressor with inter-cooling (CDP-C03). Both streams are mixed in stoichiometric ratio ($O_2:H_2S = 1.5:1.0$) to produce SO_2 and H_2O . These conditions of pressure, temperature, and inlet flow promote the oxidation of H_2S over other reactions, such as the oxidation of CH_4 (Dalrymple, 2014; Heim & Gupta, 1999).

In the second step, sulfur dioxide and nitrogen dioxide are simultaneously removed in an absorption tower operating at 22 bar (CDP-T01) (Heim & Gupta, 1999). To do this, the product stream leaving the oxidation reactor is cooled down to 38 °C and brought into contact with an aqueous solution of Na_2SO_3 . The solvent reacts with sulfur dioxide to form bisulfite (Bezuidenhout et al., 2012; Chang et al., 2004), which can then be regenerated using caustic soda in an additional step. This regeneration system is outside the scope of the study, however, a description of the process is provided in Appendix B.1. Simultaneously, nitrogen dioxide reacts to form sodium sulfate and nitrogen gas (Chang et al., 2004). The concentration and inlet flow of the solvent are defined based on data found in the literature. Accordingly, a concentration of 0.25 mol/L and a G/L volumetric flow ratio of 167 is used (Chen et al., 2002; Sun et al., 2019).

After the CO_2 stream -free of H_2S , SO_2 , and NO_2 - leaves from the top of the scrubbing tower, it is again cooled down to 38 °C and water is flashed before it enters the TSA system. TSA is a commonly used technology when high levels of dehydration are required. With superior moisture separation rates than other solvent-based processes such as treatment with Triethylene Glycol (TEG) (Terrigeol, 2012). This technology uses adsorbent materials to retain the water molecules, which are then regenerated by a temperature increase. The preferred desiccants used in industry are silica gel, activated alumina, and molecular sieves (Nastaj & Ambrozek, 2015), however, the latter are the best qualified material when extremely low dew points are required, such as in cryogenic distillation (Terrigeol, 2012). Moreover, the type 3A zeolites are commonly used in the drying of gas streams. Thus, the TSA columns in the CO_2 purification system are filled with 3A Molecular Sieves. In addition, the columns work in cycles of 8 hours, divided between adsorption and regeneration mode (Ikechukwu, 2017). Adsorption is carried out in the first column (tower A - CDP-AD1) at 38 °C and 22 bar. Wet CO_2 enters in downward flow with approximately 0.3 mol% water and exit with a water content below 10 ppm (Heim & Gupta, 1999; Ikechukwu, 2017). In parallel, regeneration is conducted in the second column (tower B - CDP-AD2) at high temperature. To achieve this, a portion of the product stream (approx. 10% - 20%) is recycled and heated to 288 °C. The recycle ratio and regeneration temperature are determined based on the guidelines from the Gass Processors Suppliers Association (GPSA, 2004). During regeneration, water is desorbed and carried over by the recycled stream flowing in upward direction. The wet gas is then cooled down (CDP-E06), water is removed in a flash drum (CDP-D02), and the stream is recycled back to the inlet of the adsorption column (tower A). After 4.5 hours, the regeneration cycle is completed. Then the gas stream flows continuously through the second column (tower B) without heating (i.e., at 38 °C) to cool down the bed material before the next adsorption cycle. Once the bed material in tower A is saturated, the operation of the columns is switched. In this way, the system can operate uninterrupted.

The final contaminants are removed in a distillation tower working under cryogenic conditions (CDP-T02). Non-condensable gases (Ar , N_2 , NO , CO and traces of O_2) leave from the top at a temperature below -100 °C. While liquid CO_2 exits from the bottom at -17 °C and a purity level of 99.99 wt% (Xu et al., 2014). On the one hand, the gases are released to the atmosphere, with Ar accounting for 89 wt% of the waste stream. On the other hand, the CO_2 is compressed and cooled to conditions suited for pipeline transportation. Thus, a final pressure of 75 bar and a temperature of 15 °C is defined (IPCC, 2005), assuming the supply of CO_2 is required within the same industrial hub.

4.1.2. Process Modeling

The flowsheet of the simulation is attached in Appendix C.1. The details and assumption used for the modeling of the CO_2 purification system are provided below:

- CO_2 is expanded from 100 to 22 bar using two turbines and two heaters. The first turbine is defined with a pressure ratio of 0.385 while the second one delivers the gas to the required pressure. The heaters were designed to supply the same amount of heat, with the condition of producing a final gas temperature of 200 °C.
- Air is compressed in 2 stages from 1.02 to 22.4 bar. Intercooling between stages is set at 40 °C to use cooling water as utility, and the second heater is designed to supply air at 110 °C, in accordance with the simulation guidelines from (Ramirez-Ramirez, 2019).

- The catalytic oxidation (CDP-R1) is modelled as an equilibrium reactor (REquil) at constant conditions of 400 °C and 21.6 bar (Sadighi, Sepehr and Seif, 2018). The oxidation reaction of hydrogen sulfide is specified with a temperature approach of 0 °C and the air inlet is determined to deliver 1.5 mol O_2 per mol of H_2S (Dalrymple, 2014).
- The absorption tower (CDP-T1) is modeled using a RadFrac column with 4 stages and considering only sodium sulfite in the aqueous solvent. This is a simplification of the actual dual-alkali FGD process, which involves the presence of more components, such as $CaCO_3$ or $NaOH$. However, research indicates Na_2SO_3 is the material that plays the major role and the one present in the larger concentration (VanNess et al., 1979). The rest of the unaccounted compounds are used in the regeneration steps.
- The first adsorption tower (CDP-AD1) is modeled as a separator block. The water content in the outlet stream is specified at 10 ppm based on information from the literature review (Heim & Gupta, 1999; Ikechukwu, 2017). Additionally, a 0.2 bar pressure drop is inputted in the flash options, according to common operating conditions. On the other hand, the regeneration column is modeled using a mixer (CDP-AD2) to simulate the water removed from the hot recycle stream (RS-CO2-2). These assumptions are used to estimate the mass and energy balances. However, for the economic evaluation, the equipment is inputted as an adsorption system.
- The distillation tower is modeled as a RadFrac column. But first, the DSTWU option is used to determine preliminary results. The calculation is conducted specifying N_2 as light key component with a recovery in the distillate of 99.99%. While CO_2 is specified as heavy key component with a recovery of 0.1% in the distillate. The results find that the column has 12 stages, a partial-Vapor condenser, kettle reboiler, a distillate to feed ratio of 0.05, and a reflux ratio of 22 (consistent with literature, (Murra, 2014)).

4.2. CO_2 Hydrogenation

4.2.1. Process Design

Figure 4.2 shows the process flow diagram for the CO_2 hydrogenation plant. This design is based on previous studies by (Kiss et al., 2016; Nyári et al., 2020), who also worked on the design of methanol production processes from CO_2 hydrogenation. However, while both studies considered an operating pressure of 50 bar for the methanol reactor, they assumed slightly different temperatures. Nyári et al., designed the reactor at 230 °C, while Kiss et al., used an operating temperature of 250 °C. Since the process model of this work resembles more that of Nyári et al., the temperature and pressure were defined following their set-up. Moreover, the reaction is supported by a commercially available Cu/Zn/Al/Zr catalyst. This choice of catalyst is made based on the existing data to simulate the kinetic model. Furthermore, in addition to the main reactions previously described in equations 1.1, 1.2, and 1.3, the production of Dimethyl Ether is included as by-product:



As already highlighted, extremely low levels of impurities are needed for the safe operation of the catalyst in the methanol reactor. Therefore, carbon dioxide is supplied from the CO_2 purification system with a purity level above 99.99 wt%, at 13 °C and 75 bar. Likewise, 100% pure hydrogen is assumed to be supplied from a SMR plant and delivered at the CO_2 hydrogenation plant at 30 bar and 80 °C. Then, to achieve the optimum inlet conditions both feedstock streams are compressed (MEOH-C01, MEOH-C-02) and heated (MEOH-E02, MEOH-E03) before entering the catalytic reactor. In addition, the stoichiometric ratio (eq. 1.4) is manipulated by adjusting the mass flow of the hydrogen stream.

After exiting the reactor, the outlet stream is cooled down to 30 °C (MEOH-E04) and sent to a flash drum to separate the denser products (consisting mainly of methanol and water) from the rest of the unreacted gases. The liquid stream from the unit is expanded to 1.02 bar to remove the majority of remaining unreacted gases in a second flash drum (MEOH-D02). On the other hand, the gas phase is compressed to 50 bar (MEOH-C03) and recycled back to mix with the inlet stream. However, before entering the compressor, 0.25% of this stream is purged to prevent inerts build-up. This value is higher than the one used by Nyári et al., 2020, because the study did not take into account impurities in the feedstock. Otherwise, some of the contaminants present in the recycling loop would exceed the maximum permissible concentrations.

The liquid methanol stream needs further treatment to achieve chemical-grade classification (i.e., 99.9 wt% purity). Thus, water, by-products, and unreacted gases still present are removed in a 2-step distillation process. From the flash drum, the liquid outlet is heated to 87 °C before entering the first tower. In this unit, 96 wt% pure methanol exits from the top at 67 °C, while virtually pure water exits the bottom at a temperature of 100 °C. The top product from the first tower then enters the second distillation column. The bottom outlet from this second column, consisting mainly of methanol and some water, is recycled back to the first unit. While the overhead stream is separated in a partial vapor-liquid condenser. Thus, the remaining gases are removed in the vapor phase to achieve a liquid methanol product of 99.9 wt% purity. Finally, the product stream is cooled down to 40 °C, ready to be transported and used for downstream chemical processes (e.g., production of MTBE or Formaldehyde).

4.2.2. Process Modeling

The Aspen flowsheet for the simulation of the CO₂ hydrogenation process is attached in Appendix C.2. The details and assumption used in the simulation are provided below:

Table 4.2: Design parameters of the Plug-flow reactor and catalyst (Nyári et al., 2020)

Parameter	Value
Number of tubes	810
Length (m)	6
Diameter (m)	0.06
Catalyst Density (kg/m^3)	1500
Bed voidage	0.68

- The methanol reactor (MEOH-R01) is modeled as an isothermal RPlug reactor (PFR). The heat generated from the exothermic reactions is removed using cooling water. However, this heat can also be used to generate high pressure steam and produce electricity (Szima & Cormos, 2018). This analysis, nonetheless, was not included in the assessment.
- The LHHW-based kinetic model developed by (Graaf et al., 1988) and adjusted for Aspen implementation by (Kiss et al., 2016) is used to simulate the interactions in the PFR. This decision is based on literature research and the reliability of available data. In fact, studies on the chemistry of the methanol synthesis suggest the Langmuir-Hinshelwood-based (LHHW) model is the best suited to represent the kinetic mechanism of the reactions (Ott et al., 2012). Moreover, Graaf's model has been validated experimentally with the use of a fibrous Cu/Zn/Al/Zr catalyst (Nyári et al., 2020).
- The design parameters for the reactor and the catalyst are shown in Table 4.2.
- The distillation towers are modelled as RadFrac columns, using the DSTWU option initially to calculate preliminary inputs. The results from the DSTWU method are used as final values for the detailed simulation. Accordingly, the first tower has 20 stages, partial-vapor condenser, kettle reboiler, reflux ratio of 0.4, and a distillate to feed ratio of 0.99. On the other hand, the second column is designed with 18 stages, partial-vapor-liquid condenser, kettle reboiler, a reflux ratio of 1.1 and a distillate to feed ratio of 0.673.

4.3. Plastic-to-methanol

4.3.1. Process Design

The process flow diagram of the plastic-to-methanol route can be seen in Figure 4.3. Additionally, a detailed step by step of the process is given in the paragraphs below.

The plastic-to-methanol route starts with the gasification of the plastic feed-stream in a dual fluidized bed gasifier (DFBG). The choice of gasifier is based on the characteristics of the technology and the raw material. Particularly, the high volatile content of plastics, the sticky behavior, and the considerable amount of TAR formation hinders the application of other conventional technologies. For example, the low thermal conductivity and the stickiness of the plastic materials impedes the optimum performance of rotary ovens and rotary kilns. Likewise, updraft and downdraft gasifiers are limited by the lower content of fixed carbon (Lopez et al., 2018). On the contrary, the DFBG technology has some comparative advantages that makes it better suited for plastic gasification, such as excellent gas-solid contact, high heat and mass transfer rates, low temperature operation, and independent syngas production with low or zero N_2 (He et al., 2012; Lopez et al., 2018). These are achieved by benefiting from the enhanced heat transfer characteristics of fluidization and by decoupling the gasification process from the combustion. Therefore, preventing the flue gases from mixing with the product gases and, consequently, reducing the requirement for downstream separation units.

Furthermore, the gasification process can be divided in three main steps. The first one is drying (100 - 200 °C), in which the moisture content of the feedstock is evaporated. The second one is pyrolysis or devolatilization. In this step, the volatile components of the fuel are thermally decomposed to form permanent gases, TARs, unreacted fixed carbon (char) and ash. This step plays a major role in fuels with larger shares of volatile compounds, such as plastics. The final one is gasification, in which char and TARs react with the gases produced from pyrolysis at high temperatures (700 - 1500 °C) to generate other products (De Jong & Van Ommen, 2014). Moreover, depending on the reactor technology, the heat needed to drive the endothermic reactions can be produced in different ways. For the case study assessed in this process model, silica sand is used as inert bed material to transfer heat between the combustion and gasifying chambers.

Considering the findings from the literature review, the gasification process is conducted at 900 °C and atmospheric pressure (Kannan et al., 2011; Saebea et al., 2020). Operating at this temperature, a balance between optimum product yield and energy demand is achieved. On the one hand, lower temperatures increase the production of TARs and reduce the H_2 content in the produce gas. On the other hand, while higher temperatures promote the degradation of primary TARs, it also boost the agglomeration of inorganic compounds and the generation of soot (Win et al., 2019), besides the higher energy requirements. Therefore a mass flow of sand of 25 kg/h per mass flow of dry inlet gas is defined to maintain a temperature of 900 °C in the gasifier (Abdelouahed et al., 2012). Additionally, the plastic feedstock is assumed to enter the gasification reactor at 15 °C and 1.02 bar.

To drive the gasification process, a mixture of air and steam is chosen as gasifying agent. There are trade-offs to be considered between the different types of materials that serve this purpose (Hantoko et al., 2019). For instance, air is a common alternative due to its low cost. However, the produce syngas suffers from low hydrogen contents, which is detrimental for the synthesis of methanol. Oxygen enhances the heating value of the gasification product, but at the expense of higher energy requirements for the air separation unit. Steam, on the other hand, is a good alternative to increase the amount of hydrogen in the syngas. Then, by using a mixture of air/steam, the inlet ratio to fuel can be adjusted to produce a syngas with the optimum composition for methanol production. Thus, eliminating the need of adding a reverse water gas shift reactor or additional hydrogen supply.

Considering the previous, the steam to fuel ratio (H_2O /carbon) is defined at 1.31 and it is mixed with air at a ratio of 4.6:1.0. In addition, the mixture is preheated to 570 °C using the available heat from the flue gases exiting the combustion chamber (PTC-E01). This heat exchange drops the flue gas temperature to 200 °C, which is suitable for stack operation according to the simulation guidelines from (Ramirez-Ramirez, 2019).

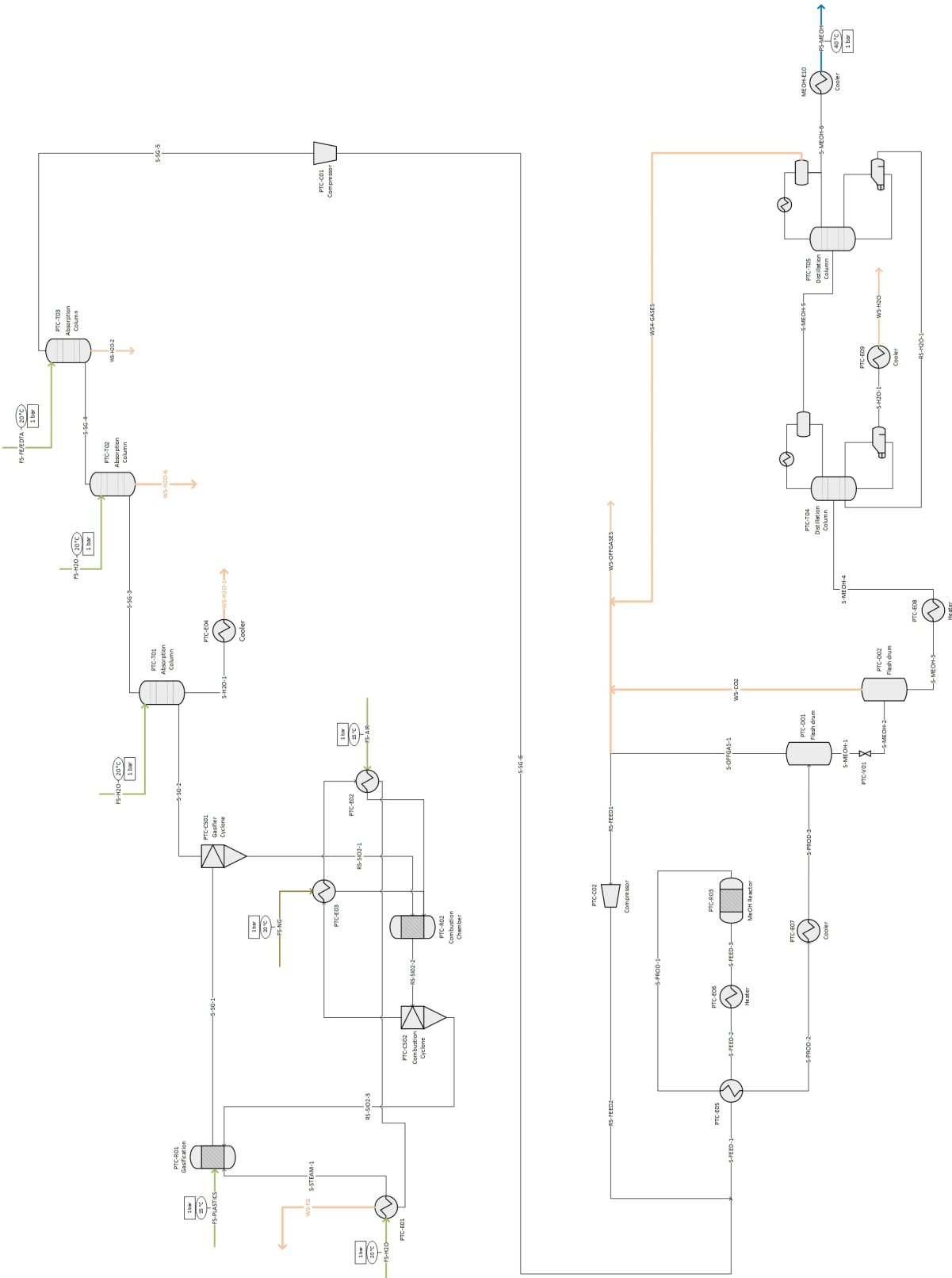


Figure 4.3: Process Flow Diagram of the plastic-to-methanol plant

The silica, unreacted char, and ash are separated from the gas products through a cyclone (PTC-CS01) and sent to the combustion chamber where carbon is combusted with excess air. The heat generated is then transported by the silica sand to maintain the 900 °C needed for the gasification. However, the unreacted char is not enough to satisfy the heat requirement, and therefore, additional fuel is supplied. Another alternative is to separate a fraction of the feedstock and burn it in the combustion chamber. However, this translated into a 40% increase in demand for plastics, with no benefit of reducing emissions. Therefore, the fuel requirement is met by introducing natural gas into the combustion reactor. Subsequently, the products from the combustion are sent to a second cyclone (PTC-CS02) where flue gases are separated from the hot sand. The bed material is then recirculated to the gasifier. Whereas the flue gases, are used to pre-heat the air and natural gas feedstreams (PTC-E02, PTC-E03) before sending them to a stack.

The main compounds generated in the gasifier are CO , CO_2 , CH_4 , H_2 , H_2O , and TARs. Furthermore, gasification often produces varying concentrations of inorganic materials depending on the nature of the feedstock. However, the sulfur content is assumed to primarily generate H_2S (Mutlu & Zeng, 2020; Ramzan et al., 2011), while similarly, nitrogen and halides will predominantly produce NH_3 and HCl (Ramzan et al., 2011; Torres et al., 2007). Therefore, the design of the purification units focuses on these 3 compounds, based on the system proposed by (Krishnamurthy et al., 2015).

First, the raw syngas is treated with two water scrubbers. The first one removes TARs, HCl , and the majority of NH_3 . Whereas the second one is designed to further reduce the NH_3 concentration below the maximum limits determined for safe catalyst operation. In the first tower, water enters from the top at ambient conditions (i.e., 15 °C and 1.02 bar), with a ratio of 7 m^3/h relative to 1000 Nm^3/h of syngas (Krishnamurthy et al., 2015). Under these conditions, TARs are cooled down, condensed, and carried over in the effluent. Additionally, NH_3 and HCl are dissolved and removed as ions.

There are other methods to remove these contaminants from gas streams. In particular, TARs can be treated by hot gas clean-up (HGC) methods, such as thermal cracking at temperatures above 1100 °C or catalytic cracking using mineral or synthetic-based catalysts. Another technology recently developed is the OLGA process (acronym for oil-based gas washer in Dutch). This method operates with two absorption columns and a regeneration unit to separate the TARs from the gas stream using oil as solvent. The liquid waste can then be burn in the combustion chamber of the gasifier, which reduces the demand for additional fuel. In addition, this technique offers some advantages such as lower temperature requirements and low operating and catalysis cost (Shahabuddin et al., 2020). Similarly, NH_3 and HCl can be treated with HGC methods, including selective catalytic oxidation or the use of sorbents (Abdoulmoumine et al., 2015). However, because of the fact that the syngas needs to be compressed and cooled before the methanol synthesis steps, maintaining the hot temperature of the gas stream is not necessary. Therefore, the main advantage of using HGC techniques is lost. Moreover, the complexity of the system is considerably reduced by combining the treatment of the three impurities into one unit.

Waste water from the first scrubber leaves from the bottom at 68 °C, while the gases exit the top at 27 °C. The rich waste water is cooled down and sent to further treatment. On the other hand, the syngas is sent to the second water scrubber to remove the remaining traces of NH_3 . In this second unit, the amount of water is adjusted to achieve a NH_3 content of 0.05 mg/Nm^3 in the syngas. Afterward, the outlet gas leaves at 20 °C and it is sent to the third cleaning unit.

This final purification step consists of an absorption column using an iron-chelate solution to remove H_2S . The process is a patented technology called LO-CAT, which converts H_2S into elemental sulfur at low temperature. This particular technique selectively removes H_2S , converts it into an innocuous component, and produces no hazardous waste as byproduct. In fact, the iron catalyst is easily and continuously regenerated with air in a subsequent regeneration unit. A description of this regeneration process is provided in Appendix B.2.

Based on literature, the inlet ratio is defined as 0.0015 m^3/h of solvent per Nm^3/h of gas (Kazemi et al., 2014), for a solvent concentration of 0.2 mol/L (Horikawa et al., 2004). The clean syngas is then compressed in 4 stages to a pressure of 50 bars, with intercooling and flash units used to remove the

water between stages. Intercooling is adjusted to maintain a temperature below 160 °C at the inlet of the subsequent compressor (Desai, 2018; Ramirez-Ramirez, 2019). Afterwards, the syngas is mixed with the recycled products from the methanol reactor, where both streams are preheated to 230 °C and sent to the inlet of the reactor.

The process then follows a similar sequence as in the CO_2 hydrogenation, considering the same kinetic model applies for the CO and CO_2 interactions with H_2 (Ott et al., 2012). Upon exiting the reactor, the outlet stream is cooled down to 30 °C to separate the denser products (methanol, water) from the rest of the unreacted gases. The gas phase is recycled to mix with the inlet stream, after compression to 50 bar. From the recycle stream, 0.25 wt% is purged to prevent build-up. On the other hand, the liquid phase containing mainly methanol is expanded to 1.02 bar to further remove the unreacted gases. Moreover, two distillation columns are designed to achieve chemical-grade methanol. The raw product is first heated to 87 °C before entering the first tower. 99.5 wt% pure methanol exits from the top at 65 °C, while water exits from the bottom at 94 °C. The top product from the first column then enters the second distillation unit. The bottom outlet, consisting mainly of methanol and some water, is recycled back to the first column. While the overhead stream is separated in a partial vapor-liquid condenser. The remaining gases are removed in the vapor phase to achieve a liquid product > 99.9 wt% purity. Finally, the methanol is cooled down to 40 °C. Under these conditions, the product is suitable for transportation to nearby chemical industries for further use in applications such as the production of MTBE or Formaldehyde.

4.3.2. Process Modeling

To reduce the data load in the simulation, the plastic-to-methanol route is divided in two Aspen flow-sheets: the gasification and syngas conditioning steps, and the methanol synthesis. The flow-sheets designed for both stages can be found in Appendix C.3 and C.4. The details and assumption used in the simulation are provided below:

- The plastic feedstock is defined as a non-conventional component. HCOALGEN and DCOALGEN models are selected for the enthalpy and density of the solids calculation, respectively.
- Because of the heterogeneity of the plastics, defined as a non-conventional material, it cannot participate in phase or chemical equilibrium calculations without transforming it into its conventional components. Thus, the plastic stream is decomposed using an RYield reactor (PTC-R04). The mass yield of H_2O , Ash , C , H_2 , N_2 , Cl_2 , S , and O_2 is determined by the Proximate and Ultimate analysis, and estimated using a calculator block.
- The gasification process is modeled with a thermodynamic approach, using an RGibss block (PTC-R01). This kinetic-free model is customary in the field of gasification/combustion for the evaluation of the gas products or the optimization of operating conditions. In this reactor, chemical and phase equilibrium are estimated based on the Gibss free energy minimization method, taking into account the constraints of the mass balances between the chemical elements. Therefore, only the chemical species potentially present in the product stream need to be identified to carry out the simulation. According to the background research, the following compounds are considered as product: C , CO , CO_2 , H_2 , CH_4 , H_2O , H_2S , NH_3 , HCl , $C_{10}H_8$, $C_{14}H_{10}$, C_9H_8 .
- TARs need to be modeled separately. When using chemical equilibrium, there is no TAR formation. However, plastics tend to produce significant amounts of TARs and they can be harmful to downstream processes. To achieve the simulation of these components, part of the feedstock is separated and sent to a second RYield reactor (PTC-R05). This unit models the production of TARs, represented in the simulation by Naphtalene, Anthracene, and Indene. The selection of the components and their mass yield in the final syngas product ($70 g/Nm^3$) is based on the work from (Wilk & Hofbauer, 2013).
- To accurately estimate the size of the gasifier and the heat transfer from the sand, the TAR stream is mixed with the rest of the unreacted plastic before entering the gasifying reactor.

- The combustion chamber (PTC-R02) is modeled using an RStoic reactor. No reactions or yields need to be entered as input to the simulation block. The oxygen requirement is met with a surplus of air of 1.05.
- The specifications for sizing the cyclones are based on literature, (de Paula et al., 2020; Miskam, 2006).
- The three absorption columns (PTC-T01, PTC-T02, PTC-T03) are modeled using a RadFrac block with 3 operating stages. Raw syngas enters from the bottom while the solvent enters from the top. The chemical interactions that remove the HCl , NH_3 , and H_2S are simulated by using ELECNRTL as the property method and specifying the chemical reactions.
- The methanol reactor (PTC-R03) is modeled as an isothermal RPlug reactor (PFR). The heat generated from the exothermic reactions can be used to generate high pressure steam (Szima & Cormos, 2018), however, it is not included for the evaluation of this model.
- The LHHW-kinetics developed by (Graaf et al., 1988) and adjusted for Aspen implementation by (Kiss et al., 2016) is used. Moreover, the model has been validated experimentally with the use of a fibrous Cu/Zn/Al/Zr catalyst (Nyári et al., 2020).
- The distillation towers are modelled as RadFrac columns, using the DSTWU option initially to calculate preliminary inputs. The results from the DSTWU method are used as final values for the detailed simulation. Accordingly, the first tower has 20 stages, partial-vapor condenser, kettle reboiler, reflux ratio of 0.4, and a distillate to feed ratio of 0.99. The second column is designed with 18 stages, partial-vapor-liquid condenser, kettle reboiler, a reflux ratio of 1.1 and a distillate to feed ratio of 0.673.

5

Pedigree Analysis

Chapter 5 gives an overview of the qualitative uncertainty evaluation. First, the topic of uncertainty is introduced in section 5.1. Then, the layout and results of the Pedigree Analysis are described in section 5.2.

5.1. Background on Process Model Uncertainty

Understanding the uncertainty of a process model is essential to correctly interpret and use its results. Historically, research in the modeling of chemical processes has focused more on the quantifiable dimensions of uncertainty. While the uncertainty behind qualitative aspects, such as the knowledge base, is rarely identified (Spek et al., 2016). Because the outcomes of the model are usually used as inputs in other studies, this gap may affect the reliability of future research or introduce biases in the decisions of policy-makers. Figure 5.1 shows some examples of inputs required for the modeling procedure that have underlying uncertainties and affect the model results. Thus, assessment of the model uncertainty improves the decision-making process of users by understanding the quality and limitations of the model.

A combination of quantitative and qualitative uncertainty assessment methods is the best approach to obtain a holistic view of the quality of a process model (Spek et al., 2016). Quantitative evaluation techniques are the most used in the modeling of industrial processes. Some examples include error propagation, sensitivity analysis, or data validation. They are based on strict and structured mathematical principles to directly demonstrate the robustness and precision of the results of a process model. However, these methods alone are limited to the quantifiable aspects of the modeling procedure. They do not provide information, for example, on the quality of the knowledge base used in the design of the process model. Qualitative assessment techniques can supplement these limitations to provide a more robust description of the uncertainties in the model. Examples of such methods are peer review, quality assurance, or pedigree analysis.

The uncertainties in this study are assessed by means of sensitivity analysis and pedigree analysis. Sensitivity analysis is used to identify the inputs in a model that contribute the greatest uncertainty to an outcome of interest (Risbey et al., 2004). It is a commonly used tool for evaluating quantifiable aspects of uncertainty. However, it does not provide any insight into the parts of the modeling process outside the quantifiable scope. The sensitivity analysis is thus complemented with a pedigree analysis. This evaluation approach is meant to qualitatively assess the strength of the knowledge base of data or models (Spek et al., 2017). Furthermore, to minimize subjectivity in the evaluation and give a structure to the qualitative assessment, pedigree matrices are used.

Details and results from the pedigree analysis are provided in section 5.2, while the outcomes of the sensitivity analysis are described in Chapter 7.

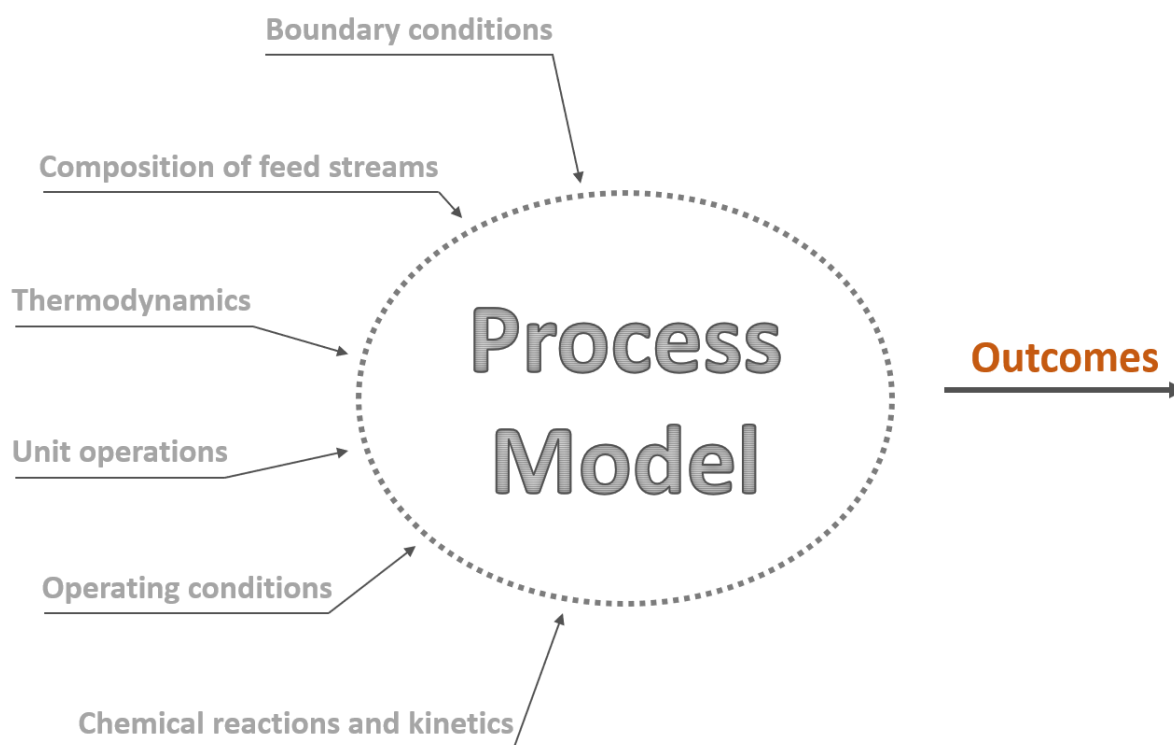


Figure 5.1: Examples of inputs in a process model with underlying uncertainty

5.2. Pedigree Analysis

Pedigree analysis is implemented in two stages of the modeling procedure: to the state of the art in the literature and to the simulation. Figure 5.2 shows the steps evaluated and the components chosen for evaluation. On the one hand, the pedigree analysis of the literature review includes the knowledge base in the composition and conditions of the feed streams, the design parameters, and how this information is used to build a coherent flow diagram of the processes. On the other hand, four key areas are selected for the second pedigree analysis to determine the quality of the simulation. First, the line ups of the flow-sheets and the corresponding representation of the PFDs in the Aspen Plus environment. Second, the choice of property method. Third, the description of chemical interactions and kinetics, and finally, the modeling of the unit operations. A description of each component evaluated is provided in Appendix A.1

5.2.1. Pedigree Workshops

Assessment of the model by independent experts is a key feature in Pedigree Analysis (Spek et al., 2017). Therefore, four members of the Energy and Industry group from the Energy Systems and Services Department of the Technical University of Delft are selected to participate in two Pedigree workshops. All of them with backgrounds in techno-economic assessments and modeling of industrial processes. Moreover, to divide the work load, the evaluation is conducted in two days. The first workshop deals with the assessment of the CO_2 purification system. While the second one is focused on the CO_2 hydrogenation to methanol process and the plastic-to-methanol route.

To facilitate the expert's assessment, an information package was provided before each workshop. The dossier was composed of: i) an overview of the process model, including references to literature and explanations on the choice of technologies; ii) a description of the flow diagram with the composition of feed streams, details of the chemistry involved in the process, and conditions of unit operations and intermediate streams; iii) the Aspen flowsheet. Together with details of the strategy followed to design

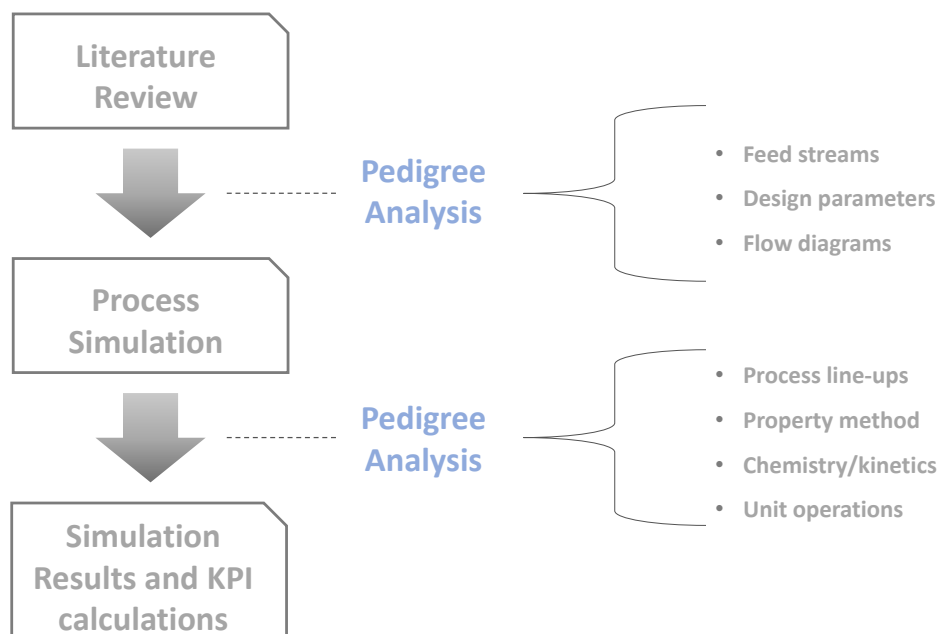


Figure 5.2: Stages in the modeling procedure in which Pedigree Analysis was conducted and the components evaluated.

the simulation according to the process described in the flow diagram; iv) every input and assumptions made to conduct the simulation; v) two pedigree matrices for each process model to evaluate separately the uncertainty in the data of the state of the art and the simulation.

The experts are required to individually assess each model using the information dossier. The evaluations are held using pedigree matrices to minimize subjectivity and structure the outcomes of the assessment. Tables 5.1 and 5.2 provide the details of the pedigree matrices used for the state of the art and for the simulations, respectively. The criteria is selected based on the work from (Spek et al., 2016), because it aligned with the assessment of data uncertainty from this study. The column headings represent the pedigree criteria, the row headings indicate the strength of the criteria, and in each box there is a brief description to help with the evaluation. The definitions of the pedigree criteria can be found in Appendix A.2.

The workshops are used to discuss the scores and clarify doubts about the modeling procedure, with emphasis on the points with the greatest variability among the experts. To improve this exercise, the experts are asked to submit their evaluations before the start of the workshops. This way, the results could be collected and averaged into an overall score beforehand, and the reviewers are already familiar with the process model and the evaluation procedure. After the discussion, the reviewers are asked to re-evaluate the state of the art and the simulation with the same pedigree matrices. The results of the discussion and the pedigree evaluation are used to improve the model. Furthermore, the averaged scores are highlighted in colours for visual aid. Depending on the evaluation, the scores are shaded according to the following categorization: red for a score between 0 - 0.5; orange for a score between 0.6 - 1.5; yellow for a score between 1.6 - 2.5; light green for a score between 2.6 - 3.5; and dark green for a score between 3.6 - 4. Where the scale indicates low to high uncertainty from 4 to 0.

In addition to the averaged scores, the variability in the responses is determined using the Interquartile Range (IQR). This is a measurement of statistical variability between the first and third quartile range of data, and it is used to steer the discussion during the workshops. Therefore, to provide a deeper understanding of the results, the variability of the scores is included in a separate column in the pedigree matrices.

Table 5.1: Pedigree matrix for the assessment of data uncertainty in the State of the Art. Based on Spek et al., 2016.

Strength	Proxy	Empirical Basis	Theoretical Understanding	Methodological Rigour
4	An exact measure of the desired quantity	Controlled experiments and large sample, direct measurements	Well established theory	Best available practice in well established discipline
3	Good fit to measure	Historical / field data, uncontrolled experiments, small sample, direct measurements	Accepted theory with partial nature (in view of the phenomenon it describes)	Reliable method common within established discipline; best available practice in immature discipline
2	Well correlated but not measuring the same thing	Modeled / derived data, indirect measurements	Accepted with partial nature and limited consensus on reliability	Acceptable method but limited consensus on reliability
1	Weak correlation but commonalities in measure	Educated guesses, indirect approximation, rule of thumb estimate	Preliminary theory	Preliminary methods, unknown reliability
0	Not correlated and not clearly related	Crude speculation	Crude speculation	No discernable rigour

Table 5.2: Pedigree matrix for the assessment of data uncertainty in the Simulations. Based on Spek et al., 2016.

Strength	Skills and Time	Theoretical Understanding	Methodological Rigour
4	High expertise from multiple practitioners in subject matter and no time constraints	Well established theory	Best available practice in well established discipline
3	Good expertise from single practitioner but limited time available	Accepted theory with partial nature (in view of the phenomenon it describes)	Reliable method common within established discipline; best available practice in immature discipline
2	Limited expertise but enough time to build skill for the specific purpose	Accepted with partial nature and limited consensus on reliability	Acceptable method but limited consensus on reliability
1	Limited expertise and limited time available	Preliminary theory	Preliminary methods, unknown reliability
0	No expertise in the subject matter and big time constraints	Crude speculation	No discernable rigour

It is important to highlight two key aspects of the pedigree evaluation. First, consensus is not sought from the reviewers. Although the role of the modeler is to clarify doubts during the workshops, there is

still room for individual interpretations of the evaluation criteria. This is allowed, since the main objective of the exercise is to find the aspects of greatest uncertainty and improve the process models. Second, the goal of the pedigree assessment is not to eliminate the uncertainty, but to understand the sources of it and the implications over the quality of the process model and its results.

5.2.2. Results from Pedigree workshops

CO_2 purification system

Tables 5.3 and 5.4 show the consolidated matrices for the state of the art and the simulation of the CO_2 purification system. The results show good agreement between the experts, with only four scores having an IQR above 0.5 between the two matrices.

Table 5.3: Pedigree scores for the data uncertainty in the State of the Art of the CO_2 purification system. Median values range from 0 (high uncertainty) to 4 (low uncertainty). Colours are used to highlight the uncertainty level

Pedigree Criterion	Proxy		Emperical Basis		Theoretical Understanding		Methodological Rigor	
	Med.	IQR	Med.	IQR	Med.	IQR	Med.	IQR
Feed streams	2.8	0.5	3.0	0.0	3.8	0.5	3.0	0.0
Design parameters	2.8	0.5	2.8	0.5	2.8	0.5	2.8	0.5
Flow diagram	2.8	0.5	2.8	0.5	3.0	1.0	3.0	1.0

Table 5.4: Pedigree scores for the data uncertainty in the Simulation components of the CO_2 purification system. Median values range from 0 (high uncertainty) to 4 (low uncertainty). Colours are used to highlight the uncertainty level

Pedigree Criterion	Skills and time		Theoretical Understanding		Methodological Rigor	
	Med.	IQR	Med.	IQR	Med.	IQR
Process line-ups	3.1	0.8	3.0	1.0	2.8	0.5
Property method	3.1	0.8	4.0	0.0	4.0	0.0
Chemistry/Kinetics	3.1	0.8	3.3	0.5	2.8	0.5
Unit Operations	3.1	0.8	3.0	0.0	2.5	1.0

The evaluation of the uncertainty in the state of the art indicates a high confidence in the composition and conditions of the feed streams. It means the experts agree that there is large empirical data available and an established theory supporting it. The methodological rigour is also scored high with absolute agreement, signifying the use of reliable methods to estimate the characteristic of the captured CO_2 . The only exception is the proxy, which has the same score for the three components. The proxy evaluation shows a majority of the experts finds the information to come from good measures of the actual values, giving it a score of 3. However, it was point out that the source of information for the components can also be considered as "well correlated data", which has a lower score of 2. This suggest there is still uncertainty associated to the proximity of the data used in the process.

The assessment of the design parameters is slightly lower, which highlights the fact that even though the CO_2 purification system operates with mature technologies, there is still no established best practice in the field. More data from laboratory and industry is needed to reduce the uncertainty levels.

On the other hand, the information used to build the flow diagram is scored more favorably, but it also shows greater variability in theoretical understanding and methodological rigour. This is explained by

the fact that some experts find that the information used for the design of the process comes from reliable methods in an accepted theory framework, thus scoring 3 or 4. While others find it to be limited in consensus, giving it a lower score of 2.

The pedigree scores for the simulation components of the CO_2 purification system reflect a high evaluation for the skills & time and theoretical understanding criteria. However, it shows mixed evaluations for the methodological rigour. While there is high certainty in the available data to decide the best property method, there is less confidence for the rest of the components. This variation comes from the fact that there is no consensus in the field for some of the methods used in the simulation. Particularly, the adsorption towers from the TSA system are not supported in the Aspen Plus environment. Thus, simplifications and assumptions have to be made. Which translates into higher levels of uncertainty.

CO_2 hydrogenation to methanol

The Pedigree assessments of the CO_2 hydrogenation to methanol process is depicted in tables 5.5 and 5.6.

Table 5.5: Pedigree scores for the data uncertainty in the State of the Art of the CO_2 hydrogenation process. Median values range from 0 (high uncertainty) to 4 (low uncertainty). Colours are used to highlight the uncertainty level

Pedigree Criterion	Proxy		Emperical Basis		Theoretical Understanding		Methodological Rigor	
	Med.	IQR	Med.	IQR	Med.	IQR	Med.	IQR
Feed streams	3.3	0.5	2.0	0.0	3.3	0.5	3.0	0.0
Design parameters	3.0	0.0	2.8	0.5	3.5	1.0	3.0	0.0
Flow diagram	3.0	0.0	2.8	1.5	3.3	0.5	2.8	0.5

Table 5.6: Pedigree scores for the data uncertainty in the Simulation components of the CO_2 hydrogenation process. Median values range from 0 (high uncertainty) to 4 (low uncertainty). Colours are used to highlight the uncertainty level

Pedigree Criterion	Skills and time		Theoretical Understanding		Methodological Rigor	
	Med.	IQR	Med.	IQR	Med.	IQR
Process line-ups	2.9	0.3	3.3	0.5	3.0	0.0
Property method	3.1	0.8	3.5	1.0	3.5	1.0
Chemistry/Kinetics	3.1	0.8	3.3	0.5	3.3	0.5
Unit Operations	2.9	0.3	3.3	0.5	3.0	0.0

Table 5.5 shows the reviewers agree there is a well established theory for the CO_2 hydrogenation process. Indeed, there is extensive literature on the subject that is used as base point for the design of the process model. However, they score lower in the criteria of empirical basis. This is explained by two factors. On the one hand, for the feed streams, the CO_2 and H_2 conditions are determined by modeled data. Even though the experts find that the theory and methods used to calculate this conditions are reliable (expressed with scores between 3 - 4), the definition of the criteria suggests a score of 2 for any input data without experimental or field measurement. On the other hand, for the design parameters and the flow diagram, the experts take into consideration the cases of commercial application, such as the George Olah Renewable Methanol Plant. The conclusion is that although limited, there are already some historical data used to corroborate the inputs to the model.

The scores in the simulation also indicate high confidence in the theoretical understanding and the methods used to represent the process. The variability in the property method shows subjectivity is

always present in the evaluation of qualitative aspects. Nonetheless, it is worth noticing the spread occurs in the low end of the uncertainty range (between 3 and 4).

The criteria of skills and time is another topic of debate that emerged during the workshops. The scoring definition leaves some room for the interpretation of what "good experience" means. It is also debatable whether only the experience of the modeler of this study should be considered. For instance, some experts argued that the assumptions and input parameters chosen for the simulation are based on earlier studies by more experienced professionals. As mentioned previously, no consensus is required, so the scores fluctuate. Although, the minimum value given to the uncertainty in the expertise of the modeler is 2.5.

Plastic-to-methanol

The last process model assessed in the second Pedigree workshop is the plastic-to-methanol. Table 5.7 shows the scores to the State of the Art and table 5.8 depicts the score to the simulation environment. From the tables, the variability in the results is immediately highlighted. Unlike the other process models, the plastic-to-methanol route has less agreement between the expert evaluations.

Table 5.7: Pedigree scores for the data uncertainty in the State of the Art of the plastic to methanol process. Median values range from 0 (high uncertainty) to 4 (low uncertainty). Colours are used to highlight the uncertainty level

Pedigree Criterion	Proxy		Emperical Basis		Theoretical Understanding		Methodological Rigor	
	Med.	IQR	Med.	IQR	Med.	IQR	Med.	IQR
Feed streams	2.5	1.0	2.5	1.0	3.0	1.0	3.0	1.0
Design parameters	2.8	0.5	2.5	1.0	2.8	0.5	3.0	0.0
Flow diagram	2.5	1.0	2.8	0.5	3.0	0.0	3.0	0.0

Table 5.8: Pedigree scores for the data uncertainty in the Simulation components of the plastic to methanol process. Median values range from 0 (high uncertainty) to 4 (low uncertainty). Colours are used to highlight the uncertainty level

Pedigree Criterion	Skills and time		Theoretical Understanding		Methodological Rigor	
	Med.	IQR	Med.	IQR	Med.	IQR
Process line-ups	2.9	0.3	3.0	1.0	2.8	0.5
Property method	2.9	0.3	3.3	0.5	2.8	1.5
Chemistry/Kinetics	2.9	0.3	3.3	0.5	3.0	1.0
Unit Operations	2.9	0.3	3.0	1.0	2.5	1.0

The results from the State of the Art in the data used to determine the characteristics of the feed streams shows the larger spread. This is explained by the fact that the plastic composition had to be assumed. The theory and the methods used to calculate this composition is regarded as reliable by the majority of the panel. However, the score is lower for proximity and empirical base. The reason behind this variation is the source for the ultimate and proximate analysis used to determine the properties of the plastics. Although TNO's Phyllis database can be considered a highly reliable source, with data gathered from experimental research, it lacks replicability from other sources. Thus, it is not sufficient to unanimously classify the uncertainty in the assumption as "low". (i.e., a score ≥ 3).

Overall, there is high confidence in the methods used in the literature to choose the design parameters and build the flow diagram. The experts also score high in the theoretical understanding criteria. The consensus is that the process of gasification and methanol production from syngas is already an

established theory. However, the source of uncertainty is found to be in the proximity of the data and the empirical basis. Similar to the feed streams, the design parameters are related to the assumption made for the plastics composition. Therefore, the same discrepancies arise in the reliability of the data. In the case of the flow diagram, the uncertainty is associated to the design of the gasification process. Despite there is high confidence in the theoretical understanding and rigor in the methods used by the modeler, there is no data available with the same plastic composition as in this study.

Table 5.8 shows there is confidence in the quality of the theory used for the simulation. It also indicates low uncertainty in the experience of the modeler. The lower scores (and variability) are present in the methodological rigor, particularly for the property method and the unit operations. The discussion on the reliability of the property method is focused in the distillation columns for the methanol synthesis. In this regard, NRTL is used as property package, following the recommendations of (Kiss et al., 2016; Nyári et al., 2020). However, it is pointed out during the workshop that because of the streams composition, NRTL with Redlich-Kwong equation of state is better suited to simulate the behaviour of the gases. This remark is considered to improve the models, and thus the property method is updated. Nonetheless, the score reflects the uncertainty from the base case.

The uncertainty in the data used to simulate the unit operations comes from the fact that there are several choices to simulate the gasification process. They depend on the scope of the study and the level of expertise of the modeler. Thus, there is no best alternative in the discipline. Each modeler then gave this criteria a score of 2 or 3, depending on their own experience and interpretation of the scoring scale.

Improvements to the Process Models

Besides assessing the strength of the data in the state of the art and the simulations, the outcomes of the pedigree workshops are used to improve the process models. This is accomplished from the discussion and suggestions of the experts. The list of improvements is summarized in table 5.9:

Table 5.9: Improvements made to the process models

Improvement Suggested during the Workshops	Implementation to the Process Model
The visualization of the PFDs can be enhanced in two ways: i) remove the temperature and pressure indicators from the intermediate flow streams; and ii) add arrows to indicate the direction of the flows	Both suggestions are taken into account. Only the conditions of the raw materials and the product stream are shown in the PFDs and arrows are included for better understanding
Add a description of the regeneration units from the absorption columns operating with sodium sulfite and iron-chelate solutions. Even though it is not included in the scope of the assessment	The description of the regeneration process for both solution is included in Appendix B
Use the conditions of the regeneration units to determine whether additional steps are needed for the inlet of the solvents to the absorption columns	A pump is included to supply the sodium sulfite solution at the required operating pressure to the absorption column in the CO_2 purification plant
If two separate plants are considered in the CO_2 hydrogenation route, then storage or supply conditions for the CO_2 are required at the end of the CO_2 purification system	Research in the field suggest that the most efficient means of CO_2 transportation is through pipeline (Onyebuchi et al., 2018). Additionally, since both plants are assumed to be in the same industrial hub, pressure drop can be considered as minimum. Therefore, two heat exchangers and a compressor are added to satisfy the conditions for the pipeline supply
Air compressor should operate with a maximum outlet temperature of 110 °C	The condition of the outlet from the air compressor of the CO_2 purification system is adjusted accordingly
Include intermediate storage for the non-condensable gases emitted from the top of the cryogenic distillation column of the CO_2 purification system	This step is addressed in the discussion, however, it is concluded that no extra units are required for the scope of this evaluation
The temperature of the methanol produced can be increased from 30 to 40 °C. This does not cause a negative impact in the transportation or subsequent use in further chemical processes	The final temperature of the product is adjusted accordingly, improving the utility consumption in the last heat exchanger.
The property method in the distillation columns should be changed from NRTL to NRTL-RK to account for non-ideality	The first choice of property method is based on literature (Kiss et al., 2016). However, this was improved considering the suggestion from the experts.
Change the simulation of the combustion reactor in the gasification and syngas conditioning flow-sheet, from an isothermal to an adiabatic design	The simulation is updated considering the comments from the experts

6

Results

Chapter 6 provides the results from the simulations and KPI calculations. First, the mass and energy balances are detailed in section 6.1. Second, with the results from the mass and energy balances, the technical KPIs are calculated and presented in section 6.2. Third, section 6.3 provides the outcomes from the estimation of the economic KPIs, and finally, the results of the environmental KPIs are given in section 6.4.

6.1. Mass and Energy Balances

The mass and energy balances are important to demonstrate the reliability of the calculations in a complex, multi-component chemical process. They represent the application of the mass and energy conservation axioms (Cerro et al., 2001), i.e., the rate of mass/energy entering the system must be equal to the rate of mass/energy exiting the system.

Table 6.1: Mass balance of the different case studies.

Mass flow (kg/h)	CO ₂ hydrogenation route	Plastic-to-MeOH
Inlet Streams		
CO ₂	42,442	-
Na ₂ SO ₃ solution	6,323	-
H ₂ O		683,733
H ₂	5,567	-
Plastic Wastes	-	22,620
Fe-EDTA solution	-	101,253
Air	20	101,013
Natural Gas	-	5,302
Total	54,352	913,919
Outlet Streams		
MeOH 99.9 wt%	27,504	27,500
Liquid wastes	22,903	779,363
Gas wastes	3,945	107,055
Total	54,353	913,918

Moreover, mass and energy balances are the basis to calculate the technical, environmental, and economic KPIs. The interaction between reacting species and the energy exchanges in the unit operations will determine raw materials consumption, composition of products, size of unit operations, utility requirements, etc. Therefore, accurate mass and energy balances are key to the techno-economic evaluation.

Tables 6.1 and 6.2 provide a summary of the mass and energy balances from the two case studies. The calculations are made in Aspen Plus, according to the flow-sheets detailed in Chapter 4.

These preliminary results already provide useful insights into the characteristics of each manufacturing process. Table 6.1 shows the mass flow in the plastic-to-methanol route is considerably higher than the one from the CO_2 hydrogenation process. This difference is mainly attributed to the feedstock requirements for the Syngas purification steps, which is given by the inlet streams of H_2O and Fe-EDTA solution. In effect, the scrubbers are designed for volumetric flows of 4 - 7 m^3/h of water relative to 1000 Nm^3/h of syngas (Krishnamurthy et al., 2015). Consequently, the generation of liquid and gas waste streams is around 33 times higher for the plastic-to-methanol route.

Table 6.2: Energy balance of the different case studies.

Energy Balance (Gcal/h)	CO_2 hydrogenation route	Plastic-to-MeOH
Inlet Streams		
CO_2	(89.3)	-
Na_2SO_3 solution	(23.5)	-
H_2O	-	(2,591.3)
H_2	1.1	-
Plastic Wastes	-	(8.7)
Fe-EDTA solution	-	(366.4)
Air	(0.0)	(0.3)
Natural Gas	-	(4.6)
Total	(111.7)	(2,971.3)
Outlet Streams		
MeOH 99.9 wt%	49.4	49.4
O_2	-	-
Liquid wastes	86.3	2,910.8
Gas wastes	3.7	60.8
Total	139.5	3,021.0
Utilities		
Hot	47.0	30.5
Cooling	(76.1)	(89.6)
Electricity	1.7	9.6
Electrolyser	-	-
Total	(27.4)	(49.5)

In the CO_2 hydrogenation route, the majority of the outlet streams are in the liquid state. Moreover, 72% of this liquid outlet is 99.99 wt% pure H_2O from the first distillation column of the methanol synthesis process. Therefore, it can readily be used as process water. Additionally, only 43% of the gas outlet

streams are emitted in the purification plant. Therefore, the CO_2 purification system plays a minor role in the generation of wastes. On the contrary, outlet streams in the plastic-to-methanol process are primarily associated with wastes generated in the gasification and syngas purification steps. Particularly, the liquid wastes from the 3 absorption columns account for 88% of all the outlet streams. While the rest is almost entirely generated as flue gases in the combustion chamber.

The results from table 6.2 show a similar trend. With higher energy exchanges in the plastic-to-methanol process between the inlet and outlet streams. This is explained by the higher energy content that results from the larger mass flow of raw materials and wastes. Furthermore, the cooling requirement is increased in the plastic-to-methanol route, while the hot utility demand decreases. These variations are also influenced by the operating conditions of the respective purification units. The details of the different mass and energy interactions between the technologies is provided in the following sections.

6.2. Results from Technical KPIs

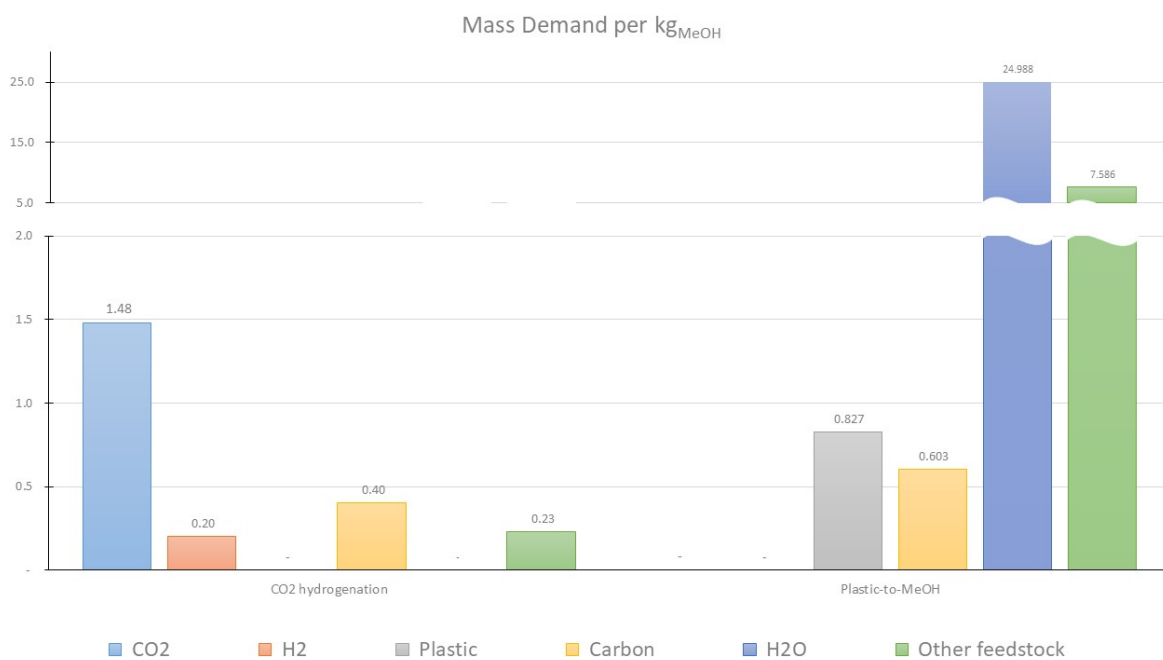


Figure 6.1: Mass demand of individual inputs in kg/kg_{MeOH}

Tables 6.3 and 6.4 summarize the mass demand and the specific utility consumption for the different technologies. Concerning Table 6.3, mass demand of the key elements for methanol production (H_2 , CO_2 , plastics) favors the plastic-to-methanol route. Showing a lower demand of plastics per kg of MeOH than the equivalent of CO_2 and H_2 for the CO_2 hydrogenation route. This is contrasted, nonetheless, by the higher need of process water -required by the absorption towers of the syngas purification steps- and the demand for other materials. The latter includes Fe-EDTA solution, and natural gas used in the gasification process. Moreover, carbon consumption is included to provide a common base of comparison. This metric refers to the carbon content in the CO_2 and the plastic feedstocks at the start of both processes. These differences in carbon consumption and other feedstock are more noticeable in Figure 6.1.

On the other hand, table 6.4 shows the difference in energy consumption from both technologies. However, a deeper analysis is needed to understand the sources of this utility demand. Therefore, the influence of the purification steps is analyzed by breaking down the utilities between the raw material purification units and the methanol synthesis. The results are shown in Figure 6.2.

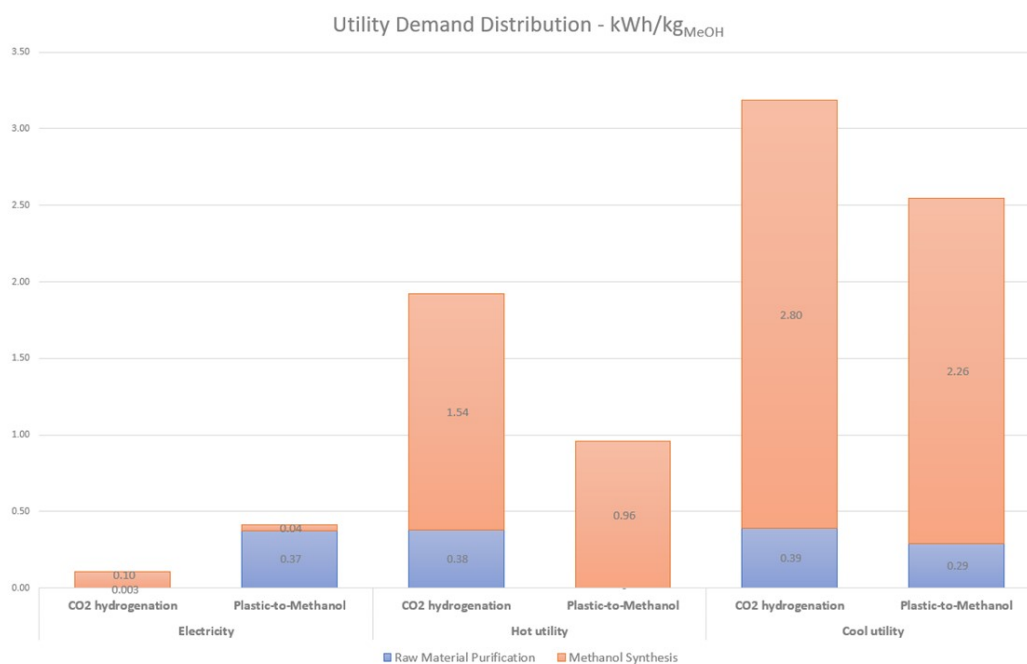
Table 6.3: Mass demand of individual inputs

	Units	CO_2 hydrogenation	Plastic-to-MeOH
CO_2	kg/kg_{MeOH}	1.479	-
H_2	kg/kg_{MeOH}	0.203	-
Plastic usage	kg/kg_{MeOH}	-	0.827
Carbon consumption	kg/kg_{MeOH}	0.404	0.603
H_2O (as feedstock)	kg/kg_{MeOH}	-	24.988
Other feedstock	kg/kg_{MeOH}	0.230	7.586

Table 6.4: Utility demand of the technologies

Utility	Units	CO_2 hydrogenation	Plastic-to-MeOH
Electricity	kWh/kg_{MeOH}	0.11	0.41
Hot	kWh/kg_{MeOH}	1.92	0.96
Cooling	kWh/kg_{MeOH}	3.19	2.54

The higher electricity demand in the plastic-to-methanol process is given by the compressor train needed to increase the pressure of the syngas. The CO_2 hydrogenation route benefits from acquiring raw materials at higher pressures. On the contrary, plastic gasification and syngas purification stages operate at atmospheric conditions. In this sense, the 4-stage compressor accounts for 90% of the whole electricity demand of the process. Moreover, the turbines in the CO_2 purification system are able to supply 92 % of the electricity requirements.

**Figure 6.2:** Utility demand distribution between the purification steps and the methanol synthesis

Furthermore, Figure 6.2 indicates the majority of hot and cool utility demand comes from the methanol synthesis. However, this consumption varies depending on the technologies, despite the fact that the unit operations and the conditions of the methanol reactor are the same. These variations can be explained by the compositions of the inlet and outlet streams to the methanol reactor. On the one hand, the heat of reaction from the CO and H_2 present in the syngas is higher than the heat generated in the

hydrogenation of CO_2 (eq: 1.1 and 1.3). Thus, the methanol reactor requires around 62% more cooling utility in the plastic-to-methanol route. On the other hand, the CO_2 hydrogenation process produces large amounts of water (around 13 wt% of the reactor outlet). This increases the heat flow required to change the temperature in the product stream. Therefore, almost twice as much energy is needed in the following heat exchangers to reach the required operating conditions. In addition, the first distillation tower needs to separate a larger water flow, which increases the energy consumption of the reboiler. On the contrary, the plastic-to-methanol route accumulate other materials, such as methane and argon, which are more easily separated in the second distillation step.

These interactions are better depicted in Figure 6.3. As stated before, the hot utility consumption in the distillation columns is reduced in the plastic-to-methanol route, because of the lower water content. On the other hand, the methanol reactor produces higher amounts of heat, which is removed with cooling water for the base case of this study. Therefore, its share in the overall cooling utility consumption increases with respect to the CO_2 hydrogenation route. It is important to highlight that no heat integration is considered within the scope of this research study. This is an important aspect of the assessment to take into consideration when comparing the different types of utility requirements. For instance, while in this case the larger heat generation from the methanol reactor translates into more costs associated with utility consumption, this heat source could also be used to generate steam and power steam turbines to produce electricity.

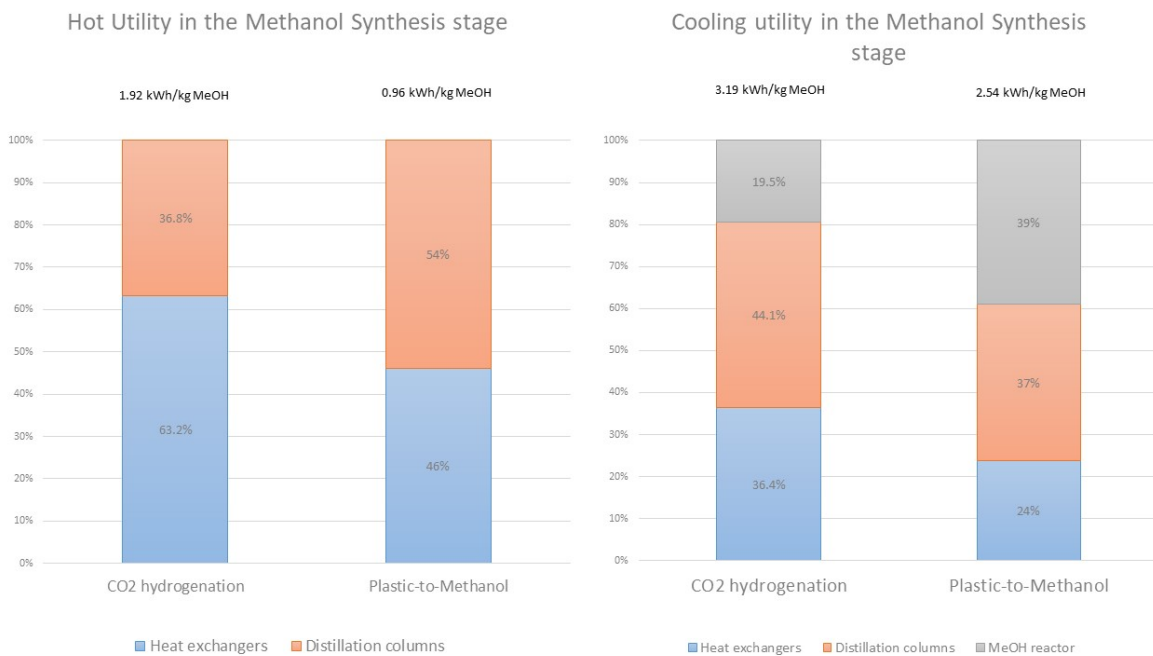


Figure 6.3: Hot and cooling utility demand by unit operations in the methanol synthesis step

Figure 6.4 depicts the results for the reactor and overall conversion efficiencies. The figure shows there is better reactor conversion efficiencies for the syngas, owing to the higher reaction rate from the hydrogenation of CO compared to the hydrogenation of CO_2 (Elsernagawy et al., 2020). Likewise, the 50% decrease in hydrogen efficiency and the production of water as byproduct (1.1) negatively affects the reactor conversions in the CO_2 hydrogenation routes.

Nonetheless, the carbon losses in the plastic-to-methanol route are considerably higher than in the CO_2 hydrogenation routes. This is translated into lower overall carbon conversions which can be appreciated in Figure 6.4. The losses are attributed to the gasification and syngas cleaning steps. Particularly, the formation of TARs during gasification consumes 25% of the carbon content in the plastic, accounting for roughly 70% of the efficiency loss in the overall carbon conversion. The rest comes mainly from the waste gases of the methanol conditioning units (i.e., the gas removed from the flash separator

before the distillation columns and the distillation columns). On the contrary, the CO_2 lost in the CO_2 purification system amounts to roughly 0.3%. Therefore, the process can achieve a higher overall conversion efficiency of 93%.

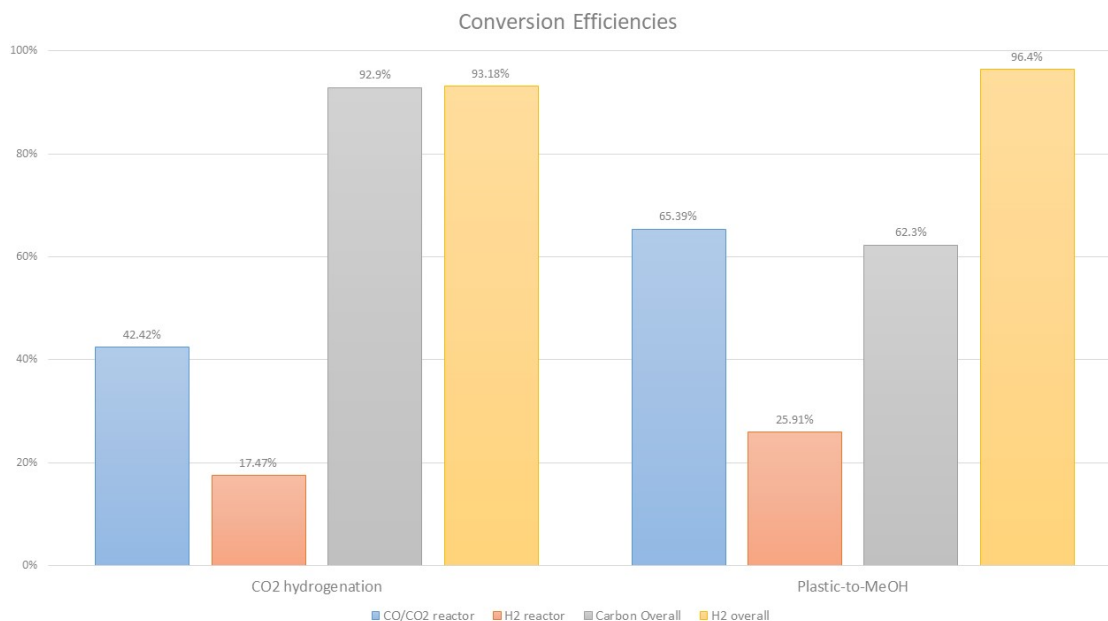


Figure 6.4: Comparison between overall and reactor conversion efficiencies.

6.3. Results from Economic KPIs

Table 6.5: Economic KPIs

	Units	CO_2 hydrogenation	Plastic-to-Methanol
CAPEX	M€	41.79	56.13
VCP	M€/yr	73.69	70.24
FCP	M€/yr	14.39	7.86
Revenues	M€/yr	90.21	90.20
NPV	M€	-54.79	9.11
LCOMeOH	€/kg _{MeOH}	0.45	0.40

A comparison of the economic KPIs is provided in table 6.5. The results indicate only the plastic-to-methanol route is economically feasible from an investor's point of view, with a positive NPV after the lifetime of the plant. Moreover, the LCOMeOH from CO_2 hydrogenation route exceeds the market cost for methanol production, estimated at 0.40 €/kg_{MeOH}. The assumptions used for the calculation of the economic KPIs and the yearly cash flows are provided in Appendix D.

The breakdown of the equipment's total installation costs and the OPEX are shown in Figures 6.5 and 6.7, respectively. From Figure 6.5, the influence of the compressors becomes evident. With a share of 40% of the total equipment cost in the CO_2 hydrogenation route and 60% in the plastic-to-methanol pathway. This larger contribution was already explained due to the extra compression needs in the syngas conditioning steps. Similarly, because of the conditions of the CO_2 hydrogenation route, more energy is required from the heat exchangers and the distillation columns. Particularly, the composition of the outlet stream from the methanol reactor influences the energy demand from the subsequent unit operations. This is more noticeable when comparing the share of these equipment in Figures 6.5a and 6.5b. On the other hand, the contribution of the methanol reactor is found to be less than 2% for the

CO_2 hydrogenation technology and below 1% for the plastic-to-methanol route. These results agree with findings from the literature (Pérez-Fortes et al., 2016).

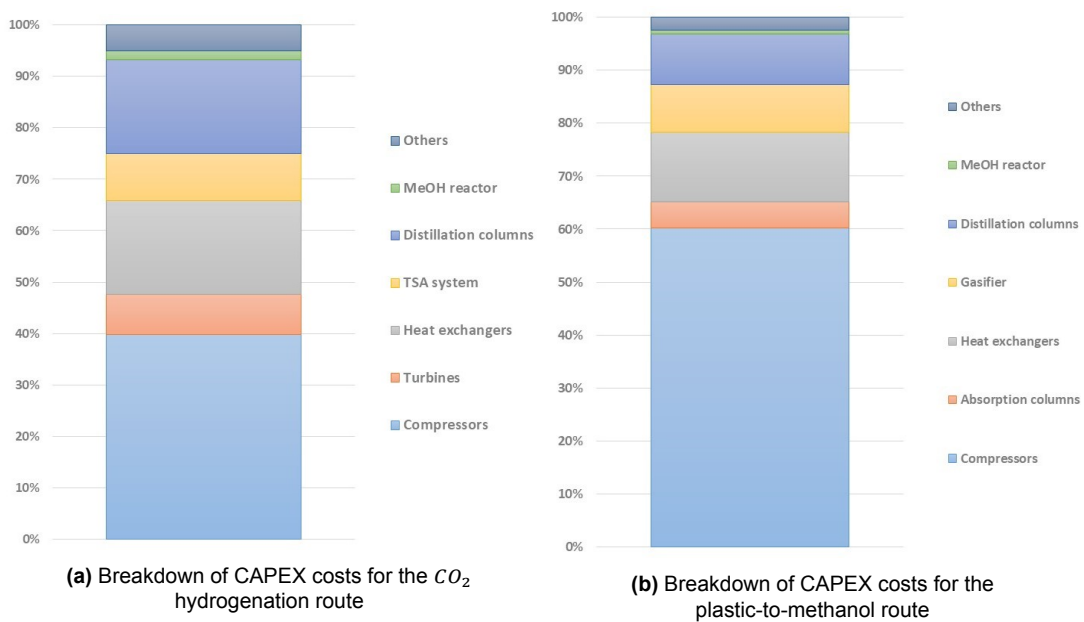


Figure 6.5: Breakdown of CAPEX costs

To understand the main sources affecting the economic feasibility of the projects, the contribution of CAPEX and OPEX to the LCOMeOH is detailed in Figure 6.6. The results show operating costs represent the larger contribution to the economic performance of the technologies. Furthermore, table 6.5 indicates that VCP are the bulk of the OPEX, accounting for 84% and 90% of the total value for the CO_2 hydrogenation and the plastic-to-methanol processes, respectively. These costs are further breakdown in Figure 6.7, which depicts that the majority of the VCP are associated to the consumption of raw materials.

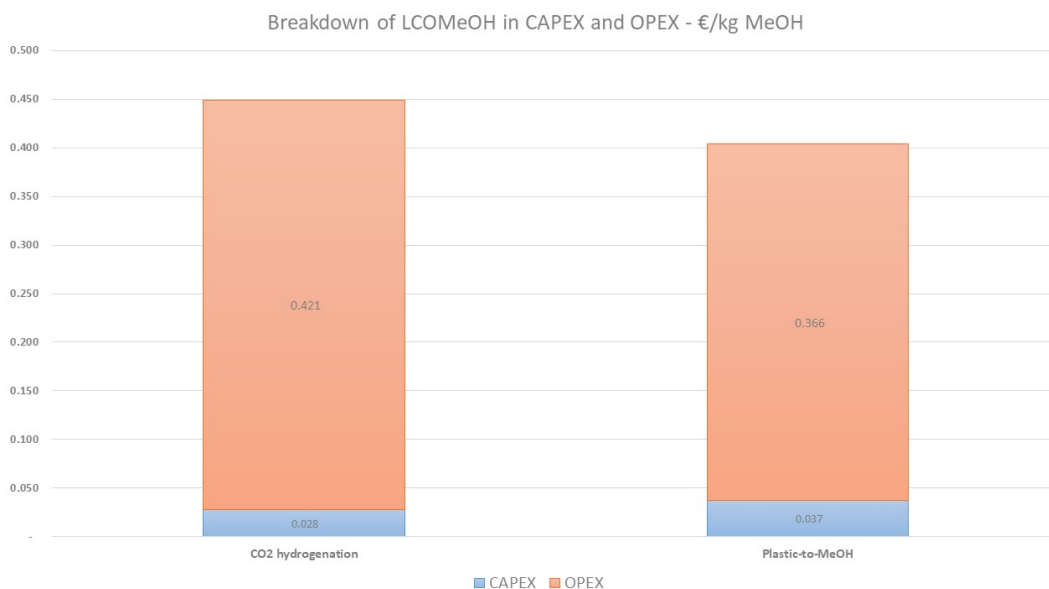


Figure 6.6: Contribution of CAPEX and OPEX to the LCOMeOH of the different technologies.

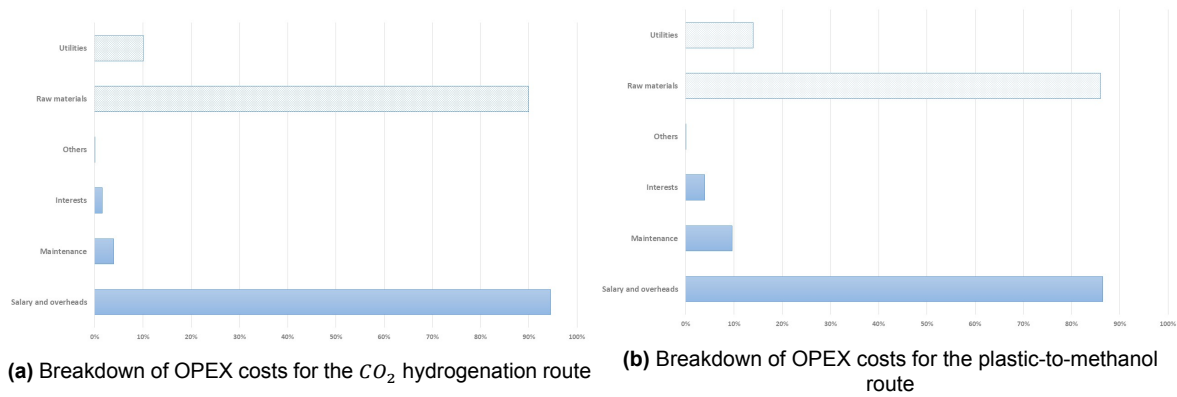


Figure 6.7: Breakdown of OPEX costs. VCP are shown with a pattern fill in the upper half. FCP are shown with a solid fill in the lower half.

6.4. Results from Environmental KPIs

Figure 6.8 shows the carbon footprint for the different case studies. The results are compared with the environmental performance of the CCU-MeOH plant simulated by Pérez-Fortes et al., 2016 and a conventional methanol synthesis process. However, there are limitations in this comparison that need to be taken into account. First, the carbon footprint is measured within the boundaries of the system. This means that no CO_2 emissions are allocated to the production and sourcing of the raw materials. Nor to the application and end of life treatment of the methanol. Second, the bio-plastic content in the plastic wastes is not considered. Likewise, the emissions avoided for using the MSW share for methanol production instead of land-filling or energy generation are not included in the assessment.

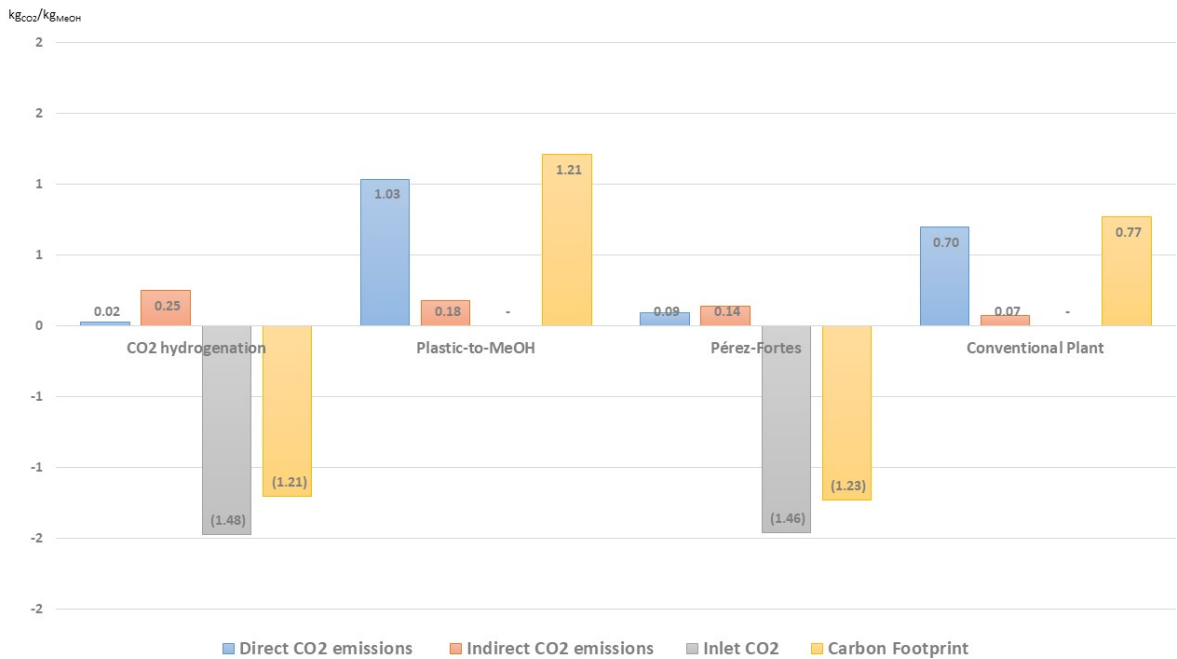


Figure 6.8: Carbon footprint of the technologies compared to two reference cases.

The carbon footprint for the CO_2 hydrogenation under the aforementioned conditions is negative, which indicates the process consumes more CO_2 than it emits. However, it is worth noting that a conventional steam methane reforming plant without carbon capture produces approximately $9.28 \text{ kg}_{CO_2}/\text{kg}_{H_2}$ (NREL, 2018). Furthermore, the plastic-to-methanol route generates more CO_2 than the natural gas

based process. The main source is related to the direct emissions, similar to the conventional reference case. The reason for this higher emissions rate is the production of flue gases during the gasification step, which includes CO_2 and CH_4 . Thus, to include the contribution of methane to the direct emissions, a GWP of 32 is used (Environmental Protection Agency, 2021).

The energy yield of the technologies and two references from (Nyári et al., 2020; Szima & Cormos, 2018) are depicted in Figure 6.9. In order to compare the results under the same basis, the purification units are excluded from the calculations. The results show that the values from this study are within the range from other techno-economic assessments. Moreover, the spread between the two reference studies can be explained by the different scopes of their evaluations. For instance, the lower value of Szima & Cormos is influenced by the on-site production of hydrogen from a water electrolysis unit. On the contrary, the higher value from the work of Nyári et al. comes from the implementation of a complete heat exchange integration network, resulting in zero demand for hot utility and reduced requirement for cooling. This exercise is outside the scope of the research. However, it provides some useful insight into potential improvements and the limits of the process model.

The plastic-to-methanol yield is affected by TARs production during gasification. In fact, the higher contribution to the inlet energy of both technologies comes from the lower heating value of the raw materials. Therefore, because more plastics are needed to account for the carbon losses, the process becomes less energy efficient.

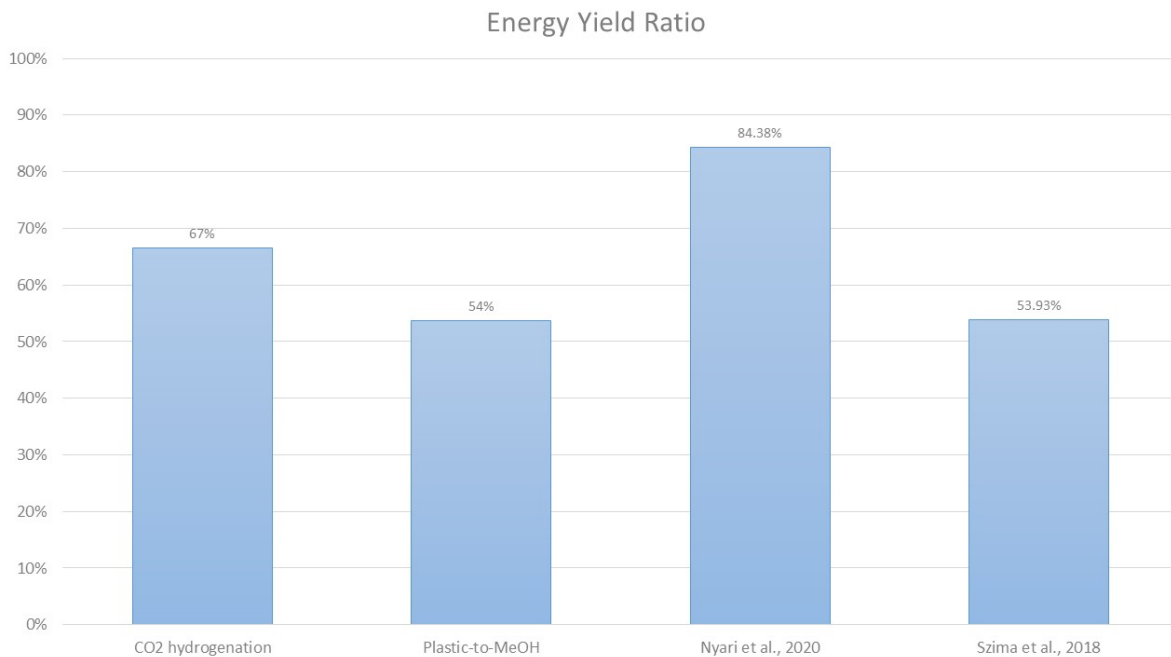


Figure 6.9: Energy yield ratio of the different case studies and two reference cases.

7

Sensitivity Analysis

Chapter 7 presents the results from a sensitivity analysis on the economic and environmental performance of the technologies in section 7.1. Afterward, section 7.2 evaluates the influence of using alternative hydrogen sources on the economic performance of the CO_2 hydrogenation route.

7.1. Sensitivity analysis on key input parameters

A sensitivity analysis is conducted for the economic and environmental models of the case studies. The choice of parameters is based on the results from Chapter 6. Thus, inputs belonging to the areas with the larger impacts are selected. The prices for the major feedstock, electricity, and methanol are chosen for the economic assessment. The effect of varying these inputs on the NPV of the projects is assessed to find scenarios of economic feasibility. Moreover, the potential for GHG emissions reduction is analyzed by measuring the influence of varying the carbon intensity of the electricity and the consumption of hot utility in the carbon footprint. A summary of the parameters included in the sensitivity analysis is provided in table 7.1.

Table 7.1: Input parameters used in the sensitivity analysis.

Input parameter	Units	Base value	% of change
NPV			
CO_2 cost	€/kg	0.025	±50%
Green H_2 cost	€/kg	4.1	±50%
Grey H_2 cost	€/kg	1.09	±50%
MeOH selling price	€/kg	0.41	±50%
Electrolyser's energy requirement	kWh/kg	50	±50%
Carbon Footprint			
Carbon intensity of electricity	$kgCO_2/kWh$	0.390	±50%
Hot utility consumption	kWh/kg_{MeOH}	100%	±50%

Figure 7.1 shows the results for the CO_2 hydrogenation case study. Production of hydrogen through steam methane reforming is a mature technology. There are several commercial plants in operation and it is the main source of hydrogen worldwide. Therefore, there is little uncertainty in the process or price of grey H_2 . Instead, the sensitivity analysis focused on the price of CO_2 , MeOH, and electricity. The results show a high influence from the methanol price. Depending on the direction of the variation, methanol price can increase or decrease the NPV of the project by 217%. Fluctuations in the price of CO_2 and electricity also influence the feasibility of the plant, but to a lesser extent. Additionally, the effect of the carbon intensity and the hot utility demand is shown in Figure 7.1b.

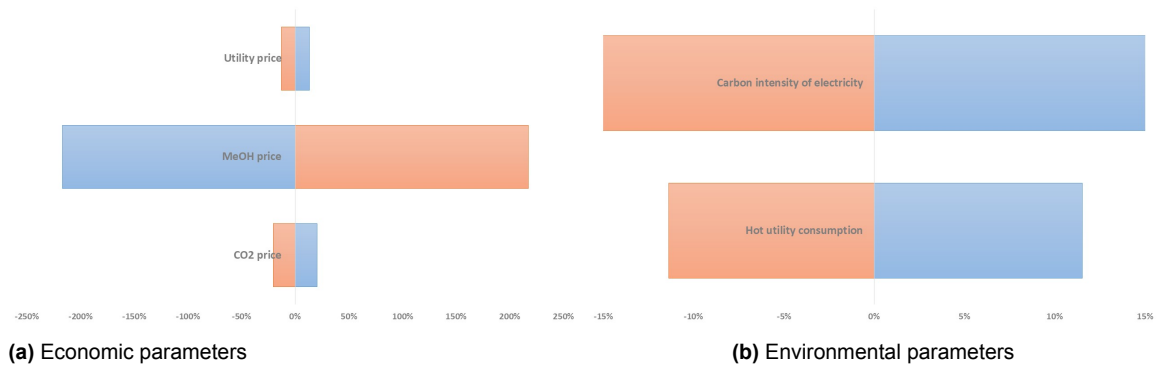


Figure 7.1: Sensitivity analysis on economic and environmental parameters for the CO_2 hydrogenation route

The sensitivity analysis conducted on the plastic-to-methanol route shows a high influence from the measured parameters (Figure 7.2). In fact, a 50% change on the price of electricity or plastic wastes can reduce or increase the NPV by 137% and 142%, respectively. The influence is even higher for the price of methanol, with variations of $\pm 1023\%$ on the NPV of the plant. This volatility suggests high levels of uncertainty in the economic performance, which is relevant for future project evaluations. Moreover, Figure 7.2b indicates neither parameter has a high influence on the carbon footprint. This agrees with the findings from section 6.4, which indicate the majority of the CO_2 emissions in the plastic-to-methanol route stem directly from the process.

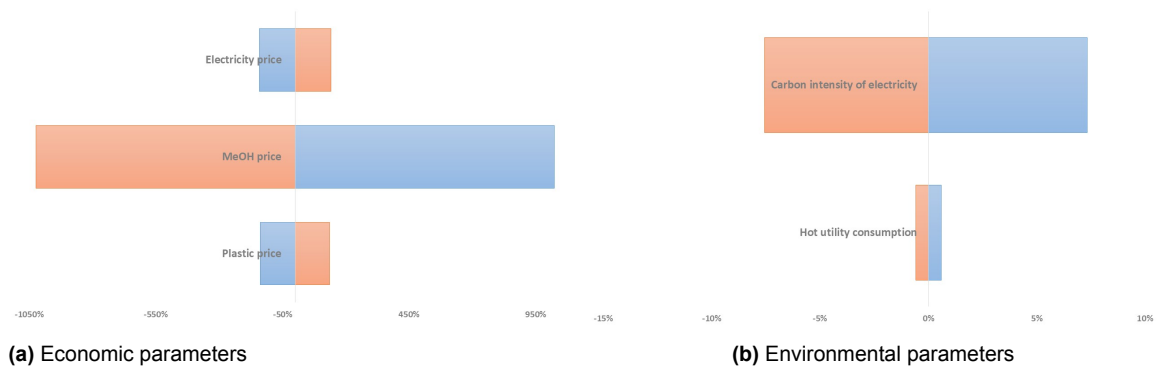


Figure 7.2: Sensitivity analysis on economic and environmental parameters for the plastic-to-methanol route

Furthermore, break-even values are estimated for the cost of CO_2 and the price of methanol on the CO_2 hydrogenation route. The results, shown in table 7.2 indicate that the process requires a neutral or negative cost of CO_2 to be financially viable. This means that the plant would have to be paid to consume the CO_2 and transform it into a valuable product. Additionally, a methanol price of 0.45 €/kg is found to be sufficient for the project to have a neutral NPV. This value is within the range of the market price for methanol over the last 3 years (Institute, 2021). Moreover, these findings are in agreement with other techno-economic studies on methanol production plants using CO_2 hydrogenation process (Nyári et al., 2020; Pérez-Fortes et al., 2016).

Table 7.2: Break-even values

	Units	CO_2 hydrogenation
CO_2 cost	€/kg	-0.0001
MeOH selling price	€/kg	0.45

7.2. Alternative Hydrogen Supply for the CO_2 Hydrogenation Route

In addition to the sensitivity analysis, two alternative cases of hydrogen supply are compared with the base case for CO_2 hydrogenation. The goal is to assess the economic impact of: i) producing the hydrogen with an on-site water electrolyser; or ii) acquiring green H_2 from a third party supplier.

7.2.1. Background on Water Electrolysis

There are different technologies used for the electrolysis of water. The main component is the electrolysis cell, where the dissociation of water takes place. These are connected in series with the addition of insulating materials, mechanical support, and end plates to form a stack, which is the core element of the system, or balance of plant (BoP). The BoP includes additional equipment such as the cooling system, compressor, transformer, water treatment, output gas purification, and re-circulation. In the cell, the fundamental mechanism is based on two electrodes divided by an electrolyte. The latter is the responsible for allowing the flow of ions from one electrode to the other, while electrons flow through the outer circuit. Depending on the technology, these ions and the choice of electrolyte varies. Which in turn, provides different physico-chemical and electro-chemical characteristics to the system (IRENA, 2020). A schematic representation of the different types of electrolysis cells and their main reactions is shown in Figure 7.3.

Experts agree there is no single technology that outperforms the rest in every dimension (O. Schmidt et al., 2017). The share in the future market for water electrolysers will be based on technological breakthroughs and better fits depending on the final application. However, AEC and PEM electrolysis are mature technologies with commercial applications today. While SOEC and AEM are still in the research and demonstration stages (IRENA, 2020; O. Schmidt et al., 2017). Therefore, AEM and PEM technologies are better suited for the techno-economic assessments of medium-term large-scale projects.

Alkaline electrolysis is chosen for the evaluation of this research. While PEM technology has faster dynamic response, studies have found both Alkaline and Solid Oxide electrolysers can be successfully operated in combination with flexible energy sources, such as wind or solar (O. Schmidt et al., 2017). In fact, the most limiting factor in the flexibility of the system comes from the BoP, not the design of the stack. This has been proven by using AEC for primary control reserve in Germany, demonstrating the technology can also be used for fast response application (IRENA, 2020). PEM electrolysers also have smaller footprint, which is something to consider. However, the advantage is almost completely diluted in large scale applications. On the contrary, because of the fact that the technologies are still developing, PEM electrolysis has a higher cost, which is not justified in cases where the benefits cannot be exploited.

Furthermore, depending on the technology, hydrogen can be produced at different conditions. This becomes particularly relevant for applications where higher temperatures or pressures are required, such as in methanol synthesis. Notwithstanding the fact that PEM electrolysis is easier to pressurize, AEC are also commercially available for high pressure operations. However, there are trade-offs between using electrolysis at high pressure and operating the electrochemical device at atmospheric conditions with a subsequent compressing stage. These include higher costs for different materials and designs of the electrolyser system versus adding a compressor to the investment and operating costs of the plant. For applications below 100 bar, research suggest it is more energy efficient to operate with a pressurized electrolysis unit. The main reason is related to the high pressure ratios of this region, as Figure 7.4 shows. Moreover, the experience from commercial units indicate that this configuration has a minimum effect on the overall cost and electricity consumption of the BoP (IRENA, 2020).

With the technology defined, economic assumptions are made for the cost calculations. For the operating costs, the latest values from IRENA's report are used to estimate energy efficiency, lifetime of the stack and CAPEX cost. These CAPEX cost are subject to economies of scales. However, research suggest the benefits of larger scales are lost beyond nominal powers of 100 MW (Zauner et al., 2019).

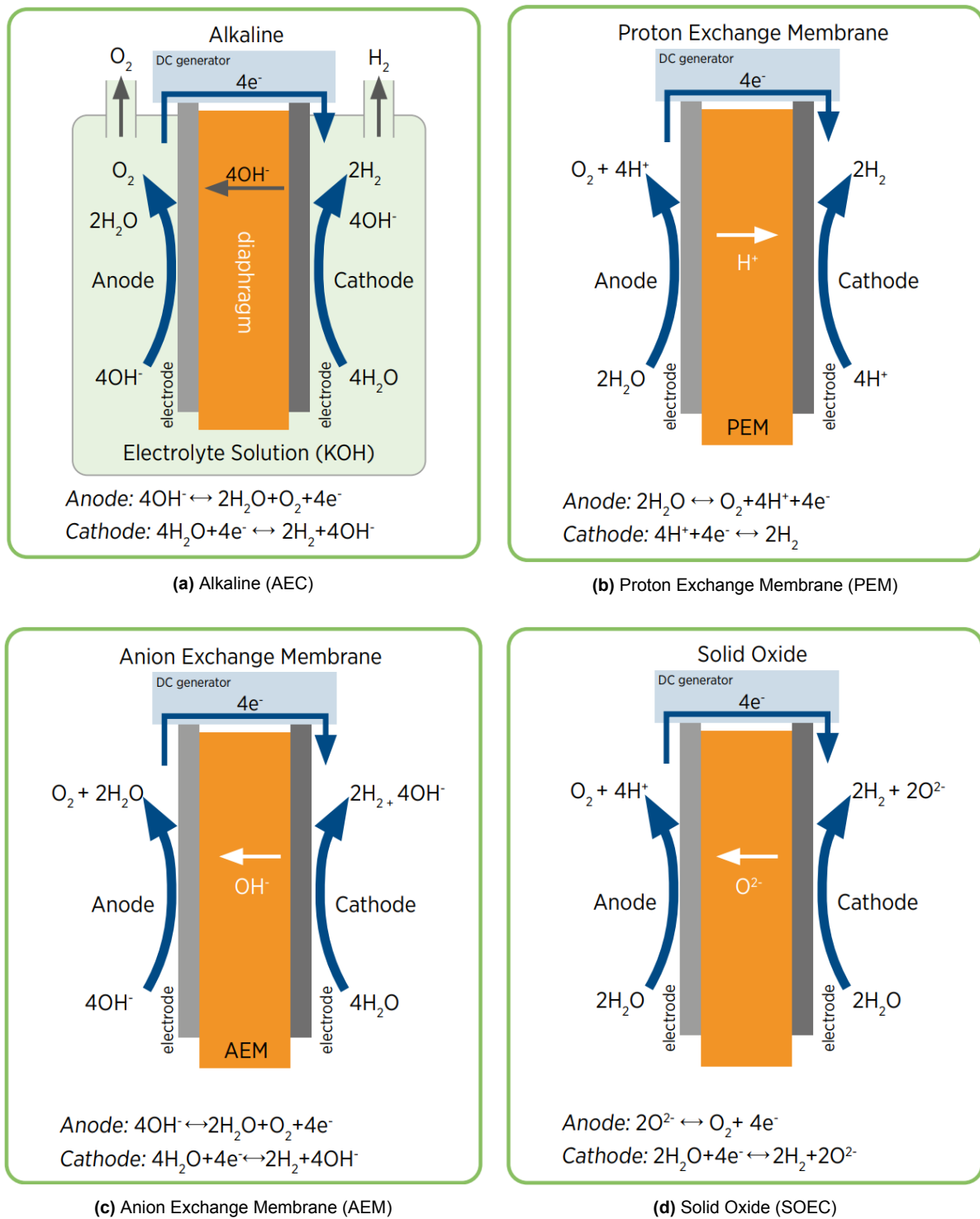
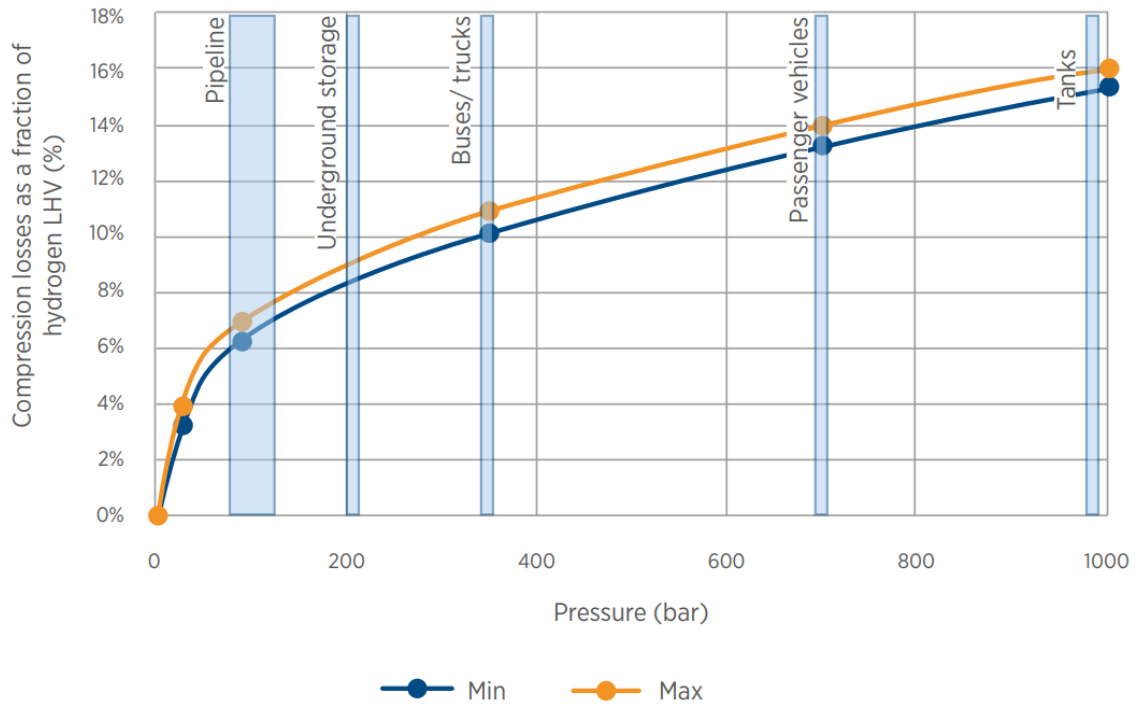


Figure 7.3: Types of water electrolysis technologies. Sourced from (IRENA, 2020)

Therefore, considering the production of hydrogen requires an electrolyzer of 278 MW for a capacity factor of 91.3, a linear estimation is made based on the values reported in (IRENA, 2020).

Table 7.3 gives a summary of the main characteristics used for the production of hydrogen with alkaline electrolysis.



Based on IRENA analysis based on BNEF, 2019.

Figure 7.4: Energy losses from mechanical compression of hydrogen, based on percentage of hydrogen LHV. Sourced from (IRENA, 2020)

Table 7.3: Specifications for the alkaline electrolyser. Based on Armijo, 2019; IRENA, 2020; Nel Hydrogen, 2019; Sánchez et al., 2020

Component	Units	Value
Operating temperature	°C	80
Operating pressure	bar	30
Load factor	%	91.3
H ₂ purity	%	99.99
Electricity Consumption of the Stack	kWh/kgH ₂	47
Electricity Consumption of the BoP	kWh/kgH ₂	50
Water consumption	l/Nm ³	0.9
Lifetime (stack)	hours	60000
Stack replacement cost	% of CAPEX (Stack)	40
CAPEX (stack)	USD/kW	270
CAPEX (BoP)	USD/kW	500

7.2.2. Comparison between different hydrogen sources

Figure 7.5 shows the economic performance of sourcing the hydrogen from 3 different alternatives. The results highlight the influence of the electrolyser. Indeed, the technology is still in development and thus suffers from high operating costs. The assessment indicates that with an electricity cost of 0.088 €/kWh, the high energy consumption is enough to produce methanol at a levelized cost of 1.36 €/kg. On the other hand, sourcing green hydrogen from a third party supplier improves the performance,

but it is still far from market prices. However, the rapid learning curve from hydrogen technology and expected growth in manufacturing capacity, might make this alternative feasible in the short to medium term.

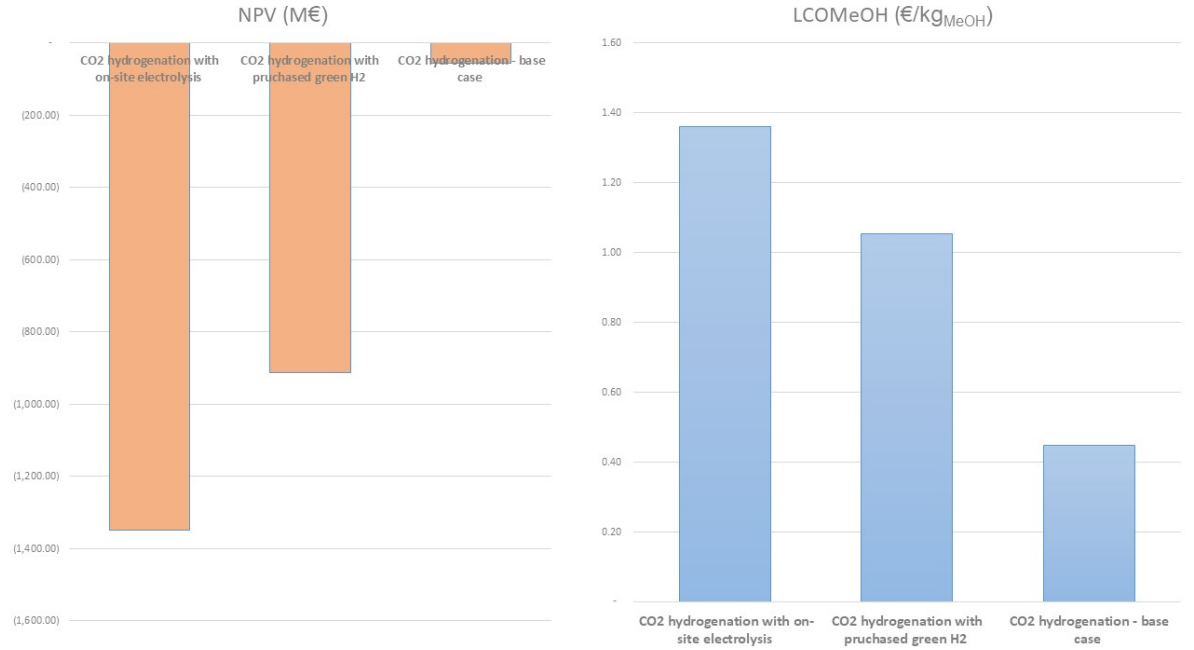
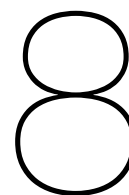


Figure 7.5: Financial indicators of the CO₂ hydrogenation route under different scenarios of hydrogen supply



Discussion

Chapter 8 presents a discussion on the results from Chapters 5, 6, and 7 to assess process bottlenecks and trade-offs between the different technologies. The results are also compared with findings from previous techno-economic studies and the benchmark.

Table 8.1 gives a summary of key performance indicators for every case study, two references, and a conventional methanol production plant. The values indicate comparative advantages from some technologies over others depending on the metric. Therefore, trade-offs can be identified.

Table 8.1: Comparative table with key performance indicators

Parameter	Units	CO_2 hydrogenation	Plastic-to-MeOH	(Nyári et al., 2020)	(Pérez-Fortes et al., 2016)	Conventional plant
CO/CO_2 reactor conversion	%	42.4	65.4	50.5	21.7	15 - 53
Overall carbon conversion	%	92.4	62.3	n.a	n.a.	72%
Electricity consumption	kWh/kg_{MeOH}	0.14	0.41	0.18	0.17	0.15
Hot utility consumption	kWh/kg_{MeOH}	0.65	0.06	-	0.44	2.26
Cool utility consumption	kWh/kg_{MeOH}	1.86	1.63	0.81	0.86	3.94
LCOMeOH	$€/kg_{MeOH}$	0.45	0.40	0.70	0.75	n.a.
Carbon footprint	kg_{CO_2}/kg_{MeOH}	-1.21	1.21	n.a	-1.23	0.77

From an economic perspective, the assessment shows a clear comparative advantage of the plastic-to-methanol route over the CO_2 hydrogenation. Higher costs of raw material and utility consumption makes the CO_2 hydrogenation project economically unfeasible. The plastic-to-methanol, on the other hand, benefits from requiring only plastics as main feedstock, i.e., no hydrogen is added to the process. However, when the carbon emissions are taken into consideration, the results show this route has the highest environmental impact. In fact, its carbon footprint is above the conventional process. This, however, is not considering the CO_2 emissions avoided for using waste plastics to produce added value materials. Nor does it take into account the bio-pastic content in the feedstock. Nonetheless, the results from the specific input demand found that the wastes generated in the gasification process and the syngas cleaning steps are considerable. Including a large presence of TARs, waste water, and flue gases from the combustion chamber.

Therefore, the environmental footprint of the plastic-to-methanol route is the main limitation in the overall performance of the technology. In particular, there are three conditions from the process that could be improved. The first one is the generation of TARs. Previous assessment of methanol production from waste have been focused on biomass. However, TAR yields can be up to 2 orders of magnitude higher

when considering plastics as the main feedstock (Wilk & Hofbauer, 2013). One option is to remove them from the produced syngas, usually by absorption processes or by reducing the temperature and condensing them into an aqueous stream. Nonetheless, this route should include post-treatment units for a more detailed assessment. Especially considering that an important share of the carbon in the feedstock is present in these compounds. For instance, they could be separated and recycled back to the combustion chamber of the gasifier. Thus, reducing the need for additional fuel. Another alternative is to eliminate them in the gasification process. The use of active bed materials, such as olivine, has proven to reduce the amount of generated TARs (Berdugo Vilches et al., 2016). However, not to the extent required by the catalyst in chemical processing. Another interesting option is to use a mix of plastics and biomass. In fact, some studies have found the interaction between the gasification products from mixed plastics with biomass can decrease TAR formation (Weiland et al., 2021). This could be an opportunity to reduce the mass demand of the process, the generation of wastes, and still promote circularity in waste management systems. Moreover, the overall cost of the process could be reduced depending on the mix of raw materials. However, more research is needed to determine ratios, compatibility between types of plastics and biomass wastes, content of the produced syngas, and optimum operating conditions.

The second condition is the flue gases generated in the combustion chamber. Unless another high temperature technology is used to heat the plastics to 900 °celsius, waste gases from the gasification will be the main bottleneck for the environmental performance of the plastic-to-methanol route. The results from the simulation estimate a production of CO_2 equal to 40% of the demand for the CO_2 hydrogenation step. This of course, using natural gas as additional fuel to the unreacted char. Therefore, there is a great opportunity for process integration and re-utilization of waste streams. Adding a CO_2 recovery unit could not only reduce the carbon emissions from the process, but it might also improve the financial feasibility of the project. This could be achieved considering the captured CO_2 as an additional carbon source for the methanol production.

The third condition is the CH_4 content in the syngas. Contrary to the CO_2 hydrogenation pathway, methane is not removed in the plastic-to-methanol process. Even though the concentration is low (1% of the syngas mass flow), the re-circulation during methanol synthesis ends up accumulating a large amount of gas. In fact, CH_4 accounts for 55% of the mass fraction of the outlet to the methanol reactor. This in turn translates into oversized equipment and utility consumption, in addition to be a potential source of GHG emissions. Although methane does not pose a threat to the catalyst, it can reduce the partial pressure of reactants and consequently, the efficiency of the process. Overall, it has an impact in the economic performance of the technology. Therefore, adding a separation unit could improve the financial conditions of the project and make it even more attractive. One alternative is to use a similar process to the one used in the CO_2 purification system. This would require the addition of a TSA system and a cryogenic distillation column, which could remove the majority of the CH_4 and Ar. The added cost would then have to be weighted against the reduction in CAPEX and OPEX from smaller unit operations and the reduction in methane emissions. Additionally, a carbon captured unit would have to be included to separate the CO_2 from the flue gases and return it to the methanol synthesis step. In this way, eliminating the highest source for carbon emissions. Furthermore, the design of the methanol synthesis was based on previous research on CO_2 hydrogenation. Naturally, operating conditions of heat exchangers and the distillation columns were adjusted to the inlet conditions of the syngas. However, there was no in depth analysis to optimize the process through variations in the layout.

Despite the better economic performance of the plastic-to-methanol route, the sensitivity analysis from Chapter 7 shows a large dependence to the variations in the market price of methanol. This uncertainty needs to be considered when deciding future investments. Especially, taking into account that the results from the Pedigree workshop also assigned medium levels of confidence to some of the parameters used as input to the process model (Chapter 5), which represent the basis for the calculations of the economic assessment. In this sense, the results show more confidence in the estimations of the economic performance for the CO_2 hydrogenation cases. Although the sensitivity analysis also showed high uncertainty with respect to the methanol price for this alternative route.

Table 8.1 also indicates a gap between the LCOMeOH calculated in this research with the ones found in

literature. This can be explained by the design of the process and the differences in the raw materials. Therefore, even though items such as fixed capital costs are higher for the CO_2 hydrogenation route, the LCOMeOH is lower. In effect, two separate plants are considered for this case study, one for the CO_2 Purification System and one for the CO_2 hydrogenation. Therefore, doubling the amount of labour for half the production output. However, both reference studies used green hydrogen as feedstock, with a cost 3 to 4 times higher than the one used for the supply of grey hydrogen. This ultimately plays a larger role in the economic performance, as it was previously demonstrated in section 6.3.

To understand the options for cost reduction, the influence of the purification steps in the levelized cost of methanol is measured and depicted in Figure 8.1. The results show the share from the purification units increase as the costs from the raw materials decline. This becomes relevant when comparing the technical and environmental advantages of the technologies to make an investment decision. For instance, addressing the costs from the purification systems may help to achieve the financial feasibility of both technologies. This highlights the relevance of the purification steps to the performance of the technologies. Nonetheless, the higher cost in the purification steps of the Plastic-to-Methanol route is influenced by two factors. First, the raw material is completely sourced during this stage of the process. Conversely, the hydrogen in the CO_2 hydrogenation route is supplied during the methanol synthesis. Second, this share includes the 4-stage compressor needed to pressurize the syngas from atmospheric pressure to 50 bars.

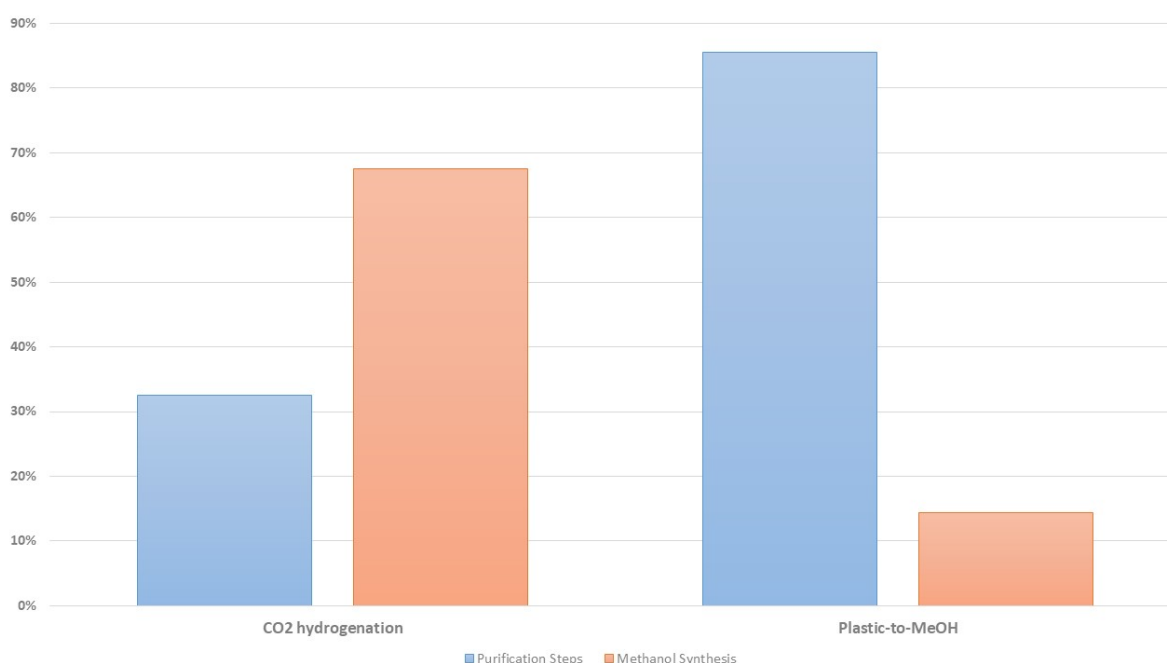


Figure 8.1: Contribution of the CO_2 Purification System to the levelized cost of MeOH

Another difference with the values reported from literature is the consumption of H_2 and CO_2 (here reported as carbon consumption). This directly relates to the impurity levels included in this research and their effect on the process design. For example, Nyári et al., 2020 recycled 99.9 wt% of the unreacted gases separated from the outlet of the methanol reactor. However, using the same specification for the simulations in this study increased the nitrogen concentration above the limit of $0.1 \text{ mg}/Nm^3$. Thus, 0.25 wt% was defined as purge instead. Likewise, the presence of other compounds changes the conditions from the distillation columns. Because of the higher content of unreacted gas materials, a larger fraction has to be separated in the liquid-vapor condenser of the second distillation column. Otherwise, the final product doesn't reach the purity specification of 99.9 wt%. Therefore, more methanol leaves the process as waste. Additionally, the property method in the simulation was improved to account for non-ideal interactions. This modification reduced the amount of methanol recovered from the unit operations. All these findings highlight the relevance of the CO_2 purification system to the techno-economic assessment, which ultimately impacts the performance of technologies in all dimensions.

The utility consumption is found to play an important role, with the majority of the demand coming from the methanol synthesis process. In this case, there is a similar opportunity for both technologies to increase their energy efficiency, and consequently, their economic performance. The findings from previous techno-economic evaluations suggest that the hot utility requirements could be completely covered by the available heat from the process. Moreover, Szima & Cormos used the excess heat from the methanol reactor to produce steam and generate electricity, covering the entire non-cooling utility demand of the plant (Szima & Cormos, 2018). In this scenario, the plastic-to-methanol route is better positioned. On the one hand, the reaction between carbon monoxide and hydrogen generates almost twice as much heat than the hydrogenation of CO_2 . Also, the absence of water in the outlet stream of the reactor creates better conditions for heat exchange. On the other hand, the only utility demand from the gasification and syngas conditioning process comes from the compressor train, which requires a minimum amount of cooling water. Therefore, potentially all the hot utility demand could be met by generating low pressure steam on-site. The excess heat could be used to power steam turbines and produce electricity to supply the demand from the overall process. In comparison, the CO_2 Purification System is responsible for about 20% of the low pressure steam demand. But more importantly, it requires 2.5 MW of high temperature heat for the catalytic oxidation unit and consumes 5.3 MW of refrigerant in the cryogenic distillation. Together, they account for 66% of the utility demand (besides electricity) from the CO_2 Purification System, which could not be sourced from a better heat integration design. Nonetheless, there is a potential of reduction in utility consumption for both processes, that becomes more evident when compared with the references. Optimizing the layout for heat integration would improve the environmental and economic performance of the two case studies. Which in turn, could make the CO_2 hydrogenation process feasible, even under a scenario sourced with green or blue H_2 .

The results from the alternative hydrogen sources showed that the electrolysis unit reduces the financial performance considerably. The economic assessment concluded a levelized cost methanol of 1.36 €/kg is achieved in the case of on-site hydrogen production. Moreover, the results are obtained assuming an operating load of 8000 hr/yr (i.e., 91.3% capacity factor) and a fixed electricity price of 0.088 €/kWh. Lower levelized cost of electricity could be assumed considering the use of renewable sources. However, the economic benefits would be offset by lower capacity factor. Other wise, storage alternatives would have to be included in the economic evaluation. Furthermore, the power consumption from the electrolysis unit would require more than a third of the capacity from the largest offshore wind farm in the Netherlands (Statista, 2021). Nonetheless, it is worth noting there is a large uncertainty behind this assumptions, and thus, on-site hydrogen production from electrolysis might be a viable alternative in geographical locations with access to cheap, continuous, renewable electricity.

The second case study analyzed the alternative for methanol production using renewable hydrogen sourced from outside the plant. Again, the results highlight the cost of hydrogen as the main bottleneck for the project to achieve financial feasibility. Considering the same operating conditions as for the base case, the results suggest that even with a green hydrogen price of 1.1 €/kg, the project would still not be feasible. Thus, reducing the hydrogen price is paramount, but not enough to achieve market competitiveness. Consequently, cost reductions from other steps of the process also need to be addressed.

Finally, there are potential incentives which could benefit the economic performance of both technologies. For instance, no incentives to the use of captured CO_2 or plastics wastes were included in the evaluations. However, this could prove difficult to quantify. Because, depending on the final application of the produced methanol, different accounting methods are considered. Based on whether or not the consumed carbon is permanently stored. Therefore, the added benefit of producing methanol for fuel consumption or to replace fossil fuel based plastics might differ. Another potential incentive relates to energy security, particularly in the Netherlands. In the framework of searching for energy independence, renewable alternatives for methanol production offer a pathway for domestic production. This type of government guidelines have been already implemented and proved successful in driving up production of alternative fuels.

Conclusions and Future Works

The purpose of this research was to comparatively assess the competitiveness of two alternative, renewable routes for methanol production through the use of techno-economic and environmental key performance indicators. To do so, two manufacturing technologies were selected and purification steps were included based on the conditions of the raw materials. The two process considered for the assessment were:

1. CO_2 hydrogenation
2. Plastic-to-methanol

The trade-offs between the technologies were weighted against each other, compared with references from literature, and to a conventional steam methane reforming plant. Additionally, opportunities for improvement in technical, economic, and environmental performance were discussed.

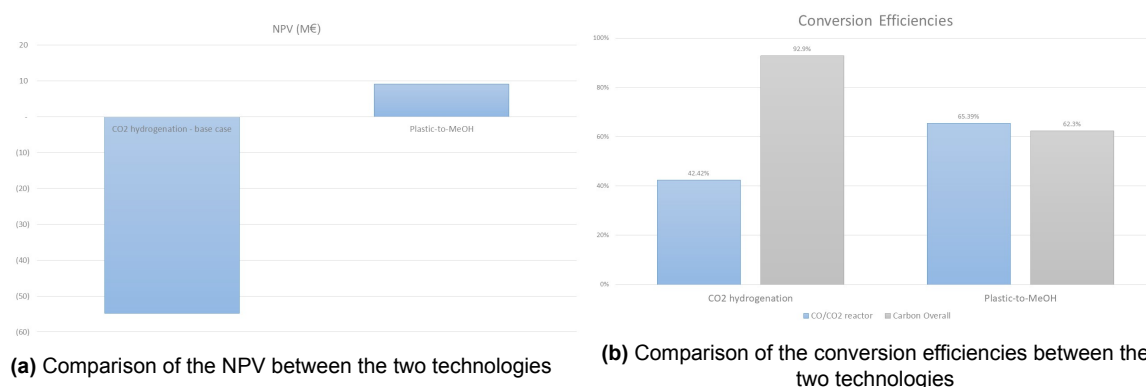


Figure 9.1: Comparative assessment of two renewable methanol production routes

The assessment showed neither technology outperforms the others in every metric. From an economic perspective, the assessment indicates the plastic-to-methanol stands as the best alternative. In fact, it is the only case study with a positive NPV over a 25 lifetime period (Figure 9.1a). Moreover, the technology showed the best reactor conversion rates when using the same stoichiometric inlet ratio. Highlighting the importance of the different reaction kinetics. However, when expanding the comparison to the overall carbon conversion, the results suggest the CO_2 hydrogenation as the best alternative (Figure 9.1b). The study showed this variation was caused by higher wastes during the gasification and syngas conditioning steps.

Moreover, the impact from the lower system efficiency in the plastic-to-methanol route was evidenced in the environmental KPIs. Contrary to the economic evaluation, the plastic-to-methanol pathway underperformed in this dimension. Particularly, due to the high emissions of flue gases during combustion

and the generation of TARs from the gasifier. Nonetheless, it was noted that the assessment was limited by not considering the intake of bioplastic nor the emissions avoided. Likewise, in the evaluation of the CO_2 hydrogenation route, the carbon content of the raw materials was not taken into account.

The comparative assessment between the different sources of H_2 showed using an on-site electrolyser is still not a viable alternative. The only condition in which this might perform better is in the presence of constant and cheap renewable electricity. But this would also have to come by the hand of lower CAPEX. On the other hand, the high cost of green H_2 is the main bottlenecks for financial feasibility of the second alternative. Nonetheless, the environmental performance could be improved by changing the source of hydrogen to renewable options.

The results also highlighted the comparative advantage of the reaction between H_2 and CO , versus CO_2 . Even though the study found large amounts of CH_4 and Ar get trapped in the plastic-to-methanol route, both H_2 and carbon conversions in the reactor outperformed the CO_2 hydrogenation technologies.

Furthermore, the main finding from this study is the influence of the purification steps. On the one hand, the assessment showed that the CO_2 purification system impacts 33 % of the LCOMeOH in the CO_2 hydrogenation route. Moreover, it did not had a great effect on the technical or environmental performance. In fact, 5% of the inlet CO_2 is accounted to be loss during the purification units. On the other hand, the purification needs from the plastic-to-methanol process played a major role in the lower environmental performance of the technology. With the majority of the wastes associated to the flue gases.

These findings underscore the relevance of including the purification steps in the techno-economic and environmental evaluations of converting CO_2 or plastic wastes to methanol.

Finally, this study designed two processes based on the main technologies, but it did not optimize the layout or the energy consumption of the unit operations. With this in consideration, the following recommendations for future works are made:

- A comparison of the results with other techno-economic studies on CO_2 hydrogenation showed there is room for improvement with respect to the utility consumption. The energy integration of the processes was out of the scope of the thesis project, however, the findings highlight the necessity to explore alternatives for cost reductions. Moreover, there is a great source of medium temperature heat from the methanol reactor that can be used for steam generation.
- The plastic-to-methanol route could benefit from adding one more purification step. Because of the characteristics of the methanol synthesis process, it was found that the accumulation of CH_4 in the recycling loop was significant. While it does not harm the catalyst, it does increase the investment and operational costs of the plant. Removing it before the inlet to the reactor could improve the financial performance of the technology.
- Now that the influence of the CO_2 purification system is highlighted, there is a need to find alternative ways of treatment and process integration. Furthermore, analysis of the overall implications of the purification steps should be included. This means studying the impacts and costs of re-generation units and/or waste treatments.
- In addition, there are immediate actions that could prove beneficial for both technologies. The first one is to include the use of by-products from both processes. These could mean, for example, to explore other treatments that add value to the generated TAR compounds. Similarly, the off-gases from the methanol synthesis could be burn in a furnace to produce steam. Or alternatively, the use of on-site electrolysis with the added value of selling the by-product oxygen.
- Finally, the environmental assessment of both routes needs to be improved by conducting a LCA with a larger scope. That includes the carbon content from the supply of raw materials and the final application of the product.

Bibliography

- Abdelouahed, L., Authier, O., Mauviel, G., Corriou, J. P., Verdier, G., & Dufour, A. (2012). Detailed modeling of biomass gasification in dual fluidized bed reactors under aspen plus. *Energy and Fuels*, 26(6), 3840–3855. <https://doi.org/10.1021/ef300411k>
- Abdoulmoumine, N., Adhikari, S., Kulkarni, A., & Chattanathan, S. (2015). A review on biomass gasification syngas cleanup. *Applied Energy*, 155, 294–307. <https://doi.org/10.1016/j.apenergy.2015.05.095>
- Adams, T. A., Salkuyeh, Y. K., & Nease, J. (2014). *Processes and simulations for solvent-based CO2 capture and syngas cleanup*. <https://doi.org/10.1016/B978-0-444-59566-9.00006-5>
- Adnan, M. A., & Kibria, M. G. (2020). Comparative techno-economic and life-cycle assessment of power-to-methanol synthesis pathways. *Applied Energy*, 278(May), 115614. <https://doi.org/10.1016/j.apenergy.2020.115614>
- Albo, J., Alvarez-Guerra, M., Castaño, P., & Irabien, A. (2015). Towards the electrochemical conversion of carbon dioxide into methanol. *Green Chemistry*, 17(4), 2304–2324. <https://doi.org/10.1039/c4gc02453b>
- Armijo, J. (2019). ScienceDirect Flexible production of green hydrogen and ammonia from variable solar and wind energy : Case study of Chile and Argentina. 5. <https://doi.org/10.1016/j.ijhydene.2019.11.028>
- Aspen Plus. (2001). *Aspen Physical Property System Physical Property Methods and Models* (tech. rep.).
- Berdugo Vilches, T., Marinkovic, J., Seemann, M., & Thunman, H. (2016). Comparing Active Bed Materials in a Dual Fluidized Bed Biomass Gasifier: Olivine, Bauxite, Quartz-Sand, and Ilmenite. *Energy and Fuels*, 30(6), 4848–4857. <https://doi.org/10.1021/acs.energyfuels.6b00327>
- Bezuidenhout, G. A., Davis, J., Van Beek, B., & Eksteen, J. J. (2012). Operation of a concentrated mode dual-alkali scrubber plant at the Lonmin smelter. *Journal of the Southern African Institute of Mining and Metallurgy*, 112(7), 657–665.
- Block, C., Ephraim, A., Weiss-Hortala, E., Pham Minh, D., Nzihou, A., & et al. (2019). Co-pyrogasification of plastics and biomass: A review. *Waste and Biomass Valorization*, Springer. 10(3), 483–509. <https://doi.org/10.1007/s12649-018-0219-8>
- Borgogna, A., Salladini, A., Spadacini, L., Pitrelli, A., Annesini, M. C., & Iaquaniello, G. (2019). Methanol production from Refuse Derived Fuel: Influence of feedstock composition on process yield through gasification analysis. *Journal of Cleaner Production*, 235, 1080–1089. <https://doi.org/10.1016/j.jclepro.2019.06.185>
- Cerro, R., Higgins, B. G., & Whitaker, S. (2001). *Material Balances for Chemical Engineers University of California at Davis*. John Wiley Sons Inc.
- Chang, M. B., Lee, H. M., Wu, F., & Lai, C. R. (2004). Simultaneous removal of nitrogen oxide/nitrogen dioxide/sulfur dioxide from gas streams by combined plasma scrubbing technology. *Journal of the Air & Waste Management Association*, 54(8), 941–949. <https://doi.org/10.1080/10473289.2004.10470965>
- Chatterton, C. (2019). "METHANOL AS A VESSEL FUEL AND ENERGY CARRIER". METHANOL INSTITUTE, PRESENTATION TO THE INTERNATIONAL TANKER TECHNICAL FORUM, SINGAPORE, 12 SEPTEMBER. <https://www.methanol.org/wp-content/uploads/2019/09/Methanol-as-a-vessel-fuel-and-energy-carrier.pdf>
- Chen, L., Lin, J. W., & Yang, C. L. (2002). Absorption of NO2 in a packed tower with Na2SO3 aqueous solution. *Environmental Progress*, 21(4), 225–230. <https://doi.org/10.1002/ep.670210411>
- Climate Tracker. (2020). Addressing global warming [Online; accessed 25/11/2020].
- Córdoba, P. (2015). Status of Flue Gas Desulphurisation (FGD) systems from coal-fired power plants : Overview of the physic-chemical control processes of wet limestone FGDs. 144, 274–286. <https://doi.org/10.1016/j.fuel.2014.12.065>
- CRI. (2011). George Olah Renewable Methanol Plant. Carbon Recycling International. <https://www.carbonrecycling.is/projects#project-goplant>

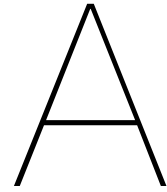
- Dalrymple, D. (2014). *Hybrid Sulfur Recovery Process for Natural Gas Upgrading. Final Report* (tech. rep.) [DOE No. DE-FC26-99FT40725]. DOE.
- Davidson, M. G., Furlong, R. A., & McManus, M. C. (2021). Developments in the life cycle assessment of chemical recycling of plastic waste – A review. *Journal of Cleaner Production*, 293, 126163. <https://doi.org/10.1016/j.jclepro.2021.126163>
- De Jong, W., & Van Ommen, J. R. (2014). *Biomass as a Sustainable Energy Source for the Future: Fundamentals of Conversion Processes* (Vol. 9781118304914). <https://doi.org/10.1002/9781118916643>
- de Paula, A. C., Hneriquez, J. R., & Figueiredo, F. A. (2020). Dimensioning a Cyclone Separator for Circulating Fluidized Bed Gasifier. Validation of a Procedure.pdf. *Heat Transfer Engineering*, 41, 1305–1314.
- Desai, M. G. (2018). Specifying carbon dioxide centrifugal compressor. *SPE Production and Operations*, 33(2), 313–319. <https://doi.org/10.2118/182992-pa>
- Elsernagawy, O. Y., Hoadley, A., Patel, J., Bhatelia, T., Lim, S., Haque, N., & Li, C. (2020). Thermo-economic analysis of reverse water-gas shift process with different temperatures for green methanol production as a hydrogen carrier. *Journal of CO2 Utilization*, 41(July), 101280. <https://doi.org/10.1016/j.jcou.2020.101280>
- Environmental Protection Agency. (2021). Understanding Global Warming Potentials. <https://www.epa.gov/ghgemissions/understanding-global-warming-potentials>
- European Commission. (2018). *A European Strategy for Plastics in a Circular Economy* (tech. rep. No. 11). <https://doi.org/10.4325/seikeikakou.30.577>
- European Commission. (2020). PORTHOS CO2 transport network. <https://ec.europa.eu/inea/en/printpdf/13766>
- European Environment Agency. (2019). Greenhouse gas emission intensity of electricity generation in Europe - Netherlands. <https://www.eea.europa.eu/data-and-maps/indicators/overview-of-the-electricity-production-3/assessment-1>
- Gao, R., Zhang, C., Lee, Y. J., Kwak, G., Jun, K. W., Kim, S. K., Park, H. G., & Guan, G. (2020). Sustainable production of methanol using landfill gas via carbon dioxide reforming and hydrogenation: Process development and techno-economic analysis. *Journal of Cleaner Production*, 272, 122552. <https://doi.org/10.1016/j.jclepro.2020.122552>
- Global Petrol Prices. (2021). Netherlands natural gas prices. https://www.globalpetrolprices.com/Netherlands/natural_gas_prices/
- Government of The Netherlands. (2019). *Climate agreement*.
- Government of The Netherlands. (2020). Government strategy on hydrogen.
- GPSA. (2004). *Engineering Data Book* (12th - FPS). Gas Processors Suppliers Association.
- Graaf, G. H., Stamhuis, E. J., & Beenackers, A. A. (1988). Kinetics of low-pressure methanol synthesis. *Chemical Engineering Science*, 43(12), 3185–3195. [https://doi.org/10.1016/0009-2509\(88\)85127-3](https://doi.org/10.1016/0009-2509(88)85127-3)
- Gradus, R. H., Nillesen, P. H., Dijkgraaf, E., & van Koppen, R. J. (2017). A cost-effectiveness analysis for incineration or recycling of dutch household plastic waste. *Ecological Economics*, 135, 22–28. <https://doi.org/https://doi.org/10.1016/j.ecolecon.2016.12.021>
- Gülşah Sönmez, H. (2017). *TECHNO-ECONOMIC EVALUATION OF A LIQUID REDOX PROCESS EMPLOYING AMINO ACID SALTS FOR SOUR NATURAL GAS TREATMENT* (Doctoral dissertation). Technical University of Berlin.
- Hantoko, D., Yan, M., Prabowo, B., Susanto, H., Li, X., & Chen, C. (2019). *Aspen plus modeling approach in solid waste gasification*. Elsevier B.V. <https://doi.org/10.1016/B978-0-444-64083-3.00013-0>
- Harkin, T., Filby, I., Sick, H., Manderson, D., & Ashton, R. (2017). Development of a CO2 specification for a CCS hub network. *Energy Procedia*, 114, 6708–6720.
- Harkin, T., Sick, H., & Ashton, R. (2017). Development of a CO 2 specification for a CCS hub network. *Energy Procedia*, 114(November 2016), 6708–6720. <https://doi.org/10.1016/j.egypro.2017.03.1801>
- He, J., Göransson, K., Söderlind, U., & Zhang, W. (2012). Simulation of biomass gasification in a dual fluidized bed gasifier. *Biomass Conversion and Biorefinery*, 2(1), 1–10. <https://doi.org/10.1007/s13399-011-0030-2>
- Heim, C. J., & Gupta, A. (1999). CO2 purification system.

- Horikawa, M. S., Rossi, F., Gimenes, M. L., Costa, C. M., & Da Silva, M. G. (2004). Chemical absorption of H₂S for biogas purification. *Brazilian Journal of Chemical Engineering*, 21(3), 415–422. <https://doi.org/10.1590/S0104-66322004000300006>
- IEA. (2020a). *Chemicals* [Online; accessed 25/11/2020]. International Energy Agency. <https://www.iea.org/reports/chemicals>
- IEA. (2020b). *The netherlands 2020: Energy policy review*. International Energy Agency.
- Ikechukwu, K. (2017). *Comparison of CO₂ dehydration processes after CO₂ capture* (Doctoral dissertation). University College of Southeast Norway.
- Institute, M. (2021). METHANOL PRICE AND SUPPLY/DEMAND. <https://www.methanol.org/methanol-price-supply-demand/>
- IOGP, & European Commission. (2019). *The potential for CCS and CCU in Europe* (tech. rep. June). IOGP. https://ec.europa.eu/info/sites/info/files/iogp_-_report_-_ccs_ccu.pdf
- IPCC. (2005). *IPCC Special Report on Carbon Dioxide Capture and Storage. Prepared by Working Group III of the Intergovernmental Panel on Climate Change* (tech. rep.) [Metz, B., O. Davidson, H. C. de Coninck, M. Loos, and L. A. Meyer (eds.)]. United Kingdom, New York, NY, USA. <https://doi.org/10.1002/9783527818488.ch15>
- IPCC. (2018). *Global Warming of 1.5°C. An IPCC Special Report on the impacts of global warming of 1.5°C above pre-industrial levels and related global greenhouse gas emission pathways, in the context of strengthening the global response to the threat of climate change* (tech. rep.) [Masson-Delmotte, V. and Zhai, P and Pörtner, H.-O. and Roberts, D. Skea, J. and Shukla, P.R. and Pirani, A. and Moufouma-Okia, W. and Péan, C. and Pidcock, R. and Connors, S. and Matthews, J.B.R. and Chen, Y. and Zhou, X. and Gomis, M.I. and Lonnoy, E. and Maycock, T. and Tignor, M, and T. Waterfield (eds.). In press].
- IRENA. (2020). *Green Hydrogen Cost Reduction: Scaling up Electrolysers to Meet the 1.5°C Climate Goal* (tech. rep.). /publications/2020/Dec/Green-hydrogen-cost-reduction%0Ahttps://www.irena.org/-/media/Files/IRENA/Agency/Publication/2020/Dec/IRENA_Green_hydrogen_cost_2020.pdf
- IRENA. (2021). *INNOVATION OUTLOOK: RENEWABLE METHANOL* (tech. rep.). International Renewable Energy Agency.
- Kajaste, R., Hurme, M., & Oinas, P. (2018). Methanol-Managing greenhouse gas emissions in the production chain by optimizing the resource base. *AIMS Energy*, 6(6), 1074–1102. <https://doi.org/10.3934/energy.2018.6.1074>
- Kannan, P., Al Shoaibi, A., & Srinivasakannan, C. (2011). Optimization of Waste Plastics Gasification Process Using Aspen-Plus. In Y. Yun (Ed.), *Gasification for practical applications*. <https://www.intechopen.com/books/advanced-biometric-technologies/liveness-detection-in-biometrics>
- Karpuk, M. E. (2003). CATALYSTS AND PROCESS FOR OXIDIZING HYDROGEN SULFIDE TO SULFUR DIOXIDE AND SULFUR.
- Kazemi, A., Malayeri, M., Gharibi kharaji, A., & Shariati, A. (2014). Feasibility study, simulation and economical evaluation of natural gas sweetening processes – part 1: A case study on a low capacity plant in iran. *Journal of Natural Gas Science and Engineering*, 20, 16–22. <https://doi.org/https://doi.org/10.1016/j.jngse.2014.06.001>
- Kiss, A. A., Pragt, J. J., Vos, H. J., Bargeman, G., & de Groot, M. T. (2016). Novel efficient process for methanol synthesis by CO₂ hydrogenation. *Chemical Engineering Journal*, 284, 260–269. <https://doi.org/10.1016/j.cej.2015.08.101>
- Kotowicz, J., Włocel, D., & Brzóczek, M. (2021). Analysis of the work of a “renewable” methanol production installation based ON H₂ from electrolysis and CO₂ from power plants. *Energy*, 221. <https://doi.org/10.1016/j.energy.2020.119538>
- Krishnamurthy, G., Higdon, C. R., Kretz, C. P., Gagliardi, C. R., Duffy, K. M., & Hsu, K.-K. (2015). PROCESS AND SYSTEM FOR SYNGAS TREATMENT.
- Kung, H. H. (1992). Deactivation of methanol synthesis catalysts - a review. *Catalysis Today*, 11(4), 443–453. [https://doi.org/10.1016/0920-5861\(92\)80037-N](https://doi.org/10.1016/0920-5861(92)80037-N)
- Lee, H. W., Kim, K., An, J. J., Na, J., Kim, H., Lee, H., & Lee, U. (2020). Toward the practical application of direct CO₂ hydrogenation technology for methanol production. *International Journal of Energy Research*, 44(11), 8781–8798. <https://doi.org/10.1002/er.5573>

- Li, S., Cañete, I., Järvinen, M., & Seemann, M. (2021). Polyethylene terephthalate (PET) recycling via steam gasification – The effect of operating conditions on gas and tar composition. *Waste Management*, *130*, 117–126. <https://doi.org/10.1016/j.wasman.2021.05.023>
- Lopez, G., Artetxe, M., Amutio, M., Alvarez, J., Bilbao, J., & Olazar, M. (2018). Recent advances in the gasification of waste plastics. A critical overview. *Renewable and Sustainable Energy Reviews*, *82*(May 2017), 576–596. <https://doi.org/10.1016/j.rser.2017.09.032>
- Marcantonio, V., Bocci, E., Pieter Ouweltjes, J., Del Zotto, L., & Monarca, D. (2020). Evaluation of sorbents for high temperature removal of tars, hydrogen sulphide, hydrogen chloride and ammonia from biomass-derived syngas by using aspen plus. *International Journal of Hydrogen Energy*, *45*(11), 6651–6662. <https://doi.org/https://doi.org/10.1016/j.ijhydene.2019.12.142>
- MarketInsider. (2021). CO2 EUROPEAN EMISSION ALLOWANCES [Accessed June 2021]. <https://markets.businessinsider.com/commodities/co2-european-emission-allowances>
- Merck. (2021). Price of Sodium Carbonate [Accessed June 2021]. <https://www.sigmaaldrich.com/HR/en/product/sigald/223530?context=product>
- MERICHEM. (n.d.). Removing H2S from Gas Streams. LO-CAT Sulfur Recovery Technology. <https://www.merichem.com/technology/sulfur-recovery-with-lo-cat/>
- Methanex. (2020). Methanol as a Marine Fuel. https://www.methanex.com/sites/default/files/methanex_brochure_marinefuel_final2_032521.pdf
- Methanex. (2021). Methanex European Posted Contract Price (Valid April 1, 2021 - June 30, 2021). <https://www.methanex.com/our-business/pricing>
- Miskam, M. A. (2006). Performance and Characteristics of a Cyclone Gasifier PERFORMANCE AND CHARACTERISTICS OF A CYCLONE GASIFIER by MUHAMAD AZMAN MISKAM Thesis submitted in fulfillment of the requirements for the degree of Master of Science NOVEMBER 2006. (November), 1–43.
- MMSA. (2021). “Methanol price and supply/demand”. *Methanol Institute*. Methanol Market Services Asia. <https://www.methanol.org/methanol-pricesupply-demand/>
- Murra, M. (2014). *Set up and test of a cryogenic distillation column for the XENON1T experiment* (Doctoral dissertation January). Westfälische Wilhelms-Universität Münster.
- Mutlu, Ö. Ç., & Zeng, T. (2020). Challenges and Opportunities of Modeling Biomass Gasification in Aspen Plus: A Review. *Chemical Engineering and Technology*, *43*(9), 1674–1689. <https://doi.org/10.1002/ceat.202000068>
- Nastaj, J., & Ambrozek, B. (2015). Analysis of gas dehydration in TSA system with multi-layered bed of solid adsorbents. *Chemical Engineering and Processing: Process Intensification*, *96*, 44–53. <https://doi.org/10.1016/j.cep.2015.08.001>
- Nel Hydrogen. (2019). The World’s Most Efficient and Reliable Electrolysers. <https://nelhydrogen.com/wp-content/uploads/2020/03/Electrolysers-Brochure-Rev-C.pdf>
- Netherlands Enterprise Agency. (2020). Stimulation of sustainable energy production and climate transition (sde++) [Online; accessed November 2020]. <https://english.rvo.nl/subsidies-programmes/sde>
- NREL. (2018). H2A: Hydrogen Analysis Production Models. <https://www.nrel.gov/hydrogen/h2a-production-models.html>
- Nyári, J., Magdeldin, M., Larmi, M., Järvinen, M., & Santasalo-Aarnio, A. (2020). Techno-economic barriers of an industrial-scale methanol CCU-plant. *Journal of CO2 Utilization*, *39*(January), 101166. <https://doi.org/10.1016/j.jcou.2020.101166>
- Onyebuchi, V. E., Kolios, A., Hanak, D. P., Biliyok, C., & Manovic, V. (2018). A systematic review of key challenges of CO2 transport via pipelines. *Renewable and Sustainable Energy Reviews*, *81*(June 2016), 2563–2583. <https://doi.org/10.1016/j.rser.2017.06.064>
- Ott, J., Gronemann, V., Pontzen, F., Fiedler, E., Grossmann, G., Kersebohm, D. B., Weiss, G., & Witte, C. (2012). Methanol. *Ullmann’s encyclopedia of industrial chemistry*. American Cancer Society. https://doi.org/https://doi.org/10.1002/14356007.a16_465.pub3
- PBL Netherlands Environmental Assessment Agency. (2020). *Netherlands climate and energy outlook 2020 summary* [PBL publication number: 4299].
- Pérez-Fortes, M., & Tzimas, E. (2016). *Techno-economic and environmental evaluation of CO2 utilisation for fuel production. Synthesis of methanol and formic acid* (tech. rep.). <https://doi.org/10.2790/89238>

- Pérez-Fortes, M., Schöneberger, J. C., Boulamanti, A., & Tzimas, E. (2016). Methanol synthesis using captured CO₂ as raw material: Techno-economic and environmental assessment. *Applied Energy*, 161, 718–732. <https://doi.org/10.1016/j.apenergy.2015.07.067>
- Puig-Gamero, M., Argudo-Santamaria, J., Valverde, J. L., Sánchez, P., & Sanchez-Silva, L. (2018). Three integrated process simulation using aspen plus®: Pine gasification, syngas cleaning and methanol synthesis. *Energy Conversion and Management*, 177(June), 416–427. <https://doi.org/10.1016/j.enconman.2018.09.088>
- Rafiee, A. (2020). Modelling and optimization of methanol synthesis from hydrogen and co₂. *Journal of Environmental Chemical Engineering*, (8), 10413.
- Ramirez-Ramirez, A. (2019). Unravelling the impacts of using alternative raw materials in industrial clusters [Simulation Guidelines. Vici DO. Research number: TTW VI.C.183.010.]. <https://www.nwo.nl/en/projects/ttw-vic183010>
- Ramzan, N., Ashraf, A., Naveed, S., & Malik, A. (2011). Simulation of hybrid biomass gasification using Aspen plus: A comparative performance analysis for food, municipal solid and poultry waste. *Biomass and Bioenergy*, 35(9), 3962–3969. <https://doi.org/10.1016/j.biombioe.2011.06.005>
- Rijk, N., & Van Dinther, J. (2019). *Rotterdam Hydrogen Hub* (tech. rep.). SmartPort.
- Risbey, J. S., Tuinstra, W., & Ravetz, J. R. (2004). *RIVM / MNP Guidance for Uncertainty Assessment and Communication : Tool Catalogue for Uncertainty Assessment*.
- Sadighi, Sepehr and Seif, R. (2018). Process simulation and optimization of catalytic reactors of sulfur recovery unit (SRU) via aspen plus. *Pet Coal*, 60(1), 71–78. <https://doi.org/10.1021/ac00060a011>
- Saebea, D., Ruengrit, P., Arpornwichanop, A., & Patcharavorachot, Y. (2020). Gasification of plastic waste for synthesis gas production. *Energy Reports*, 6, 202–207. <https://doi.org/10.1016/j.egy.2019.08.043>
- Salladini, A., Borgogna, A., Agostini, E., Annesini, M. C., & Iaquaniello, G. (2020). Power to liquid through waste as a carbon source: A technical and economic assessment. *International Journal of Hydrogen Energy*, 45(46), 24467–24476. <https://doi.org/10.1016/j.ijhydene.2020.06.232>
- Sánchez, M., Amores, E., Abad, D., Rodríguez, L., & Clemente-Jul, C. (2020). Aspen Plus model of an alkaline electrolysis system for hydrogen production. *International Journal of Hydrogen Energy*, 45(7), 3916–3929. <https://doi.org/10.1016/j.ijhydene.2019.12.027>
- Schmidt, O., Gambhir, A., Staffell, I., Hawkes, A., Nelson, J., & Few, S. (2017). Future cost and performance of water electrolysis: An expert elicitation study. *International Journal of Hydrogen Energy*, 42(52), 30470–30492. <https://doi.org/10.1016/j.ijhydene.2017.10.045>
- Schmidt, P., & Weindorf, W. (2016). *Power-to-liquids. Potentials and Perspectives for the Future Supply of Renewable Aviation Fuel* (tech. rep. september). German Environment Agency. <https://www.umweltbundesamt.de/en/publikationen/%20power-to-liquids-potentials-perspectives-for-the>
- Shahabuddin, M., Alam, M. T., Krishna, B. B., Bhaskar, T., & Perkins, G. (2020). A review on the production of renewable aviation fuels from the gasification of biomass and residual wastes. *Bioresour Technol*, 312(March), 123596. <https://doi.org/10.1016/j.biortech.2020.123596>
- Sheldon, D. (2017). Methanol production - A technical history. *Johnson Matthey Technology Review*, 61(3), 172–182. <https://doi.org/10.1595/205651317X695622>
- Solis, M., & Silveira, S. (2020). Technologies for chemical recycling of household plastics – A technical review and TRL assessment. *Waste Management*, 105, 128–138. <https://doi.org/10.1016/j.wasman.2020.01.038>
- Spek, M. V. D., Ramirez, A., & Faaij, A. (2016). Improving uncertainty evaluation of process models by using pedigree analysis . A case study on CO₂ capture with monoethanolamine. 85, 1–15. <https://doi.org/http://dx.doi.org/10.1016/j.compchemeng.2015.10.006>
- Spek, M. V. D., Sanchez, E., Henrik, N., Skagestad, R., Ramirez, A., & Faaij, A. (2017). Unravelling uncertainty and variability in early stage techno-economic assessments of carbon capture technologies. *International Journal of Greenhouse Gas Control*, 56, 221–236. <https://doi.org/10.1016/j.ijggc.2016.11.021>
- Statista. (2021). Prices of electricity for industry in the Netherlands from 2008 to 2020. <https://www.statista.com/statistics/596254/electricity-industry-price-netherlands/>
- Sun, B., Dong, K., Zhao, W., Wang, J., Chu, G., Zhang, L., Zou, H., & Chen, J. F. (2019). Simultaneous Absorption of NO_x and SO₂ into Na₂SO₃ Solution in a Rotating Packed Bed with Preoxidation

- by Ozone. *Industrial and Engineering Chemistry Research*, 58(19), 8332–8341. <https://doi.org/10.1021/acs.iecr.9b01162>
- Szima, S., & Cormos, C.-C. (2018). Improving methanol synthesis from carbon-free h₂ and captured co₂: A techno-economic and environmental evaluation. *Journal of CO₂ utilization*, (24), 555–563.
- Takahashi, K. (2009). TRANSPORTATION OF HYDROGEN BY PIPELINE. *Energy carriers and conversion systems with emphasis on hydrogen* (pp. 148–159). Encyclopedia of Life Support Systems.
- Terrigeol, A. (2012). *Molecular Sieves Contaminants: Effects, Consequences and Mitigation* (tech. rep. May 2012).
- The Minister of Justice and Security. (2019). Climate act [Online; accessed November 2020]. <https://wetten.overheid.nl/BWBR0042394/2020-01-01>
- TNO. (n.d.). Phyllis Database. Retrieved December 1, 2020, from <https://phyllis.nl/>
- Torres, W., Pansare, S. S., & Goodwin, J. G. (2007). Hot gas removal of tars, ammonia, and hydrogen sulfide from biomass gasification gas. *Catalysis Reviews - Science and Engineering*, 49(4), 407–456. <https://doi.org/10.1080/01614940701375134>
- Towler, G., & Sinnott, R. (2013). *Chemical Engineering Design: principles, practice and economics of plant and process design* (2nd). Butterworth-Heinemann, Elsevier.
- Twigg, M. V., & Spencer, M. S. (2003). Deactivation of copper metal catalysts for methanol decomposition, methanol steam reforming and methanol synthesis. *Topics in Catalysis*, 22(3-4), 191–203. <https://doi.org/10.1023/A:1023567718303>
- VanNess, R., Somers, R., Frank, T., Ramans, G., LaMantia, C., Lunt, R., & Valencia, J. (1979). *Executive Summary for Full-Scale Dual-Alkali Demonstration System at Louisville Gas and Electric Co. — Final Design and System Cost* (tech. rep. September). US ENVIRONMENTAL PROTECTION AGENCY. Office of Research and Development EPA-600/7-79-221a.
- VNCl. (2018). *Chemistry for Climate : Acting on the need for speed. Roadmap for the Dutch Chemical Industry towards 2050* (tech. rep.).
- Weiland, F., Lundin, L., Celebi, M., Vlist, K. V. D., & Moradian, F. (2021). Aspects of chemical recycling of complex plastic waste via the gasification route. *Waste Management*, 126, 65–77. <https://doi.org/10.1016/j.wasman.2021.02.054>
- Wilk, V., & Hofbauer, H. (2013). Conversion of mixed plastic wastes in a dual fluidized bed steam gasifier. *Fuel*, 107, 787–799. <https://doi.org/10.1016/j.fuel.2013.01.068>
- Win, M. M., Asari, M., Hayakawa, R., Hosoda, H., Yano, J., & Ichi Sakai, S. (2019). Characteristics of gas from the fluidized bed gasification of refuse paper and plastic fuel (RPF) and wood biomass. *Waste Management*, 87, 173–182. <https://doi.org/10.1016/j.wasman.2019.02.002>
- Woolcock, P. J., & Brown, R. C. (2013). A review of cleaning technologies for biomass-derived syngas. *Biomass and Bioenergy*, 52, 54–84. <https://doi.org/10.1016/j.biombioe.2013.02.036>
- Xu, G., Liang, F., Yang, Y., Hu, Y., Zhang, K., & Liu, W. (2014). An improved co₂ separation and purification system based on cryogenic separation and distillation theory. *Energies*, 7(5), 3484–3502. <https://doi.org/10.3390/en7053484>
- Zauner, A., Böhm, H., Rosenfeld, D. C., & Tichler, R. (2019). *Innovative large-scale energy storage technologies and Power-to-Gas concepts after optimization. D7.7 Analysis on future technology options and on techno-economic optimization* (tech. rep. No. 691797).
- Zimmermann, A. W., Wunderlich, J., Müller, L., Buchner, G. A., Marxen, A., Michailos, S., Armstrong, K., Naims, H., McCord, S., Styring, P., Sick, V., & Schomäcker, R. (2020). Techno-Economic Assessment Guidelines for CO₂ Utilization. *Frontiers in Energy Research*, 8(January), 1–23. <https://doi.org/10.3389/fenrg.2020.00005>



Pedigree Analysis

The definition of the components chosen for the Pedigree assessment and the description of the Pedigree criteria¹, covered in section 5.2, are provided here.

A.1. Components evaluated

State of the Art

- **Feed streams:** The category refers to the level of understanding of the composition and conditions of feed streams used in the model. The score should reflect the quality and reliability of the information used to determine the characteristics of the feedstock. More details about the references and assumptions were provided in the attached files sent to the experts.
- **Design parameters:** This category represents the conditions and characteristics of unit operations and intermediate streams (e.g., temperature, pressure, number of stages in a distillation column, mixing or recycling ratios, etc.). The score should reflect the strength of the data used to choose the process's design parameters. Information on the references and assumptions were provided in the attached files.
- **Flow diagram:** This section refers to the information used to build a coherent process design. How reliable is the data used for deciding which unit operations are the best suited? which technologies to use? what should be the set-up? are the different stages of the process properly interconnected? etc. Scoring should be based on the strength or weakness of the flow diagram design to achieve the goal of the model. Additional information relevant to the scoring was provided in the attached files.

Simulation

- **Process line-ups:** The process line-ups category refers to the alignment between the flow diagram and the Aspen flow-sheet. The scoring should reflect whether the data gather from literature (feed compositions, process conditions, design of the flow diagram) is well interpreted and translated into the Aspen simulation environment. More information on the references and assumptions used for this section was shared with the experts on the attached files.
- **Property method:** The property method is a key parameter for the simulation. Choosing the wrong property package can considerably alter the accuracy of the model or prevent the software from performing the simulation. For this section, the score is meant to reflect the correctness of

¹The description of the Pedigree criteria is taken from Spek et al., 2016

the property method(es) used in the process model. Information on decisions, references, and assumptions were provided in the attached files.

- **Chemistry/Kinetics:** This category refers to how well are the chemical interactions from the process represented in the simulation. Scoring should reflect the level of understanding and the strength of the information and assumptions used to simulate the chemical reactions and/or kinetics of the process. Relevant information for the evaluation was shared in the attached files.
- **Unit operations:** This category is meant to assess the modeling of process steps (equipments). The goal is to score on the accuracy of the modeling inputs based on the available data from the literature and the experience of the experts. All the information regarding the inputs, assumptions, and references was provided in the documents shared with the experts.

A.2. Pedigree Criteria

- **Proxy:** Sometimes it is not possible to represent directly the thing we are interested in by a parameter so some form of proxy measure is used. Proxy refers to how good or close a measure of the quantity that we model is to the actual quantity we represent. Think of first order approximations, over simplifications, idealisations, gaps in aggregation levels, differences in definitions, non representativeness, and incompleteness issues. If the parameter were an exact measure of the quantity, it would score four on proxy. If the parameter in the model is not clearly related to the phenomenon it represents, the score would be zero.
- **Empirical basis:** Empirical basis typically refers to the degree to which direct observations, measurements and statistics are used to estimate the parameter. When the parameter is based upon good quality observational data, the pedigree score will be high. Sometimes directly observed data are not available and the parameter is estimated based on partial measurements or calculated from other quantities. Parameters determined by such indirect methods have a weaker empirical basis and will generally score lower than those based on direct observations.
- **Theoretical understanding:** The parameter will have some basis in theoretical understanding of the phenomenon it represents. If our theoretical understanding of some mechanism is very high, we may well be able to make reliable estimates for the parameters that represent that mechanism, even if the empirical basis is weak. On the other hand a strong empirical basis may not be sufficient to estimate future values of parameters if our theoretical understanding of the mechanisms involved is absent. In that case extrapolation from past data is not warranted. This criterion aims to measure the extent and partiality of the theoretical understanding that was used to generate the numeral of that parameter. Parameters based on well-established theory will score high on this metric, while parameters whose theoretical basis has the status of speculation will score low.
- **Methodological rigour:** Some method will be used to collect, check, and revise the data used for making parameter estimates. Methodological quality refers to the norms for methodological rigour in this process applied by peers in the relevant disciplines. Well-established and respected methods for measuring and processing the data would score high on this metric, while untested or unreliable methods would tend to score lower.
- **Skills & time availability:** This metric refers to the amount of resources that are available to construct a process model. It includes the skill, and the amount of resources involved in the modelling exercise, as well as the time that was available to construct the model, or to learn more about the simulated technology. The best results, with least uncertainty, is expected when a group of very skilled scientists is working on the model, and when they have ample time to educate themselves in the technology of interest. In the other extreme, one inexperienced modeller has to do the modelling work, without time to appropriately study the details of a technology. In between the extremes are cases where there are skilled resources available, but time is limited, or where the resource is somewhat less experienced, but is given time to fully familiarize him/herself with the knowledge base of the technology.

B

Regeneration Units

B.1. Dual-alkali process

The dual-alkali process is a widely used desulfurisation method. The main chemical interactions involve sodium sulfite and sodium dioxide to form bisulfite. The latter is removed in the rich solvent stream and can be regenerated using calcium hydroxide. Moreover, research has shown that sodium sulfite is also suitable to simultaneously remove NO_2 . The product, Na_2SO_4 can then be discarded using the same regeneration and filtration process designed for the dual-alkali technology.

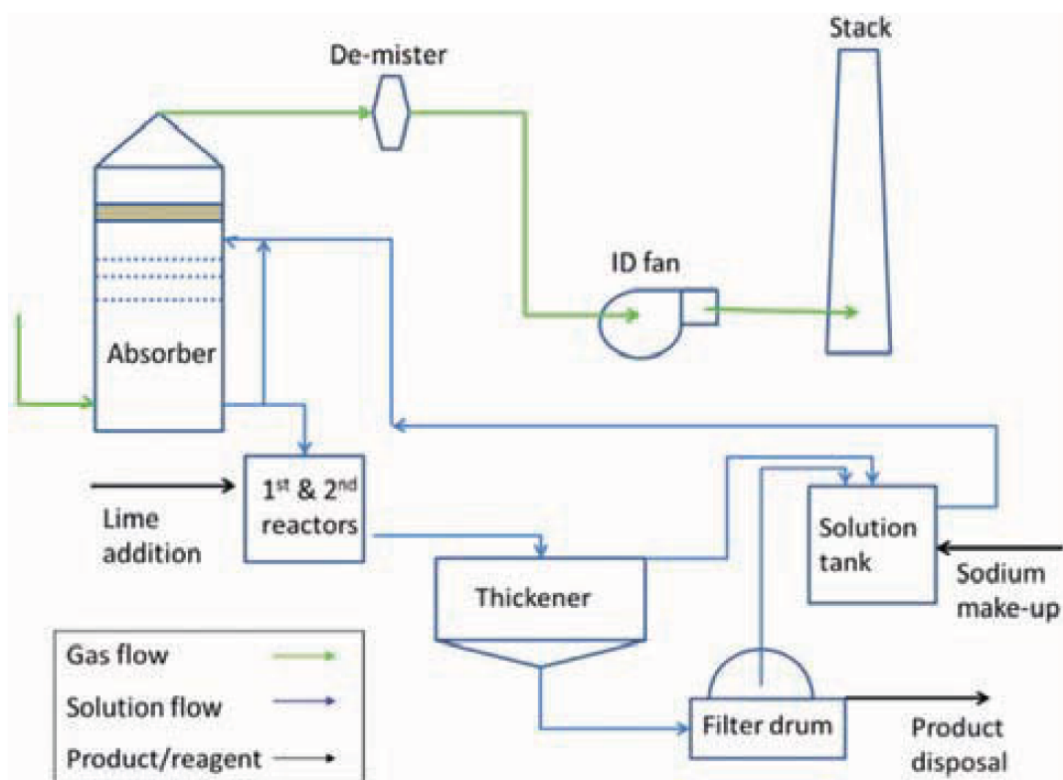


Figure B.1: Schematic of an absorption and regeneration process for a dual-alkali process. Sourced from (Bezuidenhout et al., 2012)

The overall process is comprised of 3 steps: absorption, regeneration, and filtration. In the absorption process, SO_2 and NO_2 are removed as $NaHSO_3$ and Na_2SO_4 . The rich solvent is bled continuously to a

lime reactor where sodium sulfite is regenerated. During this step, part of the sodium salts is lost with the filter cake. Thus, solvent losses are made up from a make-up tank. The make up is usually done using soda ash, which reacts with $NaHSO_3$ to form Na_2SO_3 .

The regeneration system consists of a lime reactor, a thickener, and a surge tank. In the lime reactor, the sodium bisulfite present in the rich solvent stream reacts with hydrated lime to form sodium sulfite and calcium sulfite. The product is a slurry consisting of solid salts ($CaCO_3$, Na_2NO_3) suspended in an aqueous solution of sodium sulfite that flows to a thickener tank. In here, the solid particles settle and are sent to the filtration system. On the other hand, regenerated sodium sulfite overflows and is recycled back to the absorber column.

Finally, the filtration system is responsible to remove, dewater, and store the precipitated solids. Concentrated slurry from the thickener tank is pumped to a rotary vacuum filter where a final cake consisting of about 55% solids is obtained.

Figure B.1 shows a representation of a typical scrubbing system with the regeneration and filtration steps included.

B.2. LO-CAT process

LO-CAT is a commercially available technology used to remove H_2S . The system provides significant advantages, such as 99% to 100% single stage removal efficiency, the ability to process a variety of gas streams, low temperature requirements, and minimum to non environmental footprint. To achieve all of this, the method is based on a proprietary liquid solvent composed of an iron-chelate (Fe-EDTA) catalyst.

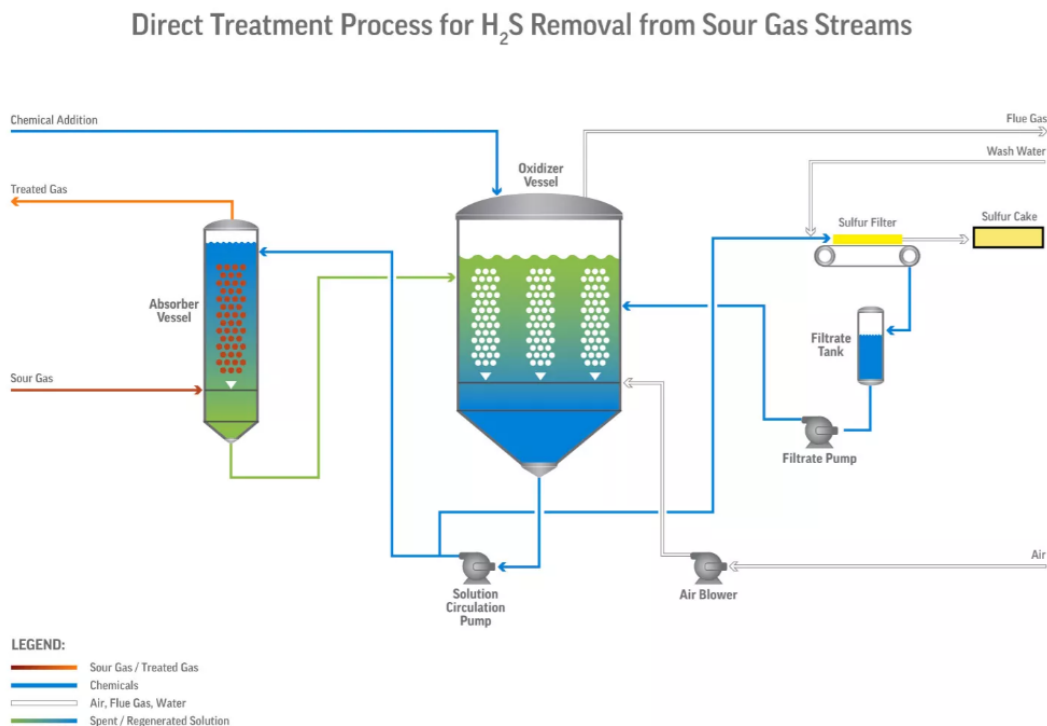


Figure B.2: Schematic representation of the LO-CAT technology. Sourced from (MERICHEM, n.d.)

Figure B.2 shows the unit operation and process streams from a typical LO-CAT process. The main reaction occurs in the absorption column, where H_2S is converted to S , by means of an iron-based catalyst. The Fe^{3+} ions are used as reagent (i.e., electron donor and acceptor) and as a catalyst,

by accelerating the overall reaction. On the other hand, the EDTA does not participate in process chemistry. Its function is to prevent the iron ions from precipitating in the aqueous solution.

Subsequently, regeneration takes place in a second unit by injecting air into the rich solution. In this step, oxygen present in the air reacts with the ferrous ions to regenerate the ferric elements according to reaction B.1. Additionally, a filter is used to remove a sulfur "cake", while the regenerated solution is recycled back to the absorption column.



C

Aspen Flowsheets

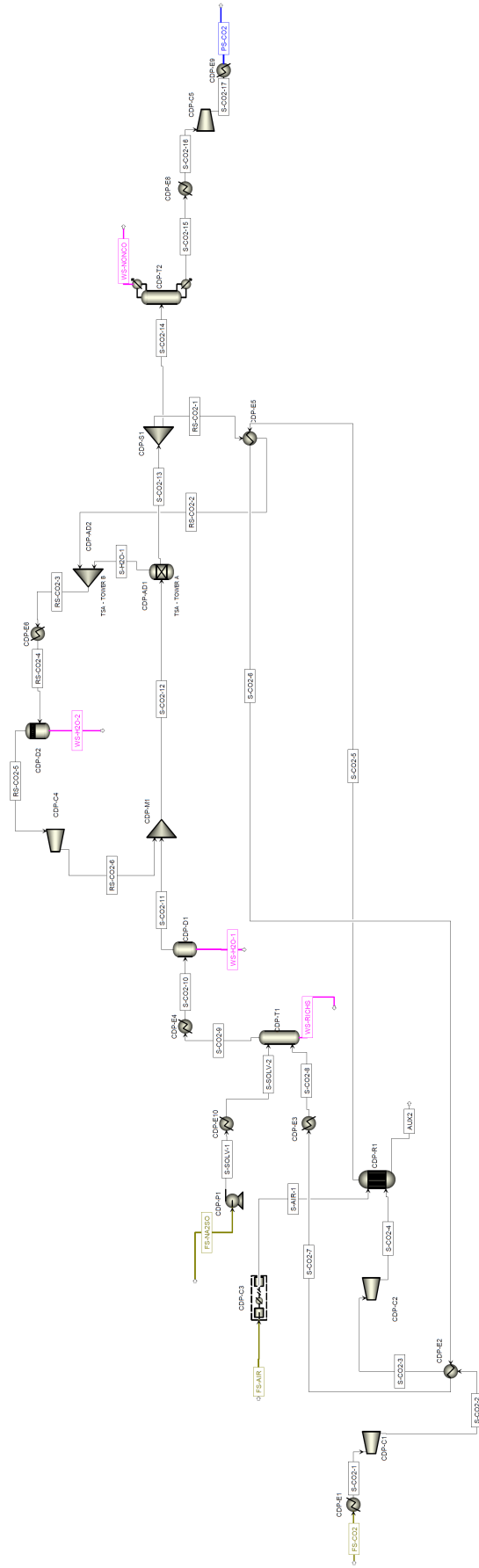


Figure C.1: Simulation flowsheet of the CO₂ purification system

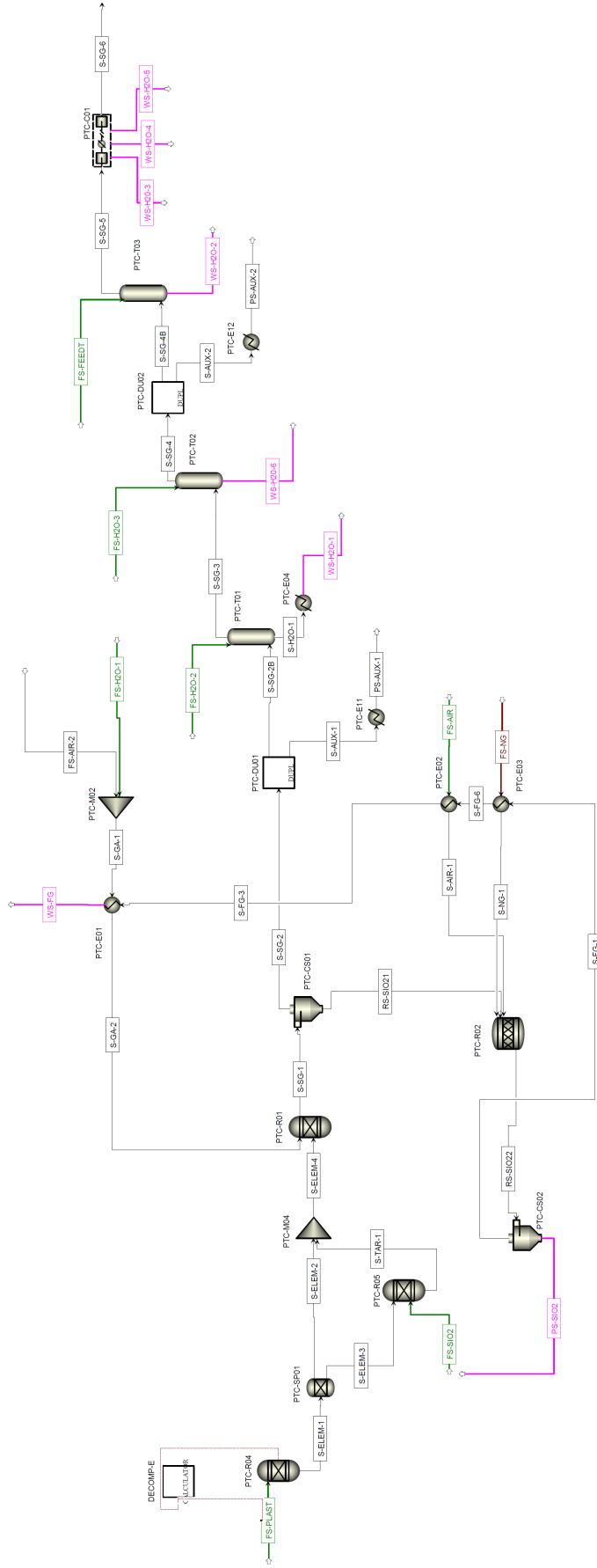


Figure C.3: Simulation flowsheet of the gasification and syngas conditioning units


```

function [ParEnt,ParReal,CorSal]=usermodel(ParEnt,ParReal,CorEnt)

tam = size(CorEnt);
n = tam(1) - 9; %Number of components
CorSal = CorEnt; %It makes the Output stream matrix equal to the Inlet stream matrix

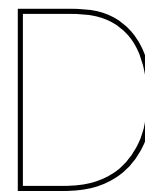
%ParEnt(2,1) = 12;
%ParEnt(4,1) = 98;
%ParReal(3,1) = 1.9*ParReal(1,1);

CorSal(n+2,1) = 80 + 273.15; % It changes the output stream temperature of stream number 1 (K)
CorSal(n+2,2) = 80 + 273.15; % It changes the output stream temperature of stream number 2 (K)
CorSal(n+3,1) = 3*1e6; % It changes the output stream pressure of stream number 1 (Pa)
CorSal(n+3,2) = 3*1e6; % It changes the output stream pressure of stream number 2 (Pa)

h2o=CorEnt(4,1);
h2o_consumption=0.9; % L of water per Nm3 of H2
h2_ratio=11.13; % Nm3 of H2 per kg of H2
M_h2o=CorEnt(n+9,1); % kg/kmol
d_h2o=CorEnt(n+8,1)/1000; % kg/L
Pc=64; % Power Consumption kWh/kg H2
CorSal(3,1)=h2o*M_h2o*d_h2o/h2o_consumption/h2_ratio/2; % kmol/s of H2 - kmol/s*kg/kmol*L_h2o/kg*Nm3_H2/L_h2o*kg_H2/Nm3_h2*kmol_h2/kg_h2
CorSal(4,1)=0; % kmol/s of water in H2 stream
CorSal(3,2)=0; % kmol/s of H2 in O2 stream
CorSal(10,2)=CorSal(3,1)/2; % kmol/s of O2
CorSal(4,2)= (h2o*18-CorSal(3,1)*2-CorSal(10,2)*32)/18; % kmol/s of water in O2 stream
ParReal(1,1)= CorSal(3,1)*2*Pc; % kWh per second
end

```

Figure C.5: Matlab code for the alkaline water electrolyser



Economic Evaluation

Assumptions for economic calculations

The assumptions and values used in the assessment are stated in the followings:

- The initial CAPEX is divided in 3 years prior to the start of the plant. 30% is allocated on the first year, 60% on the second year, and 10% on the third year.
- No revenues are considered for the first 2 years. The methanol production in years 3 and 4 is equal to 30% and 70% of the total capacity (8000 hours per year). This affects the revenues and VCP.
- Base year of total installed costs is 2014. These costs are updated to 2019 values using the Chemical Engineering Plant Cost Index.
- The capacity factor of the plants is considered as 91.3% (i.e., 8000 h per year).
- The catalyst is assumed to last for 3 years (Nyári et al., 2020).
- The raw material cost for the Fe-EDTA scrubbing unit is estimated at 300 US\$ per ton of sulfur removed (Gülşah Sönmez, 2017).
- For the scrubber in the CO_2 Purification System, $CaCO_3$ consumption is considered assuming an adjacent regeneration unit. The demand is estimated using a factor of 0.045 and 2 kmol of $CaCO_3$ per kmol of SO_2 and NO_2 removed, simultaneously. This represent a worst case scenario for the regeneration of Na_2SO_3 from Na_2SO_4 (i.e., all the Na_2SO_4 is removed from the system, without recycling any regenerated Na_2SO_3 to the absorption column). The factors were determined using data from (Bezuidenhout et al., 2012).
- 3 shifts of 5 operators are considered to operate the plastic-to-methanol plant, the CO_2 hydrogenation plant, and the CO_2 purification system (Pérez-Fortes et al., 2016).
- No cost associated to the disposal of waste streams, nor revenues by selling of by products.
- 25 years of lifetime was assumed for all the plants (Nyári et al., 2020)

Prices of raw material, utilities, and produced methanol

Table D.1: Prices of raw materials, utilities, and product

Raw Material	Price (eur/kg)	Reference
CO_2	0.025	Cost of CO_2 European emissions allowance (MarketInsider, 2021)
Green H_2	4.10	(Nyári et al., 2020)
Grey H_2	1.09	(NREL, 2018)
Plastic waste	0.066	(Gradus et al., 2017)
Natural gas	1.01	(Global Petrol Prices, 2021)
$CaCO_3$	47.17	(Merck, 2021)
H_2O	0.001	Assumed price of 1 <i>eur/m</i> ³
Product	Price (eur/kg)	Reference
MeOH	0.41	(Methanex, 2021)
Utility	Price (eur/kWh)	Reference
Electricity	0.088	(Statista, 2021)
Low pressure steam	0.006	Aspen Plus
High pressure steam	0.009	Aspen Plus
High temperature needs	0.015	Aspen Plus
Cooling water	0.001	Aspen Plus
Chilling water	0.001	Aspen Plus
Refrigerant	0.001	Aspen Plus

Total Installation Cost

The total installation cost, used as input to calculate the results in Section 2.3.2, are obtained from the Aspen Economic Analyzer tool. These include PEC, piping, insulation, civil works, site preparation, and engineering costs associated with the ISBL.

Plastic Gasification and Syngas Conditioning

Table D.2: Total installation cost of equipment for the Plastic Gasification and Syngas Conditioning process

Name	Total Equipment Cost [EUR]
PTC-T03	\$ 374,338
PTC-E03	\$ 159,448
PTC-R01	\$ 225,153
PTC-E05	\$ 71,416
PTC-C01	\$ 14,031,538
PTC-T02	\$ 389,045
PTC-M02	\$ 140,826
PTC-R02	\$ 236,263
PTC-CS01	\$ 184,630
PTC-M01	\$ 18,074
PTC-E04	\$ 93,571
PTC-CS02	\$ 213,726
PTC-T01	\$ 484,058

Methanol Synthesis in the Plastic-to-Methanol Route

Table D.3: Total installation cost of equipment for the Methanol Synthesis process

Name	Total Equipment Cost [EUR]
PTC-T05	\$ 1,244,161
PTC-E09	\$ 97,023
PTC-R03	\$ 129,399
PTC-M02	\$ 87,924
PTC-E07	\$ 121,570
PTC-D01	\$ 145,588
PTC-E05	\$ 164,209
PTC-E06	\$ 548,599
PTC-E08	\$ 42,005
PTC-T04	\$ 1,141,212
PTC-D02	\$ 174,261
PTC-C02	\$ 1,356,208

CO₂ Purification System

Table D.4: Total installation cost of equipment for the CO₂ Purification System

Name	Total Equipment Cost [EUR]
CDP-T2	\$ 755,765
CDP-P1	\$ 49,305
CDP-AD1	\$ 327,572
CDP-AD2	\$ 327,572
CDP-E6	\$ 72,900
CDP-D2	\$ 107,286
CDP-C4	\$ 668,793
CDP-M1	\$ 86,443
CDP-C1	\$ 497,918
CDP-E3	\$ 106,546
CDP-E2	\$ 163,574
CDP-C5	\$ 1,659,339
CDP-T1	\$ 197,432
CDP-E9	\$ 142,413
CDP-E10	\$ 48,564
CDP-C3	\$ 997,529
CDP-E4	\$ 70,043
CDP-D1	\$ 107,286
CDP-E8	\$ 50,152
CDP-E11	\$ 79,989
CDP-R1	\$ 228,116
CDP-C2	\$ 723,177
CDP-E1	\$ 122,099
CDP-C6	\$ 1,381,284

CO₂ Hydrogenation

Table D.5: Total installation cost of equipment for the CO₂ Hydrogenation process

Name	Total Equipment Cost [EUR]
MEOH-C01	\$ 295,937
MEOH-C02	\$ 2,053,357
MEOH-C03	\$ 1,666,640
MEOH-D01	\$ 173,732
MEOH-D02	\$ 184,206
MEOH-E02	\$ 1,025,356
MEOH-E03	\$ 101,044
MEOH-E04	\$ 547,752
MEOH-E05	\$ 172,991
MEOH-E06	\$ 96,388
MEOH-E07	\$ 101,573
MEOH-E01	\$ 73,323
MEOH-M02	\$ 78,296
MEOH-M03	\$ 76,603
MEOH-R01	\$ 325,985
MEOH-T01-cond	\$ 227,798
MEOH-T01-cond acc	\$ 189,603
MEOH-T01-reb	\$ 190,555
MEOH-T01-reflux pump	\$ 53,114
MEOH-T01-tower	\$ 1,201,627
MEOH-T02-cond	\$ 239,860
MEOH-T02-cond acc	\$ 171,192
MEOH-T02-reb	\$ 128,765
MEOH-T02-reflux pump	\$ 58,616
MEOH-T02-tower	\$ 912,251
MEOH-EL01	\$ 147,233,655

Cash Flows

Table D.6 shows the details for the yearly cash flows used to calculate the economic KPIs in Section 2.3.2.

Table D.6: Yearly cash flows

	CO ₂ hydrogenation	Plastic-to-MeOH
ISBL	18.76	25.20
OSBL	6.57	8.82
Engineering costs	5.07	6.80
Contingency	7.60	10.21
TFCC	37.99	51.03
Working Capital	3.80	5.10
TOTAL CAPEX	41.79	56.13
Fixed Cost of Production		
Labour	7.50	3.75
Supervision (25% of labour)	1.88	0.94
Overhead (45% labour and supervision)	4.22	2.11
Maintenance (3% ISBL)	0.56	0.76
Interest (6% of WC)	0.23	0.31
TOTAL FCP	14.39	7.86
Raw materials		
CO ₂	8.47	-
CaCO ₃	9.16	-
H ₂ O	-	5.49
Green H ₂	-	-
Grey H ₂	48.64	-
Plastic Wastes	-	11.99
Fe-EDTA	-	0.00
NG	-	42.94
Utilites		
Elec	2.77	8.01
LLPS	2.52	1.30
HPS	0.13	0.09
FHT	0.29	-
CW	0.46	0.41
CHW	0.02	-
Refrigerant	1.23	-
Catalyst consumption		
Cu/Zn/Al/Zr	0.01	0.01
Stack replacement of electrolyser		
TOTAL VCP	73.69	70.24
Every 7.5 years	-	-
REVENUES from MeOH production	90.21	90.20